2019 RMZ – M&G **Vol. 66** No. 2

RMZ

MATERIALS and GEOENVIRONMENT

MATERIALI in GEOOKOLJE

RMZ – M&G, **Vol. 66**, No. 2
pp. 075–138 (2019)

Ljubljana, June 2019

ISSN 1408-7073

RMZ – Materials and Geoenvironment
RMZ – Materiali in geookolje
ISSN 1408-7073

Old title/Star naslov
Mining and Metallurgy Quarterly/Rudarsko-metalurški zbornik
ISSN 0035-9645, 1952–1997

Published by/Izdajatelj
Faculty of Natural Sciences and Engineering, University of Ljubljana/
Naravoslovnotehniška fakulteta, Univerza v Ljubljani

Associated Publisher/Soizdajatelj
Institute for Mining, Geotechnology and Environment, Ljubljana/
Inštitut za rudarstvo, geotehnologijo in okolje
Velenje Coal Mine/Premogovnik Velenje
Slovenian Chamber of Engineers/Inženirska zbornica Slovenije

Editorial Office/Uredništvo
Technical editors/Tehnična urednika Teja Čeru and Jože Žarn
Secretary/Tajnica Nives Vukič

Editorial Address/Naslov uredništva
RMZ – Materials and Geoenvironment
Aškerčeva cesta 12, p. p. 312
1001 Ljubljana, Slovenija
Tel.: +386 (0)1 470 46 10
Fax.: +386 (0)1 470 45 60
E-mail: rmz-mg@ntf.uni-lj.si

Published/Izhajanje
4 issues per year/4 številke letno

Partly funded by Ministry of Education, Science and Sport of Republic of Slovenia./Pri financiranju revije sodeluje Ministrstvo za izobraževanje, znanost in šport Republike Slovenije.

Articles published in Journal "RMZ M&G" are indexed in international secondary periodicals and databases:/Članki, objavljeni v periodični publikaciji „RMZ M&G", so indeksirani v mednarodnih sekundarnih virih:
CA SEARCH® – Chemical Abstracts®, METADEX®, GeoRef.

Annual subscription for individuals in Slovenia: 20 EUR, for institutions: 30 EUR. Annual subscription for the rest of the world: 30 EUR, for institutions: 50 EUR/Letna naročnina za posameznike v Sloveniji: 20 EUR, za inštitucije: 30 EUR. Letna naročnina za tujino: 30 EUR, inštitucije: 50 EUR

Transaction account/Tekoči račun
Nova Ljubljanska banka, d. d., Ljubljana: UJP 01100-6030708186

VAT identification number/Davčna številka
24405388

Online Journal/Elektronska revija
www.rmz-mg.com
www.degruyter.com/view/j/rmzmag

Table of Contents

Kazalo

Historical Review

More than 90 years have passed since the University Ljubljana in Slovenia was founded in 1919. Technical fields were united in the School of Engineering that included the Geologic and Mining Division, while the Metallurgy Division was established only in 1939. Today, the Departments of Geology, Mining and Geotechnology, Materials and Metallurgy are all part of the Faculty of Natural Sciences and Engineering, University of Ljubljana.

Before World War II, the members of the Mining Section together with the Association of Yugoslav Mining and Metallurgy Engineers began to publish the summaries of their research and studies in their technical periodical Rudarski zbornik (Mining Proceedings). Three volumes of Rudarski zbornik (1937, 1938 and 1939) were published. The War interrupted the publication and it was not until 1952 that the first issue of the new journal Rudarsko-metalurški zbornik – RMZ (Mining and Metallurgy Quarterly) was published by the Division of Mining and Metallurgy, University of Ljubljana. Today, the journal is regularly published quarterly. RMZ – M&G is co-issued and co-financed by the Faculty of Natural Sciences and Engineering Ljubljana, the Institute for Mining, Geotechnology and Environment Ljubljana, and the Velenje Coal Mine. In addition, it is partly funded by the Ministry of Education, Science and Sport of Slovenia.

During the meeting of the Advisory and the Editorial Board on May 22, 1998, Rudarsko-metalurški zbornik was renamed into "RMZ – Materials and Geoenvironment (RMZ – Materiali in Geookolje)" or shortly RMZ – M&G. RMZ – M&G is managed by an advisory and international editorial board and is exchanged with other world-known periodicals. All the papers submitted to the RMZ – M&G undergoes the course of the peer-review process.

RMZ – M&G is the only scientific and professional periodical in Slovenia which has been published in the same form for 60 years. It incorporates the scientific and professional topics on geology, mining, geotechnology, materials and metallurgy. In the year 2013, the Editorial Board decided to modernize the journal's format.

A wide range of topics on geosciences are welcome to be published in the RMZ – Materials and Geoenvironment. Research results in geology, hydrogeology, mining, geotechnology, materials, metallurgy, natural and anthropogenic pollution of environment, biogeochemistry are the proposed fields of work which the journal will handle.

Editor-in-Chief

Zgodovinski pregled

Že več kot 90 let je minilo od ustanovitve Univerze v Ljubljani leta 1919. Tehnične stroke so se združile v Tehniški visoki šoli, ki sta jo sestavljala oddelka za geologijo in rudarstvo, medtem ko je bil oddelek za metalurgijo ustanovljen leta 1939. Danes oddelki za geologijo, rudarstvo in geotehnologijo ter materiale in metalurgijo delujejo v sklopu Naravoslovnotehniške fakultete Univerze v Ljubljani.

Pred 2. svetovno vojno so člani rudarske sekcije skupaj z Združenjem jugoslovanskih inženirjev rudarstva in metalurgije začeli izdajanje povzetkov njihovega raziskovalnega dela v Rudarskem zborniku. Izšli so trije letniki zbornika (1937, 1938 in 1939). Vojna je prekinila izdajanje zbornika vse do leta 1952, ko je izšel prvi letnik nove revije Rudarsko-metalurški zbornik – RMZ v izdaji odsekov za rudarstvo in metalurgijo Univerze v Ljubljani. Danes revija izhaja štirikrat letno. RMZ – M&G izdajajo in financirajo Naravoslovnotehniška fakulteta v Ljubljani, Inštitut za rudarstvo, geotehnologijo in okolje ter Premogovnik Velenje. Prav tako izdajo revije financira Ministrstvo za izobraževanje, znanost in šport.

Na seji izdajateljskega sveta in uredniškega odbora je bilo 22. maja 1998 sklenjeno, da se Rudarsko-metalurški zbornik preimenuje v RMZ – Materiali in geookolje (RMZ – Materials and Geoenvironment) ali skrajšano RMZ – M&G. Revijo RMZ – M&G upravljata izdajateljski svet in mednarodni uredniški odbor. Revija je vključena v mednarodno izmenjavo svetovno znanih publikacij. Vsi članki so podvrženi recenzijskemu postopku.

RMZ – M&G je edina strokovno-znanstvena revija v Sloveniji, ki izhaja v nespremenjeni obliki že 60 let. Združuje področja geologije, rudarstva, geotehnologije, materialov in metalurgije. Uredniški odbor je leta 2013 sklenil, da posodobi obliko revije.

Za objavo v reviji RMZ – Materiali in geookolje so dobrodošli tudi prispevki s širokega področja geoznanosti, kot so: geologija, hidrologija, rudarstvo, geotehnologija, materiali, metalurgija, onesnaževanje okolja in biokemija.

Glavni urednik

Original scientific paper

Received: Jul 17, 2018
Accepted: Jun 04, 2019
DOI: 10.2478/rmzmag-2019-0008

Contribution to Understanding of Ore Fluids in the Zletovo Mine Based on Fluid Inclusion Data

Raziskave Rudnih Fluidov v Rudniku Zletovo s Pomočjo Tekočinskih Vključkov

Goran Tasev[1], Todor Serafimovski[1], Matej Dolenec[2], Nastja Rogan Šmuc[2,*]

[1]Goce Delcev University, Faculty of Natural and Technical Sciences, Stip, R. Macedonia

[2]University of Ljubljana, Faculty of Natural Sciences and Engineering, Department of Geology, Ljubljana, Slovenia

*nastja.rogan@guest.arnes.si

Abstract

The Zletovo is lead–zinc (Pb–Zn) deposit, adjacent to the Plavica volcanic centre (R. Macedonia) with high-sulphidation and porphyry mineralisation. The analysis of fluid inclusions showed homogenisation temperatures in the range 335–145°C, which reflects phases of pulsation of hydrothermal solutions and defined into four groups from the lowest to the highest temperatures. The frequency of the homogenisation temperatures ranged from 265 to 125°C and with the most dominant from 245 to 225°C, from 225 to 205°C and from 145 to 125°C. Also, it was confirmed that hydrothermal ore-bearing solutions were defined as NaCl-type with range from 4.4 to 8.6 wt% NaCl equivalent. The latest stage salinities ranged from 3 to 12 wt% NaCl equivalent, where those from 10 to 12 wt% and from 6 to 8 wt% NaCl equivalent, prevailed. This suggests that hydrothermal solutions within analysed quartz grains were at final mineralizing phase. Density of fluid inclusions ranged from 0.7 to 0.95 g/cm^3. Calculated pressures and paleo-depths of mineralisation ranged from 14 to 130 bar and from 0.6 to 0.8 km.

Key words: lead–zinc, quartz, fluid inclusions, temperature, salinity, Zletovo mine.

Izvleček

Svinčevo cinkovo (Pb-Zn) rudišče Zletovo z bogato sulfidno in porfirsko mineralizacijo leži v bližini vulkanskega centra Plavica (R. Makedonija). Analiza tekočinskih vključkov je pokazala, da so se homogenizacijske temperature gibale od 335 do 145°C, kar odraža različne faze prisotnosti hidrotermalnih raztopin. Frekvence homogenizacijskih temperatur so se gibale od 265 do 125°C, z najbolj prevladujočimi od 245 do 225°C, od 225 do 205°C in od 145 do 125°C. Z raziskavami smo potrdili, da so bile hidrotermalne rudonosne raztopine tipa NaCl, in sicer z razponom od 4,4 do 8,6 ut.% ekviv. NaCl. Slanost v zadnjih fazah prisotnosti raztopin je znašala od 3 do 12 ut.% ekviv. NaCl. Podatki tako kažejo na to, da so bile hidrotermalne raztopine znotraj analiziranih kremenovih zrn v zadnji fazi mineralizacije. Gostota tekočinskih vključkov je znašala od 0,7 do 0,95 g/cm^3. Tlaki in paleo-globine pojava mineralizacije so znašali od 14 do 130 barov in od 0,6 do 0,8 km.

Ključne besede: svinec-cink, kremen, tekočinski vključki, temperatura, slanost, rudnik Zletovo.

Introduction

Research and exploitation of lead–zinc ore from Zletovo mine have recorded history of nearly a century, but detailed studies of ore fluids, as presented in this paper, are very rare. Namely, the Zletovo lead–zinc deposit has been the subject of exploitation since 1941. After the end of the Second World War, a modern mine with an annual production capacity of 400,000 t of ore was built at the Zletovo ore deposit. Thus, the Zletovo mine has been in continuous production for more than 75 years, with an average content of 8% of Pb + Zn within the ore.

During the exploration of the Zletovo deposit, numerous detailed and special mineralogical and geochemical studies on evolution and lead–zinc mineralisation were performed. The most complex and complete published materials are as follows [1, 3, 4, 5–10].

The aim of this paper is to investigate the fluid inclusions in quartz samples taken from the ore parageneses in order to define the ore deposit origin through values of homogenisation temperature, salinity and pressures.

Materials and methods

Geological setting and mineralisation

The Zletovo lead–zinc deposit, located in the east of the Kratovo–Zletovo volcanogenic complex, occupies the central parts of the Kratovo–Zletovo ore district or the south-eastern parts of the Zletovo ore field. The Zletovo lead–zinc deposit was formed by hydrothermal activity intimately associated with tertiary volcanism along the active continental margin. The major rock types in the area are andesite, dacite, dacitic ignimbrite and volcanic tuff [1, 3, 11]. Dacitic ignimbrite is the most common volcanic unit. The Pb–Zn mineralisation at Zletovo is spatially and genetically related to fracture zones in the NW, NNW and ENE directions, which have served as the main conduits and depositional sites for hydrothermal fluids.

Ore bodies occur as veins, accompanied by impregnation and stockwork-disseminated ore mineralisation, most commonly in the selvage parts of the mineralized vein structures. The ore bodies are of variable dimensions in terms of strike, dip and size. Vein-type ore bodies have been determined to be 100–300 m in length (depending on the length of veins), and rarely over 5 km (the vein no. 10), whereas they have been traced as over 500 m in dip, and according to the data available so far, no change in continuity has been noticed with depth, which is very important fact for the deposit reserve potential. The ore veins are also variable, ranging from several centimetres to 2 m and rarely over 5 m in size. Thickening of veins occurred at places with great changes in their direction in both strike and dip. Investigations done so far have determined about 16 veins from NW–SE to NNW–SSE and ENE–WSW to E–W extension, most commonly subparallel to each other. Occasionally they bend and intersect (commonly under a sharp angle) such as ore veins 2, 3, 4, 6 and 7 (Figure 1). Termi-

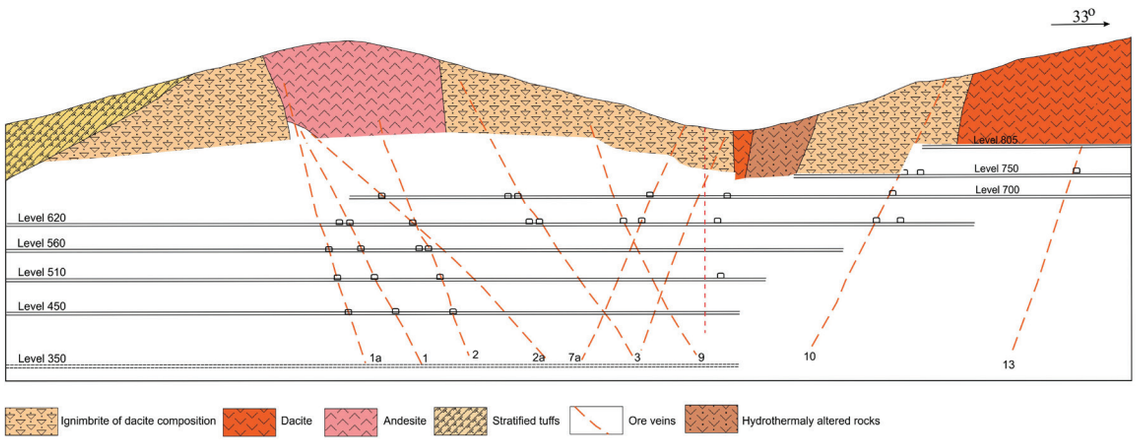

Figure 1: *Geological cross section through the Zletovo Mine.*

nal branching of the main ore veins is common (ore vein 1) and results in the formation of apophyses of small dimensions.

The ore mineral association comprises galena as the principal ore mineral together with sphalerite and subordinate pyrite, siderite and chalcopyrite and rare pyrrhotite, marcasite and magnetite [12, 13]. Veins typically contain large clasts or screens of altered dacitic and andesitic wall rocks. The altered clasts are weakly mineralized or barren.

Analysis

Fluid inclusion studies were conducted on doubly polished thin sections, made of six quartz samples (S1–S7, omitting S2) from the Zletovo mine, in which more than 130 separate fluid inclusions were investigated. Transparent, 150 μm thick, polished plates were utilised, in which fluid inclusions (5–40 μm in size) in quartz were analysed. Fluid inclusions were almost evenly distributed in the studied quartz grains and only those with strong indications of primary origin [14], and thus interpreted as having been trapped during the mineralising event, were taken into account during the microthermometric studies; however, the possibility that some secondary inclusions have also been investigated cannot be excluded [15]. The study was performed using Nikon and Olympus BX51 optical microscopes, and at least 20 inclusions were found and defined in each analysed sampleQQ. Microthermometric data were obtained using a Linkam THMSG600 heating–freezing stage (with temperature range from −196 to +600°C) and TMS 90 controller attached to a conventional petrographic microscope. The stage was calibrated using the Synflinc set of synthetic fluid inclusions and revealed a precision of ±0.1°C for the freezing runs and ±5°C for temperatures near to or higher than 360°C. Salinities were expressed as weight percent NaCl equivalent and were estimated from the melting temperatures of the last crystal of ice for two-phase fluid inclusions [16, 17]. Eutectic temperatures were used to estimate the overall composition of the studied fluid inclusions by comparison with published data for different salt–water systems [15, 18]. The pressure of heterogeneous fluids was determined using the method of sections of isochors and isotherms [19].

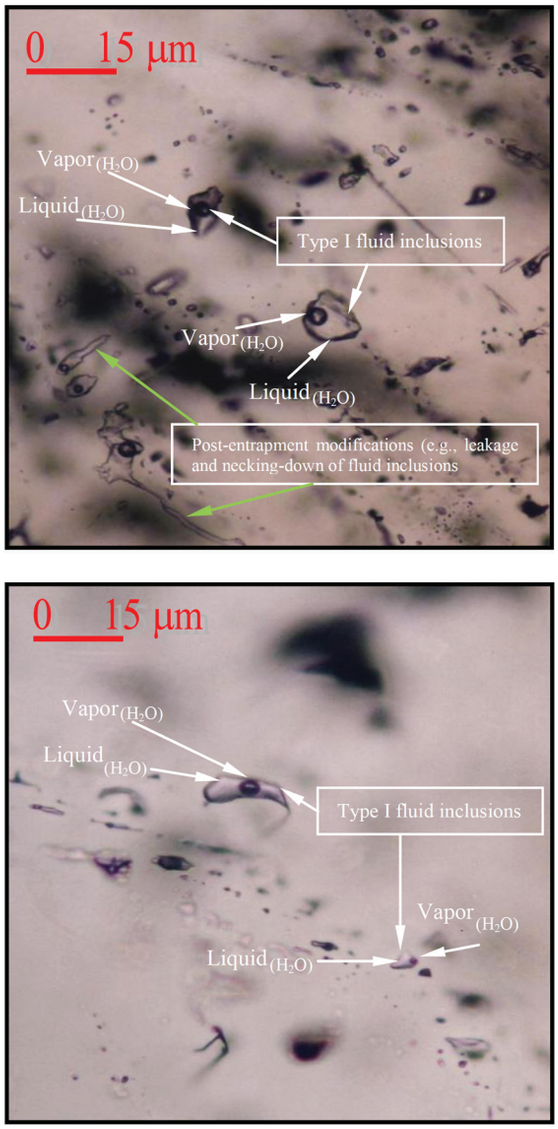

Figure 2: *a) Large primary type I (V+L) fluid inclusions; b) Large and minute primary type I (V+L) fluid inclusions.*

As mentioned above, the fluid inclusions as remnants of ancient ore-bearing solutions from the Zletovo deposit were analysed by the analytical facilities of the Geological Department of Royal Holloway University in London, Egham, UK.

During the analysis, the following phenomena were analysed and interpreted: the homogenisation temperature (T_h), the temperature of melting of the last ice crystal (T_m), salinity (wt% NaCl equivalent), density, pressure and determination of the primary or secondary ori-

Table 1: *Microthermometry data of studied fluid inclusions from the Zletovo deposit (R. Macedonia).*

Locality and sample label	Mineral	Fluid inclusion type	Salinity (wt% NaCl equivalent)		Homogenisation temperature (°C)	
			Range	Average	Range	Average
Zletovo (*S*-1)	Quartz	P	3.1–11.8	8.6	137.8–265.4	196.2
Zletovo (*S*-2)	Quartz	P	1.7–5.4	4.4	233–285	251.2
Zletovo	Quartz	P	–	–	304.0–368.0	335.0
Zletovo	Quartz	Ps	–	–	210.0–265.0	235.0
Zletovo	Quartz	P	–	–	109.0–163.0	145.0

Note: *P—Primary fluid inclusions; Ps—Pseudosecondary fluid inclusions; samples S-1 and S-2 are from [11] and others are from [8].*

gin of inclusion (Table 1). At least 20 inclusions were taken into account in each specimen, which should provide sufficient data to ensure the reliability of the parameters mentioned above. All the studied fluid inclusions were colourless. The analysed fluid inclusions were mainly of two phases type (L + V, where L is liquid and V is vapour; see Figures 2a and 2b), or liquid phase (L) and vapour phase (V), without the presence of CO_2.

Results and discussion

Primary fluid inclusions in quartz vary in size from 3 to 7 μm and locally up to 12–13 μm (Figure 2). Some secondary liquid-rich inclusions occur along healed fractures that cut across different quartz grains and range from 1 to 5 μm and typically have irregular shapes (Figure 2a, green arrows). The degree of fill of the fluid inclusions was calculated by the following equation:

$$D_f = \frac{L}{L+V}$$

where D_f stands for degree of fill of the inclusion, L for liquid phase and V for vapour phase. The degree of fill of the studied fluid inclusions was high, ranging from 0.70 to 0.95. They consist of two phases (L + V) with 5–30 vol.% vapour. This gave us a basis for calculation of fluid inclusions densities later on. All the studied fluid inclusions were homogenized into a liquid phase. The salinity of solutions, in general, was low, ranging from 1.7 to 11.8 wt% NaCl equivalent, with an average of 4.4–8.6 wt% NaCl equivalent. In more than 120 individual fluid inclusions, in six quartz samples from Zletovo deposit, homogenisation temperatures (T_h) were within the range of 109–368°C. This range of homogenisation temperatures showed high consistency, bearing in mind the range of 150–350°C determined by former studies [6, 20]. The T_h range given above is characterised by two peak values of 130–180°C and 200–275°C, which can be easily related to the polymetallic stage characterised by the assemblages of sphalerite–galena–pyrite–chalcopyrite and less abundant pyrite–galena–quartz. This is very similar to the data of [21] for the Maouduan deposit, where sulphides followed the sequence pyrite–sphalerite–chalcopyrite–galena. The capture temperatures of inclusions can be determined as medium to high. Here, it is necessary to point out that the homogenisation temperatures define the lowest temperature of mineralisation, while the temperatures determined by stable sulphur isotope geothermometers define the "real" temperatures of mineralisation [22–25]. For all of the studied fluid inclusions, temperatures of first ice melting (T_m) within the range of –26 to –20°C were determined, which suggests temperatures close to the eutectic temperature of the system H_2O–NaCl (–20.8°C), or the solution NaCl with (±K), while Ca and Mg are absent since their eutectic temperature is significantly lower.

In accordance with data obtained from micro-thermometric analyses, diagrams show relations between parameters of the fluid in-

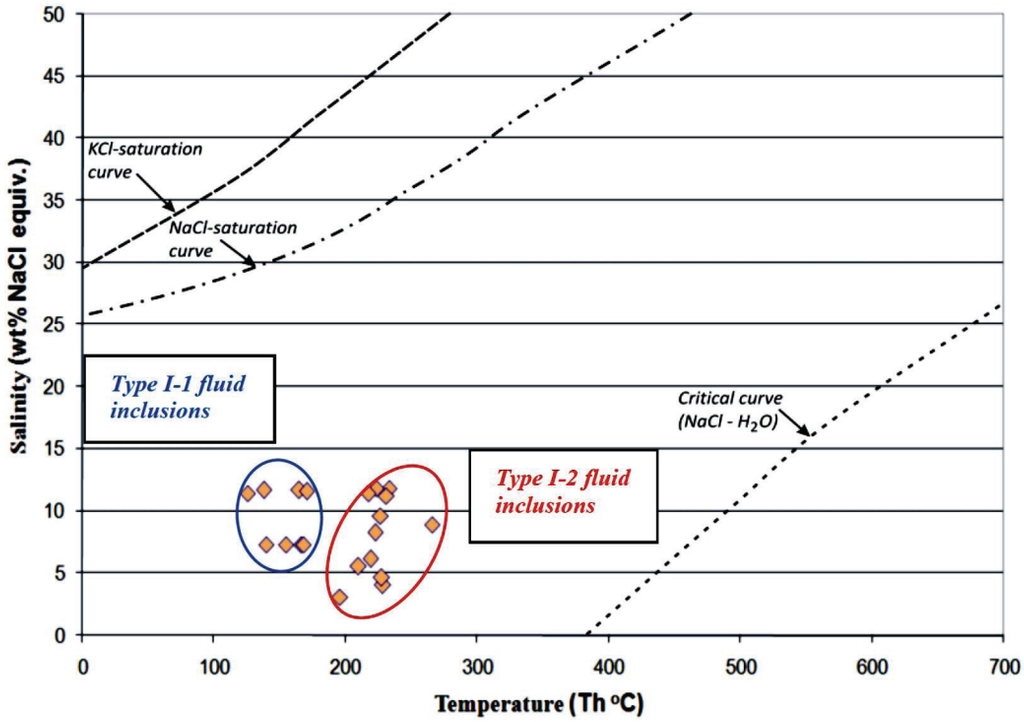

Figure 3: *Relations of homogenization temperatures and salinities in fluid inclusions from Zletovo deposit.*

clusions: salinity (wt% NaCl equivalent) versus homogenisation temperature (Figure 3).

It points to a wide temperature range of fluid inclusions capture, indicating a long process of new material deliveries, which is supported by a salinity difference of up to 10 wt% NaCl equivalent units. Such occurrences are very indicative of mineralisations with multiple pulsations and phase deposition of mineralisations. Fluid inclusion studies of ore-related minerals (in our case, quartz) constrain the fluid evolution in the later stages of development of the hydrothermal system. Homogenisation temperatures plotted against bulk salinity values clearly separate two types of fluid inclusions into two distinct groups, which strongly suggests the involvement of two distinct fluid types in the Pb–Zn mineralisation event: a higher temperature (>200°C), low-to-medium salinity (>7.5 wt% NaCl equivalent) brine, represented by type I-2 fluid inclusions, and a lower temperature (<200°C), low salinity (<5.5 wt% NaCl equivalent) type I-1 fluid inclusion (Figure 3). Post-entrapment modifications (e.g., leakage and necking-down; Figure 2a) could be invoked to explain the broad and contrasting range of homogenisation temperatures and salinities displayed by types I-1 and I-2 fluid inclusions. Data on the melting temperatures of the last ice crystal and homogenisation temperatures, as expected, have shown the very same grouping as in the Figure 3.

Also, that data shows that there is no direct relation between the melting temperature of the last ice crystal and the homogenisation temperature. Ice melting temperatures ranging from −5.5 to −8.18°C yield salinities between 7.2 and 11.8 wt% NaCl equivalent for type I-1 inclusions. In contrast, ice melting of type I-2 inclusions invariably takes place at temperature values ranging from −1.8 to −8.3°C, indicating a broader range of salinities (3.0–11.8 wt% NaCl equivalent). Upon heating, total homogenisation of type I-1 fluid inclusions invariably occurred via the disappearance of vapour into the liquid phase between 130 and 180°C. Fluid inclusions of type I-2, on the other hand, show vapour disappearance within the interval of 200–275°C. Probably, type I-2 is representative of mixing of less saline and colder (probably

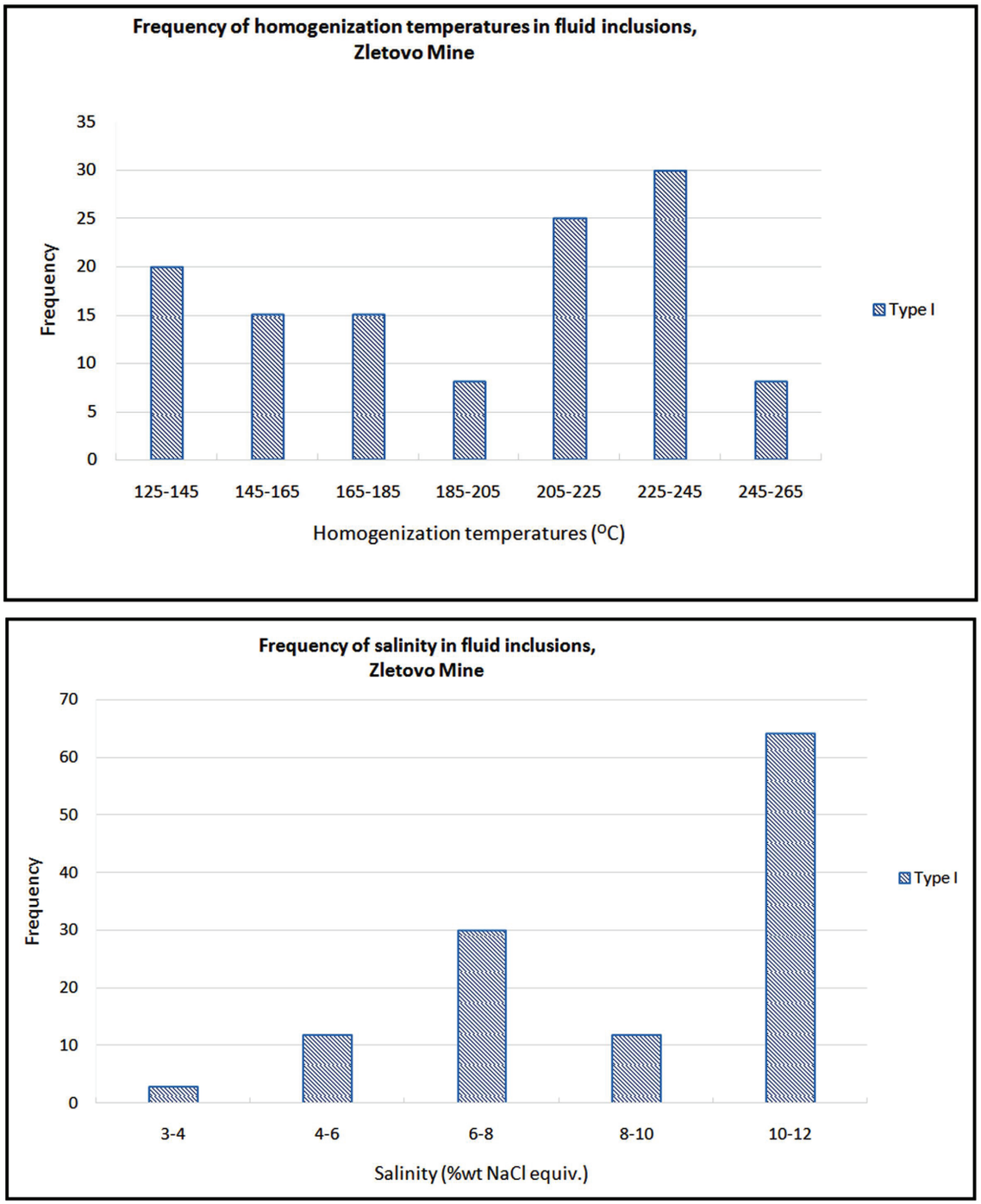

Figure 4: *Relations of homogenization temperature vs. last ice crystal melting temperature in fluid inclu¬sions from the Zletovo deposit [9].*

meteoric water) with magma water. Type I-1 shows a clear connection to I-2, that are inclusions with cooler fluid that survived the "leakage" and their T_h increased significantly.

However, the most common were inclusions with homogenisation temperatures within the ranges of 225–245°C and 205–225°C, while salinities showed the highest frequencies within the ranges of 10–12 wt% and 6–8 wt% NaCl

Table 2: *Several the most crucial fluid inclusion parameters calculated from ours fluid inclusions study.*

	x (NaCl)	w% (NaCl)	Molar volume (cm^3/mol)	Density (g/cm^3)	Temperature homogenisation (°C)	Pressure (MPa)
Sample 1	0.0282	8.6	20.490	0.93	198.2	1.41
Sample 3	0.0183	5.7	26.155	0.72	334.1	13.14
Sample 4	0.0220	6.8	21.779	0.87	244.5	3.48
Sample 5	0.0187	5.8	24.760	0.76	312.8	9.94
Sample 6	0.0155	4.9	21.099	0.88	217.9	2.16
Sample 7	0.0224	6.9	20.890	0.91	213.1	1.94

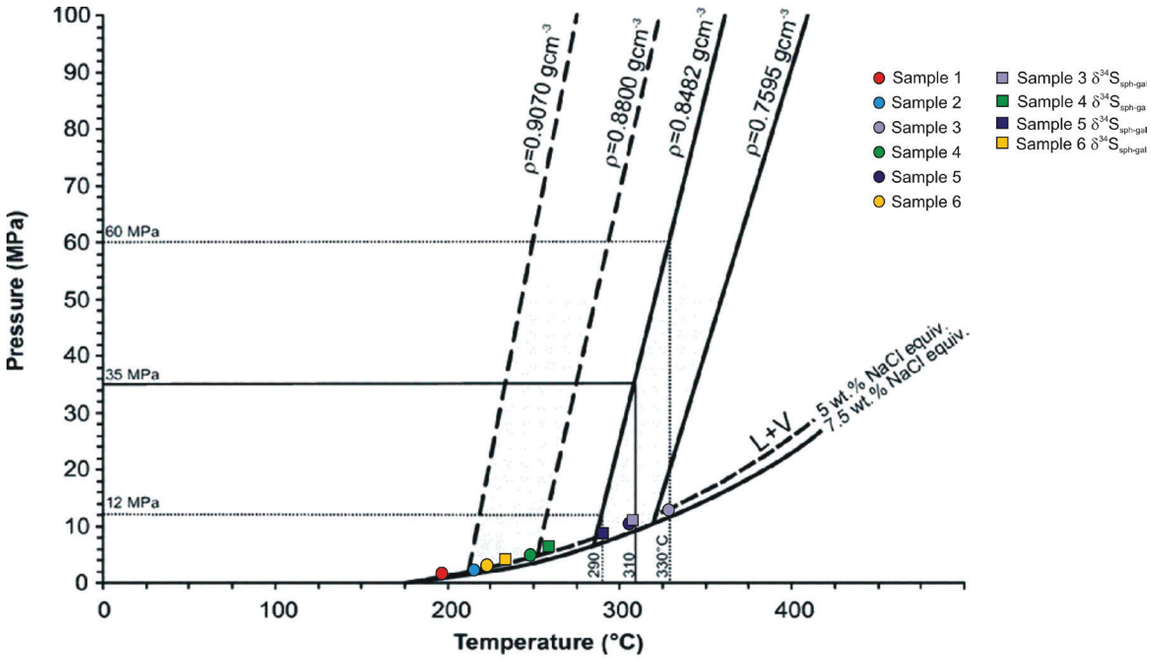

Figure 5: *Histograms of a) homogenization temperatures and b) salinities of fluid inclusions in ore associated quartz samples from the Zletovo Mine.*

equivalent (Figure 4). According to eutectic temperatures, solutions were probably of Na–Cl± Cl composition.

Calculations all fluid inclusions data from ours latest study, made in FLINCORE and AqCl following instructions [22], yielded the following parameters (Table 2).

Several findings emerged during the data processing from this study. Densities ranged from 0.72 to 0.93 g/cm^3. Here, we would like to remind that at high pressures the supercritical fluid has a density similar to liquid water at the Earth's surface (1 g/cm^3), while at low pressures and high temperatures its density differs significantly from 1 g/cm^3. Low densities resulted in low solubility of ion materials, leading to relatively low mineralizing capacity of the ore-bearing solution [15]. Combining microthermometric data for the majority of fluid inclusions from the quartz (4.9–8.6 wt% NaCl equivalents, T_h = 198–334°C) with P-T stability field limits maximum formation temperature

at 334°C and total fluid pressure at 13.14 MPa. The data above (temperature of homogenisation, salinity, molar volume and density) gave us an opportunity to determine the pressures of formation of these particular parageneses (Figure 5, circles).

As it can be seen from the plot, the pressures ranged from 1.41 to 13.14 MPa. Based on this information, the palaeo-depths of mineralisation (during the capture of fluid inclusions [15]) ranged between 0.6 and 0.8 km [23], which is largely consistent with the depths around 1 km in data given by [2] and indicates that the deposit was generated at subvolcanic levels and under strong influence of lithostatic and explosive pressures. Additionally, the spatial coexistence of types I-1 and I-2 fluid inclusions within the same assemblage also suggest that both fluids may have been present during the precipitation of the ore-related quartz within the timeframe of the Pb–Zn mineralizing episode.

Studied fluid inclusions in quartz samples taken from the ore veins no. 2, 3 and 12, Zletovo mine, were also followed by analysis of the sulphur isotopic compositions in galenite and sphalerite, as basic ore minerals in the paragenesis in which the treated quartz is located. The results of the isotopic analyses of sulphur in the main sulphide minerals were used for calculation of geothermometer temperatures and comparison with the values obtained from fluid inclusions in quartz. After that those values were used to obtain the pressures at which these parageneses had been deposited. Temperatures calculated from sulphur stable isotopes for sulphide–sulfide mineral pairs from the Zletovo deposit, followed directions given in representative literature [24–28]. Namely, our recent stable sulphur isotope data ($d^{34}S$; see Table 2) in samples from the Zletovo deposit have shown strong value compatibility with some of the previous researchers [29, 12]. In regards to sulphur stable isotopes geothermometers, we would like to stress out that a number of experimental studies have been performed to determine the temperature (in degrees Kelvin) dependence of equilibrium fractionation factors of sulphur isotopes between coexisting galena and sphalerite [30]. Through the years several equations occurred in literature. Some of the most common examples were those given below:

Some of the earliest equations addressing sulphur stable isotopes thermometers [31], it was found that:

$$\Delta_{ZnS-PbS} = (0.63/T^2) \cdot 10^6. \quad (1)$$

Certain researchers [32] later have proposed the equation:

$$\Delta_{ZnS-PbS} = (0.80/T^2) \cdot 10^6. \quad (2)$$

While particular variation of the equation was suggested some other authors too [33]:

$$\Delta_{ZnS-PbS} = (0.70/T^2) \cdot 10^6. \quad (3)$$

Detailed study of equations above has shown good agreement between values calculated from Equation (3) and filling temperatures of fluid inclusions from several ore deposits [34].

One of the most preferred equations was the one given below [24]:

$$\Delta_{ZnS-PbS} = (0.73/T^2) \cdot 10^6. \quad (4)$$

Authors of this paper, based on numerous references, have decided to use Equation (4) to calculate temperatures (Table 3). We have used sphalerite–galena (in paragenesis with quartz from which originated measured fluid inclusions), as the most commonly used pair that in many cases yields temperatures consistent with those obtained from fluid inclusion data, which suggests that sphalerite and galena in numerous deposits are precipitated by similar mechanisms and under similar conditions [35] while eventual inconsistent temperatures obtained from this geothermometer in some studies elsewhere has been attributed to isotopic disequilibrium [36, 30].

The isotopic sphalerite–galena geothermometer yielded temperatures ranging from 154 to 309°C according to Equation (4) already mentioned above. Temperatures for the Zletovo deposit estimated with the sulphur isotope sphalerite–galena geothermometer are plotted versus fluid inclusion homogenisation temperatures in Figure 6.

Table 3: *Analytical data for coexisting sphalerite and galena crystallized during simultaneous mineralisation within the same ore vein, distribution, sulphur isotope fractionation and estimated mineralisation temperatures.*

No.	Sample No.		Mineral	No. of vein or horizon	$^{34}S/^{32}S$	$\delta^{34}S‰$	δ A - δ B	Pair	1000 lnα	T (Kelvin)	T (°C)
1	69 z	δ A	Sphalerite	vein 3,h-625	22.231110	0.5	−2.3	69z-70zA	-2.29621226	563.8394	290.6894
2	70zA	δ B	Galena	vein 3,h-625	22.282216	2.8					
3	12 z	δ A	Sphalerite	vein 2,h-510	22.224444	0.2	2.9	12zs-12zg	2.903631577	501.4073	228.2573
4	12z	δ B	Galena	vein 2,h-510	22.160006	−2.7					
5	M 71	δ A	Sphalerite	vein 12,h-490	22.155562	−2.9	−4	M71s-M71g	-4.003608591	427.0076	153.8576
6	M 71	δ B	Galena	vein 12,h-490	22.244442	1.1	−2.5	M71s-M76g	-2.504133126	539.9241	266.7741
7	M 76	δ B	Galena	vein 12,h-490	22.211112	−0.4					
8	M 39	δ A	Sphalerite	vein 3,h-700	22.225545	0.3	2	M39s-M39g	2.156966909	581.7544	308.6044
9	M 39	δ B	Galena	vein 3,h-700	22.177657	-1.7					

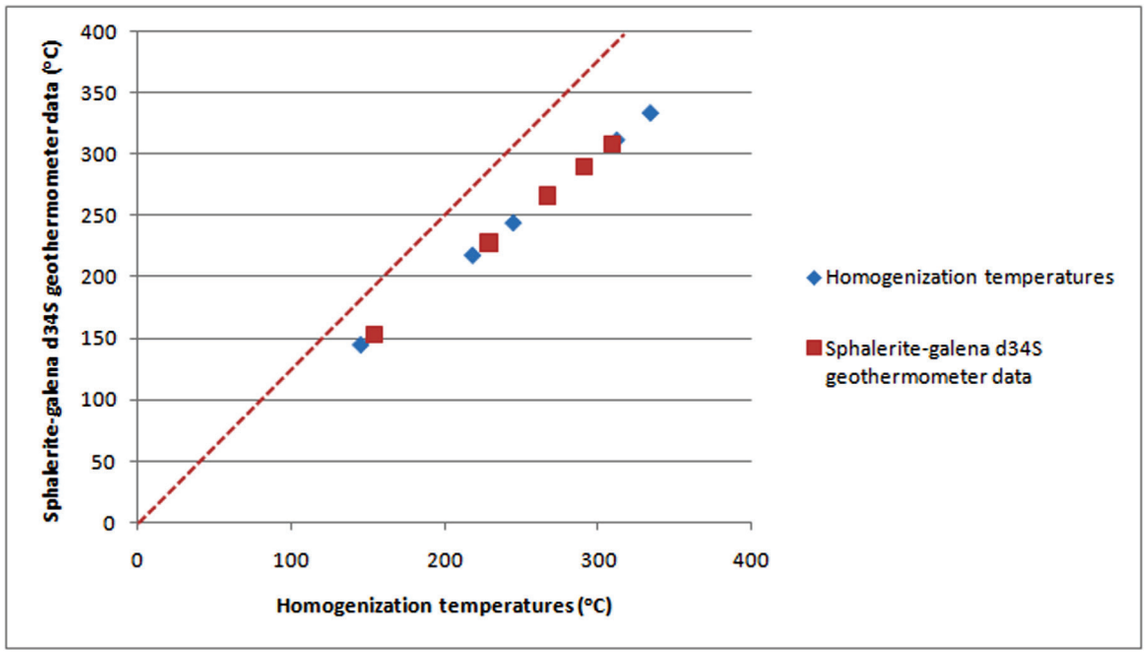

Figure 6: *Changes in density and gas pressure of the liquid water [24, 9].*

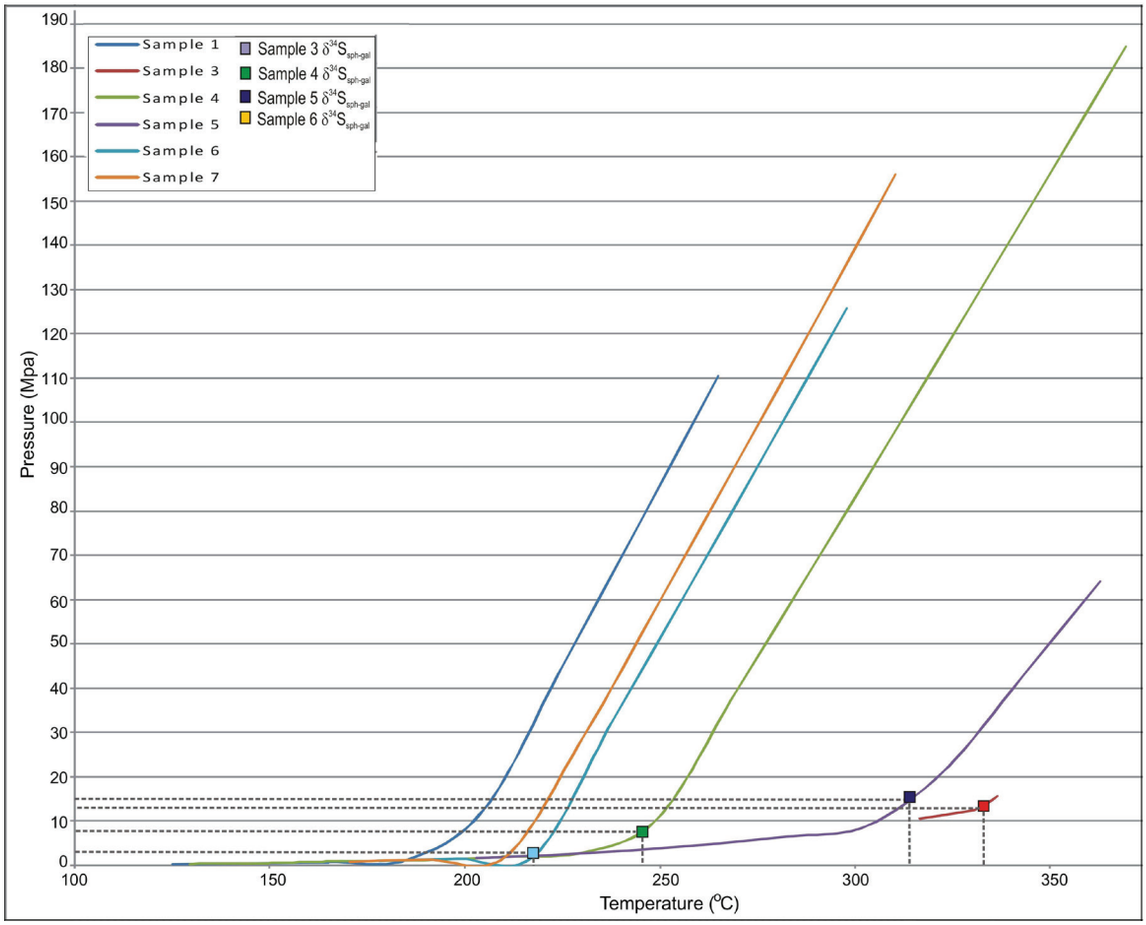

Figure 7: *Density changes of supercritical fluid as a function of pressure and temperature (basic plot data [25] and [9]).*

The majority of sulphur isotope mineral pair (sphalerite–galena) data yield isotopic temperatures (154–309°C ±6°C) in general agreement with fluid inclusions data. This suggests that isotopic equilibrium was established between the sphalerite and galena and was not affected by an eventual re-equilibration. Thus, the sphalerite–galena geothermometer, along with fluid inclusion results, appears to give correct temperatures for ore formation. Here, we would like to stress out that Equation (4) yielded values are in good agreement with homogenisation temperatures (Figure 6).

Using solely the data from our research (fluid inclusions and sulphur stable isotopes), as well as their compilation in Excel, an isochore diagram was constructed (Figure 7).

From the plot above (Figure 7), we obtained confirmation of the data obtained from the similar diagram above (Figure 5). As it can be seen, these pressures only slightly or not at all differ from the pressures determined solely based on fluid inclusions data, which point out to an equilibrium of the system at the moment of paragenesis deposition.

Conclusions

The main ore parageneses in the Zletovo mine are galena–sphalerite ones, usually followed by quartz, pyrite and chalcopyrite, which determines the hydrothermal nature of this famous vein type of lead–zinc deposit. The selected quartz grains, where fluid inclusions have been identified and measured originates from the main ore parageneses with galena and sphalerite prevailing, followed by pyrite, chal-

copyrite, calcite, kaolinite and others. Homogenisation temperatures were within the range of 335–145°C and reflect phases of pulsation of hydrothermal solutions that have been classified into four separate and consecutive groups from the highest temperature down to the lowest. Also, it was confirmed that the hydrothermal ore-bearing solution was of NaCl-type with salinity ranging from 4.4 to 8.6 wt% NaCl equivalent. Density or fulfilment of fluid inclusions with liquid phase was within the range of 0.7–0.95 g/cm^3. Calculated pressures and paleo-depths of mineralisation were probably within the range of 1.41–313.14 MPa and 0.6–0.8 km, respectively. The latest data obtained with the study of fluid inclusions within the quartz from ore veins from the Zletovo mine are quite similar to some older data [6], with certain differences in the concentration of NaCl (10–25 wt% NaCl equivalent), which is probably due to analysis of fluid inclusions from cleophane varieties of sphalerite and barites in former studies. Calculation of the homogenisation temperature frequencies and salinities clearly points to the productive solutions from which the primary parageneses were deposited.

References

[1] Serafimovski, T. (1990): *Metallogeny of the Lece-Chalkidiki zone*. Ph.D. Thesis. Faculty of Mining and Geology-Stip: University "Sts. Cyril and Methodius"-Skopje; 390 p.

[2] Serafimovski, T., Janković, S., Čifliganec, V. (1995): Alpine Metallogeny and Plate Tectonics in the SW Flank of the Carpatho-Balkanides. *Geologica Macedonica,* 9(1), pp. 3–14.

[3] Serafimovski, T., Aleksandrov, M. (1995): Lead-zinc deposits and occurrences in the Republic of Macedonia. Faculty of Mining annd Geology-Stip, University "Sts. Cyril and Methodius"-Skopje, Special Issue No. 4, 387 p. [in Macedonian with extended English summary].

[4] Janković, S. (1997): The Carpatho-Balkanides and adjacent area: a sector of the Tethyan Eurasian metallogenetic belt. *Mineralium Deposita,* 32(5), pp. 426–433.

[5] Petković, M. (1982): *Regional and detailed metallogenetic explorations of the Zletovo ore fie*ld. Faculty of Mining and Geology-Belgrade, 78 p. [in Serbian].

[6] Blečić, N. (1983): *Sources of ore components in hydrothermal deposits (comparative analysis of genetic models on the example of the Zletovo mine deposit)*. Ph.D. Thesis: Faculty of Mining and Geology, Belgrade, 247 p. [in Serbian].

[7] Serafimovski, T. (1993): Structural-metallogenetic features of the Lece-Chalkidiki zone: Types of deposits and zonation*.* Faculty of Mining and Geology-Stip, Special issue No. 2, 235 p. [in Macedonian].

[8] Efremov, I. (1993): *Metalogenija na Kratovsko-Zletovskata vulkanska oblast.* Ph.D. Thesis. Rudarsko-geološki fakultet: Štip; 286 p.

[9] Serafimovski, T., Lazarov, P., Tasev, G. (2005): Sulfosalt mineral compositions from the № 10 vein, Zletovo lead-zinc deposit, Macedonia. Mineral Deposit Research: Meeting the Global Challenge, Ed.Jingwen Mao and Frank P. Bierlein. 8th SGA Biennial Meeting, Beijing, China, pp. 461–464.

[10] Serafimovski, T., Dolenec, T., Tasev, G. (2006): New data concerning the major ore minerals and sulphosalts from the Pb-Zn Zletovo Mine, Macedonia. *RMZ-materials and geoenvironment*, 52(3), pp. 535–548.

[11] Tasev, G. (2003): *Polymetallic mineralizations related to the Tertiarymagmatism in the Republic of Macedonia.* Master thesis. Stip: Faculty of Mining and Geology; 176 p.

[12] Mudrinić, C., Serafimovski, T. (1990–91): Geochemical and geochronological examinations by isotopes in Zletovo ore field. *Geologica Macedonica*, 5(1), pp. 105–120.

[13] Serafimovski, T., Tasev, G. (2003): The Zletovo Subvolcanic Hydrothermal Pb-Zn Mineral Deposit in the Republic of Macedonia. Geodynamicsand Ore Deposit Evolution of the Alpine-Balkan-Carpathian-Dinaride Province. *Final GEODE-ABCD Workshop. Programme and Abstracts.* Seggauberg, Austria, 22–24 March, 2003, pp. 50–51.

[14] Goldstein, R.H., Reynolds, T.J. (1994): *Systematics of fluid inclusions in diagenetic minerals*, SEPM Short Course 31. Society for Sedimentary Geology, 199 p.

[15] oedder, E. (1984): *Fluid inclusions.* Reviews in mineralogy, 12, Mineralogical Society of America, 644 p.

[16] Bodnar, R.J. (1993): Revised equation and table for determining the freezing point depression of H_2O-NaCl solutions. *Geochimica et Cosmochimica Acta*, 57, pp. 683–684.

[17] Sterner, S.M., Hall, D.L., Bodnar, R.J. (1988): Synthetic fluid inclusions. V. Solubility relations in the system NaCl-KCl-H_2O under vapor saturated conditions. *Geochimica et Cosmochimica Acta,* 52, pp. 989–1005.

[18] Vanko, D.A., Bodnar, R.J., Sterner, S.M. (1988): Synthetic fluid inclusions. VIII. Vapor-saturated halite solubility in part of the system NaCl-$CaCl_2$-H_2O, with application to fluid inclusions from oceanic hydrothermal systems. *Geochimica et Cosmochimica Acta,* 52, pp. 2451–2456.

[19] Thiery, R., Kerkhof, A.M., Dubessy, J. (1994): VX properties of CH_4–CO_2 and CO_2–N_2 fluid inclusions: modeling for T <31ºC and P <400 bars. *European Journal of Mineralogy,* 6, pp. 753–771.

[20] Tasev, G., Serafimovski, T. (2012): Fluid inclusions study in the quartz from the Zletovo Mine. Macedonian Geological Society, Second Congress of Geologists of the Republic of Macedonia, Proceedings book (eds. Jovanovski, M., Boev, B.), *Special Issue of Geologica Macedonica*, 3, pp. 83–90.

[21] Li, Y.J., Wei, J.H., Chen, H.Y., Tan, J., Fu, L.B., Wu, G. (2011): Origin of the Maoduan Pb–Zn–Mo deposit, eastern Cathaysia Block, China: geological, geochronological, geochemical, and Sr–Nd–Pb–S isotopic constraints. *Mineralium Deposita*, 47(7).

[22] Bakker, R.J. (2003): Package FLUIDS 1. Computer programs for analysis of fluid inclusion data and for modelling bulk fluid properties. *Chemical Geology*, 194, pp. 3–23.

[23] Prokof'ev, V.Y., Pek, A.A. (2015): Problems in Estimation of the Formation Depth of Hydrothermal Deposits by Data on Pressure of Mineralizing Fluids. *Geology of Ore Deposits*, 2015, 57(1), pp. 1–20.

[24] Ohmoto, H., Rye, R.O. (1979): *Isotopes of sulphur and carbon*. In: Geochemistry of Hydrothermal Ore Deposits, 2nd edn., Barnes, H.L. (ed.). John Wiley and Sons: New York; pp. 509–567.

[25] Ohmoto, H. (1986): Stable istope geochemistry of ore deposits. In: Stable istope in high temperature geological processes, Valley, J.W., Taylor, H.P. Ir., O'Neil, J.R (eds.). *Reviews in Mineralogy and Geochemistry*, 16, pp. 491–559.

[26] Rye, R., Hall, W., Ohmoto, H. (1974): Carbon, Hydrogen, Oxygen and Sulphur isotope Study of the Lead-Silver-Zinc Deposit, Southern California. *Economic Geology*, 69, pp. 468–481.

[27] Shelton, K.L., Rye, D.M. (1982): Sulfur isotopic compositions of ores from Mines Gaspe´, Quebec: an example of sulfate-sulfide isotopic disequilibra in ore-forming fluids with applications to other porphyry-type deposits. *Economic Geology*, 77, pp. 1688–1709.

[28] Brownlow, H.A. (1996): *Geochemistry*. 2nd Edition. U.S.A: Prentice Hall, Inc., 580 p.

[29] Drovenik, M., Leskovsek, H., Pezdic, I., Strucl, I., (1970). Isotopic composition of sulfur in sulfides from some Yugoslavian deposits (Izotopska sestava zvepla v sufidih nekaterih jugoslovenskih rudisc). Materials and Geoenvironment (former Mining and Metallurgy Quaterly), 17: 153–173 [in Slovenian].

[30] Bortnikov, N.S., Dobrovol'skaya, M.G., Genkin, A.D., Naumov, V.B., Shapenko, V.V. (1995): Sphalerite-Galena Geothermometers: Distribution of Cadmium, Manganese and the Fractionation of Sulfur Isotopes. *Economic Geology*, 90, pp. 155–180.

[31] Grootenboer, J., Schwarcz, H.P. (1969): Experimentally determined sulfur isotope fractionations between sulfide minerals. *Earth and Planetary Science Letters,* 7, pp. 162–166.

[32] Kajiwara, J., Krouse, H.R. (1971): Sulfur isotopic partitioning in metallic sulfides systems. Canadian Journal of Earth Sciences, 8, pp. 1397–1422.

[33] Czamanske, G.K., Rye, R.O. (1974): Experimentally determined sulfur isotope fractionations between sphalerite and galena in the temperature range 650ºC to 275ºC. *Economic Geology*, 69, pp. 17–25.

[34] Rye, R.O. (1974): A comparison of sphalerite-galena sulfur isotope temperatures with filling temperatures of fluid inclusions. *Economic Geology*, 69, pp. 26–32.

[35] Misra, C.K. (2000): Understanding Mineral Deposits. Kluwer Academic Publishers, Dodrecht, Netherland, 845 p.

[36] Yamamoto, M., Endo, M., Ujihira, K. (1984): Distribution of selenium between galena and sphalerite. *Chemical Geology*, 42, pp. 243–248.

Original scientific paper

Received: Sep 07, 2018
Accepted: Nov 13, 2019
DOI: 10.2478/rmzmag-2019-0016

Sustainability and Conceptual Groundwater Hydraulic Models of Basement Aquifers

Trajnost in konceptualni hidravlični modeli podzemne vode v vodonosnikih podlage

Olanrewaju Akinfemiwa Akanbi[1,*], Moshood 'Niyi Tijani[2]

[1] Department of Earth Sciences, Ajayi Crowther University Oyo, Oyo Town, Nigeria

[2] Department of Geology, University of Ibadan, Ibadan, Nigeria

* oa.akanbi@acu.edu.ng

Abstract

Groundwater flow of the basement terrains of the Ibarapa region was studied by carrying out pumping test and measurement of borehole inventory. The view was to identify the associated aquifer systems from the time-drawdown curves, quantify the estimable hydraulic properties and develop hypothetical models for the understanding of the groundwater flow in the area underlain by diverse crystalline bedrocks. Three aquifer types were identified namely, dual, leaky and regolith. The yield of groundwater in dual and leaky aquifers that dominated terrains underlain by amphibolite and gneisses was sustainable, but the discharge of regolith aquifers mainly associated with migmatite and granite terrains declined at late pumping stage. The transmissivities of the dual and leaky aquifers were between 2.02 and 11.65 m^2/day, while those of regolith aquifers were mostly less than 1.00 m^2/day. The average aquifer transmissivities in m^2/day by bedrocks were: 6.85, 2.57, 0.76 and 1.72, correspondingly. The inter-relationships between transmissivities and groundwater discharge showed diverse aquifer representations, from sustainable high-yielding to unsustainable low-yielding types. Conscientious effort is, therefore, required for well construction in the area.

Key words: groundwater, well-inventory, time-drawdown, aquifer-types, yield

Povzetek

Tok podzemne vode na območju Ibarapa je bil proučevan s pomočjo črpalnih preizkusov in popisov vrtin. Namen članka je indentificirati povezane sisteme vodonosnikov iz krivulj časovnega znižanja gladine podzemne vode, oceniti hidravlične lastnosti in razviti hipotetične modele za razumevanje toka podzemne vode na območju z raznoliko kristalinično kamninsko podlago. Identificirani so bili trije tipi vodonosnikov: dvojni, polzaprti in regolitni vodonosnik. Izdatnost podzemne vode v dvojnem in polzaprtem vodonosniku, ki prevladujejo in imajo za podlago amfibolit ter gnajs, je bila trajna. Izdatnost regolitnega vodonosnika, ki ima za podlago migmatit in granit, je v pozni fazi črpanja upadla. Transmisivnost dvojnih in polzaprtih vodonosnikov je bila med 2.02 in 11.65 m^2/dan, medtem ko je bila transmisivnost regolitnih vodonosnikov večinoma manj kot 1.00 m^2/dan. Povprečne transmisivnosti vodonosnikov v m^2/dan glede na omenjene kamninske podlage so bile 6.85, 2.57, 0.76 in 1.72. Povezava med transmisivnostjo in izdatnostjo kaže na raznolika stanja vodonosnikov, od trajnega visoko izdatnega do ne-trajnega nizko izdatnega tipa. Ugotovitve je potrebno upoštevati pri izdelavi vrtin na tem območju.

Ključne besede: podzemna voda, popis vrtin, časovno znižanje gladine podzemne vode, tipi vodonosnikov, izdatnost

Introduction

In the Sub-Sahara tropical climatic region of Africa, basement aquifers are of particular importance due to the extensive availability of weathered overburden and/or the occasional occurrences of bedrock fracturing [1, 2]. Besides, as there is no alternative source of water supply for the increasing population and the developing economies, groundwater has become the major reliable water resource for both domestic and industrial usages [3, 4]. However, the yield of basement aquifers is known to be generally poor and erratic as a result of the discrepancy in the structural and textural systems [4, 5] associated with the crystalline basement of igneous and/or metamorphic rocks.

In respect of this, the Nigerian hydrogeological setting is complex because approximately half of the landmass is underlain by diverse intrusive crystalline rocks [6, 7] including the Ibarapa region, which is within the southwestern (SW) Nigeria basement complex. The study lies inside coordinates- 7° 21' N–7° 37' N and 3° 07' E–3° 21' E (Figure 1) and has human population that is well above 200,000 [8]. At the moment, towns and adjoining communities have no functioning town water supply [3, 4], and the residents of the Ibarapa region rely on groundwater for domestic water needs and even for agricultural purposes. The groundwater is supplied from hundreds of hand pump boreholes that tapped into the weathered-regolith and underlying bedrocks, which include granite, gneisses, amphibolite and migmatite [4] (Figure 2). These boreholes were largely funded by the government and other foreign agencies under the water supply and sanitation scheme for rural communities' development (formerly WATSAN) [3]. However, even with these provisions, the availability of potable water is still inadequate as a result of unsustainable yield and improper management. Recently in the study area, there is a dire need to expand the groundwater supply due to the increasing population, the unavailability of town water supply and the poor yield of most of the drilled wells. Hence, it is now mandatory to characterise the sustainable yield of the aquifer systems across the various bedrocks terrains within the Ibarapa region of SW Nigeria to ensure the effective management and sustainable groundwater resources.

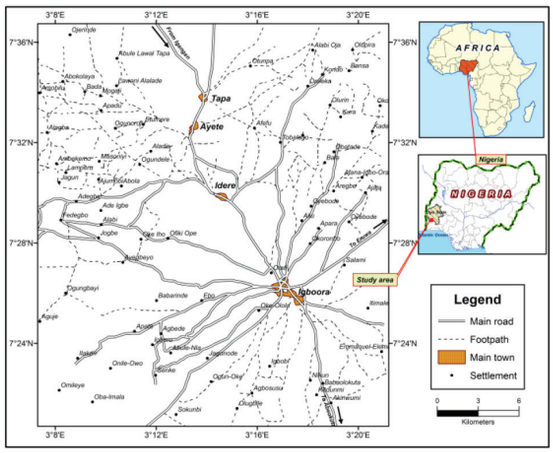

Figure 1: *Location map of the study area.*

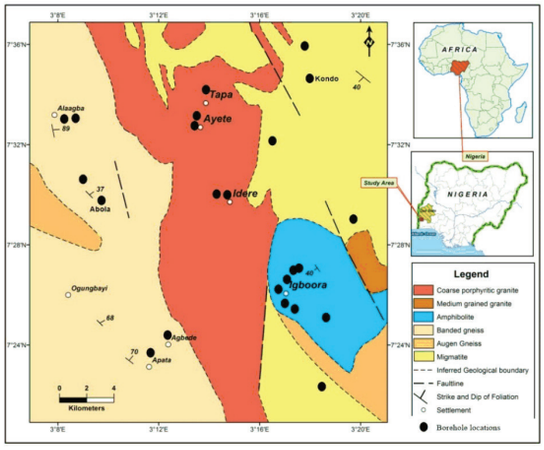

Figure 2: *Geological map of the study area with wells' points.*

For the appropriate analyses of the aquifer system, pumping tests provide enough information in evaluating the safe yield of an aquifer and estimating aquifer properties like transmissivity[9]. However, despite the importance of hydraulic characterisation, documented or published reports of aquifer characterisation using pumping tests are scarce in developing nations like Nigeria due to cost factor and lack of technical expertise in analysing pumping and recovery tests data. Because the essential aquifer properties, like transmissivity, can be reliably estimated from single-well test and that there is no need for observation wells [10], make it appropriate for the present study, this method is less cumbersome and relatively

less expensive to conduct as compared to others. Moreover, single-well pumping tests can provide hydraulic conditions of a local aquifer system. It is, therefore, suitable for characterising the basement aquifers of the Ibarapa region where the hydrogeology is expected to be complex as a result of lithological and structural complications [11, 12], even within the same bedrock terrain.

Materials and Methods

The hydraulic characterisation of the crystalline aquifers of the Ibarapa regions was carried out by conducting single-well pumping tests on 23 wells across the various bedrocks terrains within the study areas. Seven wells were tested on terrains underlain by amphibolite, six on gneisses, and five each in areas underlain by both migmatite and porphyritic granite (Figure 2).

Before the pumping tests were conducted, well inventory, including coordinates, pre-pumping level and the elevation and depth of the well were taken. The measurable and estimable hydraulic properties from single-well pumping included the water table, discharge, change in drawdown per log cycle of time, total drawdown for the entire pumping time and transmissivity. The discharge (Q), which is the groundwater yield, was measured at every time interval in cubic metre per day to an accuracy of 0.0001 m^3 (or 0.1 l). The static water level and the depths of individual wells were measured using the automatic water level and a well-depth indicator. In most cases, the drawdowns were measured every 30 s for the first 5 min. The time intervals were then increased as pumping continues. The wells were pumped continuously till steady-state conditions were reached. When discharge is no longer sustainable with the same constant discharge, the yield can no longer support the rate of discharge and the aquifer is unsustainable.

The total drawdown is the difference between the final drawdown in the well after pump cessation and the pre-pumping water level, while the drawdown per log cycle (Δs) is the drawdown for one log cycle of pumping time. The unit of measurement of transmissivity is m^2/day. The coordinates of wells were taken using Garmin Etrex GPS, and all field measurements were carried out using the following standard procedures [10].

Data Processing

For single-well test where no piezometer is used, only the time-drawdown curve is applicable. The semi-log plot is reputable to be more diagnostic of the aquifer characteristics than the log-log scale plots [10, 4]. The drawdowns are plotted on a vertical linear scale and time on the log scale on the horizontal axis. From the semi-log plots, the flow regimes and aquifer boundary can be identified and analysed using the appropriate equations. Typical aquifer boundary conditions have been defined from the time-drawdown curves by various workers [10, 9, 13].

For the present work, Jacob's straight-line method is applicable for the analysis of the time-drawdown data from the single-well pumping test. This method does not require the correction for non-linear well losses and can be used to analyse the time-drawdown data obtained from the single-well test for both confined and leaky aquifers [10]. From the straight-line plot obtained from the semi-log graph of drawdowns against time, the transmissivities, T of the aquifers, were estimated using the following equation:

$$T = 2.3Q/4\pi\Delta s \text{ [14]} \quad (1)$$

where Q = pumping rate and Δs = drawdown across one log cycle. From this approach of study, theoretical hydraulic models of the basement aquifers of the study area were then developed from the cross-plots of aquifers' transmissivities and yields. The statistical evaluation and cross-plots were also constructed to establish the type and degree of inter-relationships existing between well inventory and estimated hydraulic parameters.

Results and discussion

Aquifer Systems

From the response of the aquifer to pumping on the time-drawdown diagnostic curves as

Table 1: *Well inventory and hydraulic parameters by aquifer systems.*

s/n	Well location	Well Elevation (m)	Well Depth (m)	Water Table (m)	Q (m^3/d)	Δs1 (m)	Δs2 (m)	DD (m)	T_1 (m^2/d)	T_2 (m^2/d)	$T_t = T_1 + T_2$ (m^2/d)	Bedrock
Dual aquifers												
1	Ajegunle	159	18.90	1.46	93.58	3.80	2.40	8.50	4.51	7.14	11.65	Amphibolite
2	Agbede	143	34.60	6.42	78.92	7.00	2.00	10.03	2.07	7.23	9.30	Gneiss
3	Pako	187	31.60	6.40	73.24	2.00	3.70	7.90	6.71	3.63	10.34	Amphibolite
4	Igboole I	170	38.00	4.95	71.73	4.00	1.60	5.20	3.29	8.23	11.52	Amphibolite
5	Ayete I	141	28.00	2.00	56.81	4.00	8.50	19.70	2.00	0.95	2.95	Por. granite
Leaky aquifers												
1	Abola	171	34.1	14.48	32.78	11.00	2.82	14.82	0.55	2.13	2.68	Gneiss
2	Apata	139	38.00	9.40	37.87	14.50	4.5	22.38	0.48	1.54	2.02	Gneiss
3	Igboole II	175	30.40	3.23	67.92	11.20	1.19	13.51	1.11	10.45	11.56	Amphibolite
Regolith aquifers												
s/n	Well Location	Well Elevation (m)	Well Depth (m)	Water Table (m)	Q (m^3/d)	Δs (m)		DD (m)	T (m^2/d)			Bedrock
1	Onilado	176	22.90	6.10	43.56	13.75		12.96	0.58			Amphibolite
2	Sagaun	162	22.80	3.30	98.12	14.00		15.36	1.28			Amphibolite
3	Itaagbe	172	27.70	10.70	55.97	10.60		11.49	1.03			Amphibolite
4	Alaagba I	174	43.0	4.15	40.43	29.50		31.90	0.25			Gneiss
5	Alaagba II	164	99.5	2.90	54.79	19.40		33.50	0.52			Gneiss
6	Lamperu	169	30.9	6.68	75.91	21.50		19.32	0.65			Gneiss
7	Alabi-Oja	188	26.36	3.34	41.91	13.80		18.63	0.56			Migmatite
8	Sekere	142	29.10	7.05	77.04	16.00		18.70	0.88			Migmatite
9	Faju	182	29.72	4.20	99.79	25.00		21.23	0.73			Migmatite
10	Tobalogbo	188	17.80	3.50	69.48	14.00		11.49	0.91			Migmatite
11	Kondo	199	35.60	11.83	53.15	13.40		18.40	0.71			Migmatite
12	Ayete II	140	27.85	3.65	45.62	15.00		19.91	0.56			Por. Granite
13	Tapa	155	36.50	2.05	57.70	11.00		22.04	0.96			Por. Granite
14	Idere I	215	20.30	5.32	91.10	5.65		9.27	2.94			Por. Granite
15	Idere II	209	15.86	6.48	70.42	10.80		7.00	1.19			Por. Granite

presented in Figures 3 (A) to (C), three aquifer categories were identified, namely, the double porosity (dual), leaky and unconsolidated/ regolith aquifers. The measured and estimated well inventory and hydraulic properties of the aquifer systems that included discharge (Q), drawdown per log cycle (Δs), total drawdown (DD) and transmissivity (T) are presented in Table 1.

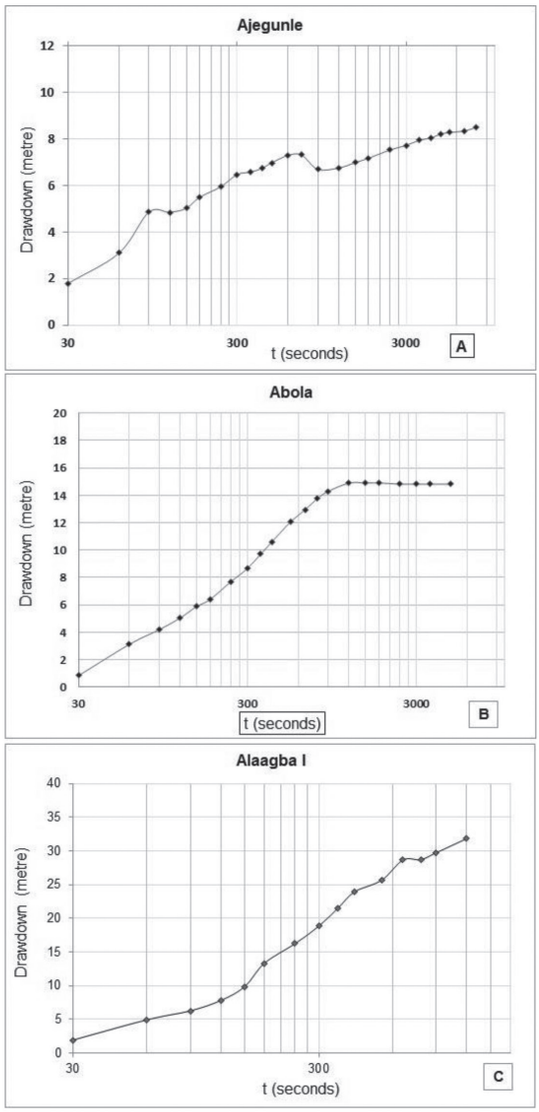

Figure 3: *Typical time-drawdown semi-log plots obtained for: (A) dual aquifers, (B) leaky aquifers and (C) regolith aquifer systems.*

Dual Aquifers

Aquifer systems with this type of time-drawdown curves (Figure 3A) are consolidated fractured aquifers of double porosity type [10, 4], denoted as dual aquifers in this study, because they are characterised by two distinct flow regimes separated by a transition period (Figure 3A). Each flow regime represents a water-bearing zone that is clearly distinguishable from the other one. The early pumping time signifies water contribution solely from the fractured system. This is succeeded by a transition zone and significant water contribution from the overlying weathered layer at the later pumping time. For dual aquifers, the transmissivity of each flow regime is independently analysed within the domain of its drawdown intervals. The total transmissivity, T_t, is the sum of the transmissivities of the upper and the lower aquifers [15] denoted by T_1 and T_2 respectively as given in Table 1. Dual aquifer systems are generally characterised by good groundwater yield that is sustainable for the entire pumping period and relatively larger transmissivity (Table 1). Generally, in most of the dual aquifer systems, the transmissivities of the second flow regime are larger because the overlying matrix units also contributed water just as the fractured bedrocks. The occurrence of dual aquifer systems revealed that multi-layer water-bearing zones can develop in basement terrains.

Leaky Aquifers

Leaky aquifers are characterised by prolific highly permeable densely fractured bedrock underlying the weathered/regolith units. As typical of leaky aquifers, the diagnostic semi-log plots for these aquifers were notably characterised by the development of dynamic-equilibrium at late time (Figure 3B). The equilibrium state is characterised by flattened drawdown at the late pumping stage regardless of the length of pumping. These wells were found at Abola, Apata and Igboole II. This type of aquifer system is somehow referred to as semi-confined aquifers whereby the overlying regolith is an aquitard and also permeable, though not as prolific as the fractured bedrock under it.

Regolith Aquifers

Regolith aquifers are the water-bearing weathered layers that developed upon the impermeable or slightly fractured bedrock units. The in-situ regolith units (or the weathered

Table 2: *Statistical summary of well inventory and hydraulic parameters by aquifer systems.*

Aquifer systems	n	Statistics	Well Elevation (m)	Well Depth (m)	Water Table (m)	Discharge Q (m^3/d)	Total drawdown (m)	Transmissivity T (m^2/d)
Dual	5	Min	141	18.90	1.46	56.81	5.20	2.95
		Max	187	38.00	6.42	93.58	19.70	11.65
		Mean	160	30.22	4.25	74.86	10.27	9.15
		Std.Dev.	19	7.33	2.38	13.28	5.56	3.60
Leaky	3	Min	139	30.40	3.23	32.78	13.51	2.02
		Max	175	38.00	14.48	67.92	22.38	11.56
		Mean	162	34.17	9.04	46.19	16.90	5.42
		Std.Dev.	20	3.80	5.63	18.99	4.79	5.33
Regolith	15	Min	140	15.86	2.05	40.43	7.00	0.25
		Max	215	99.50	11.83	99.79	33.50	2.94
		Mean	176	32.39	5.42	65.00	18.08	0.92
		Std.Dev.	22	19.92	2.82	20.10	7.47	0.62

layers) that developed upon the intrusive bedrock in the tropical climatic Sub-Sahara region of Africa are somewhat porous and permeable [1, 3, 4, 5, 12]. From the time-drawdown curves (Figure 3C), wells in this category were dominated initially by water from well storage, and afterward by flows from the matrix component (or weathered layer). The water input from the regolith units was, however, not substantial enough to guarantee the constant discharge for the entire pumping period. Therefore, the discharge dropped at the later stage of pumping. This is noticeable by the sharp decline in drawdown (Δs) as water table drops (Figure 3C).

The yield of regolith aquifers was between 40.43 and 99.79 (av. of 65.00) m^3/day, and the drawdowns in the wells were typically large ranging from 7 m to over 33 m at an average of 18.08 m (Table 2). The transmissivities of most of the regolith aquifers were typically below 1.50 m^2/day with an average of 0.92 m^2/day (Table 2). In regard to the transmissivity and the abrupt decline of water level during pumping, the regolith aquifer system is not regarded as being sustainable. Regolith aquifers are the most widespread, found in all terrains; however, they are more common in migmatite and granite terrains.

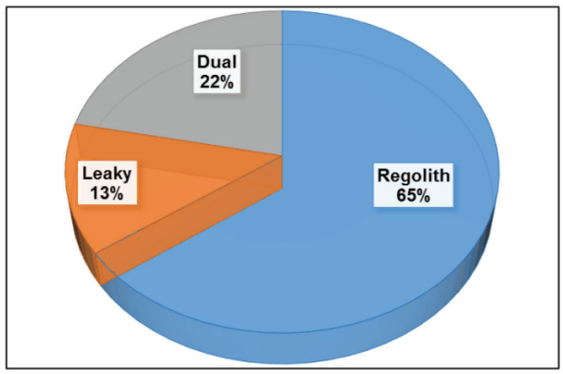

Figure 4: *Percentage frequency of aquifers occurrences.*

The frequency of the occurrence of regolith aquifer system was 15, which was about 65% of the total number of tested wells. The frequency of the dual aquifer system was 5 representing 22% of occurrences, while that of leaky aquifers was just 3, which is just about 13% of occurrences (Figure 4). The fact that the occurrence of regolith aquifers is higher due to the shortage of water supply in the study area.

Bedrocks and Associated Aquifer Systems

The general statistics of the well inventory data and hydraulic properties by bedrocks is pre-

Table 3: *Statistics of well inventory and hydraulic parameters by bedrocks.*

Bedrock	n	Statistics	Well Elevation (m)	Well Depth (m)	Water Table (m)	Q (m^3/day)	Draw-down (m)	T (m^2/day)
Amphibolite	7	Min.	159.00	18.90	1.46	43.56	5.20	0.58
		Max.	187.00	38.00	10.70	98.12	15.36	11.65
		Mean	171.57	27.47	5.16	72.02	10.70	6.85
		Std dev.	9.32	6.49	3.00	19.29	3.61	5.53
Gneisses	6	Min.	139.00	30.90	2.90	32.78	10.03	0.25
		Max.	174.00	99.50	14.48	78.92	33.50	9.30
		Mean	160.00	46.68	7.34	53.45	21.99	2.57
		Std dev.	15.13	26.20	4.16	19.97	9.30	3.43
Migmatite	5	Min.	142.00	17.80	3.34	41.91	11.49	0.56
		Max.	199.00	35.60	11.83	99.79	21.23	0.91
		Mean	179.80	27.72	5.98	68.27	17.69	0.76
		Std dev.	22.00	6.49	3.59	22.33	3.65	0.14
Porphyritic Granite	5	Min.	140.00	15.86	2.00	45.62	7.00	0.56
		Max.	215.00	36.50	6.48	91.10	22.04	2.95
		Mean	172.00	25.70	3.90	64.33	15.58	1.72
		Std dev.	37.05	7.95	1.99	17.35	6.91	1.14

sented in Table 3. It is clearly seen that based on the average values as illustrated in Figure 5, groundwater discharge of amphibolite, migmatite and porphyritic granite terrains exceeded 60 m^3/day, while gneissic aquifers have the lowest average yield of nearly 54 m^3/day (Table 3, Figure 5A). Consequently, the total drawdown in gneisses is the largest, and the average value is greater than 20 m while it is below 18 m for other bedrocks (Table 3, Figure 5B). This does not necessarily mean that wells in gneisses are less productive because wells in gneisses are deeper (Table 3) as a result of pronounced weathering [14]. The transmissivities of aquifers in amphibolite are relatively larger with a range of 0.58–11.65 m^2/day and an average of 6.85 m^2/day, as compared to those in other terrains having a range of 0.25–9.30 m^2/day, (Table 1, Figure 5C). Amphibolite aquifers have the highest potential for the provision of prolific wells within the study area. The transmissivities of four of the aquifers is greater than 10 m^2/day. Six wells were tested in areas underlain by gneisses. The two wells located at Alaagba and the one tested at Lamperu are regolith and terminate on fresh gneissic bedrocks [12]. The transmissivities ranged from 0.25 to 0.65 m^2/day (Table 3). Wells at Abola, Apata and Agbede were characterised by water-bearing matrix and bedrock. However, the aquifer at Agbede is the most prolific aquifer within the gneissic terrain with transmissivity of 9.03 m^2/day (Table 1). Generally, the mean transmissivity of wells in gneissic terrains is 2.57 m^2/day. This value is comparatively lower than the average value of 6.85 m^2/day estimated for amphibolite aquifers (Table 3). The dynamic equilibrium water level was obtained at Agbede, Abola and Apata at corresponding depths of 10.03 m, 14.82 m and 22.38 m. The dynamic equilibrium water level of aquifers in gneisses is deeper than those in amphibolite. The depth of dynamic equilibrium is less than 9 m except at Igboole II for aquifers in amphibolite. Water-bearing zones tested on migmatite terrain are similar, and all the five wells penetrated regolith aquifers (Figure 6). The migmatite aquifers are characterised by fairly large

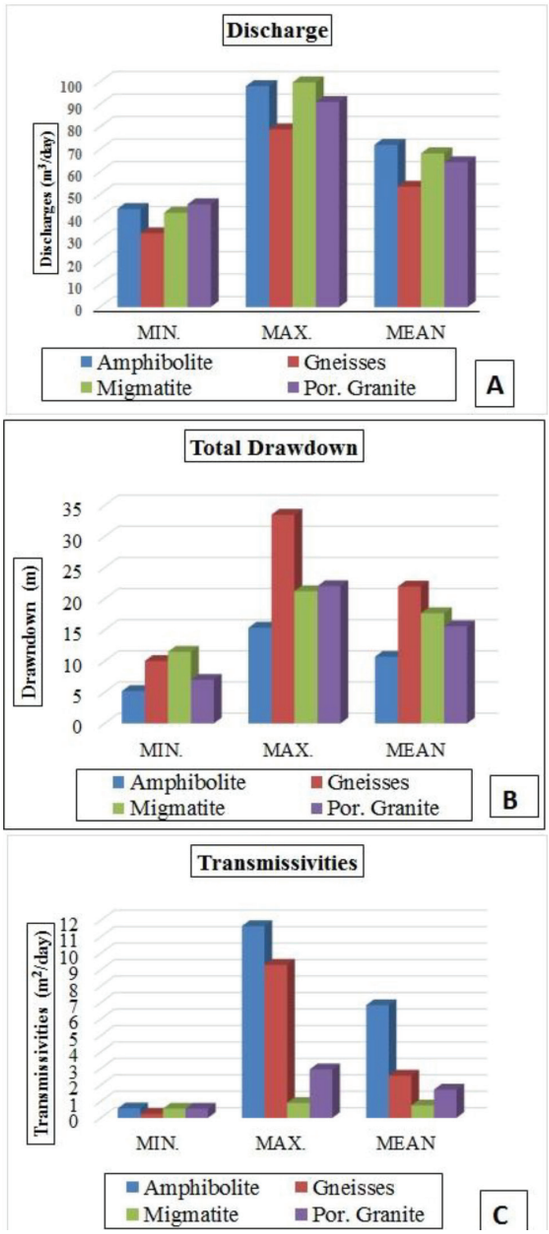

Figure 5: *Statistical illustrations of aquifer parameters.*

discharge and drawdowns with the average values of 68.27 m^3/day and 17.69 m (Table 3), respectively. Comparatively, the water-bearing zones in the migmatite terrain have the lowest transmissivity between 0.56 and 0.91 m^2/day and the mean value of 0.76 m^2/day (Table 3).

Granitic aquifers are still fairly better than those in migmatite but not as prolific as those in amphibolite and gneisses. The only sustainable well tested on the granitic terrain was Ayete I. The two wells tested at Idere are also

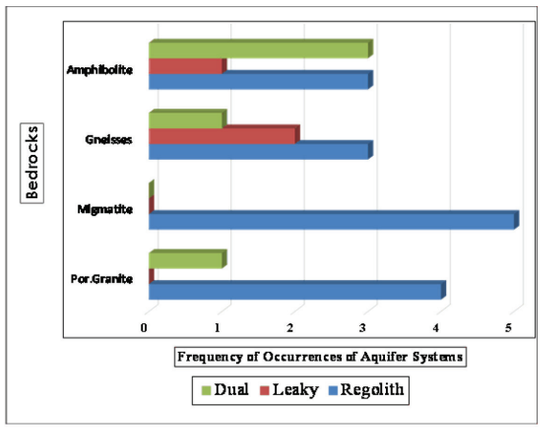

Figure 6: *Frequency of occurrences of aquifer systems in bedrocks.*

on the granitic terrain with transmissivities of 2.94 and 1.19 m^2/day, respectively; they are not sustainable over a large period of pumping as Ayete I. The rates of pumping rapidly decline during pumping at Idere.

In general, the widespread occurrence of the regolith aquifer is an indication of rarity and localised nature of dual and leaky aquifers in the study area (Figure 4). This is a result of the infrequency of bedrock fractures in the area as revealed by the previous work on lithological and structural mapping of the subsurface environment of the study area using a geophysical method [4, 12]. Dual aquifers with about 22% of occurrences are mostly associated with amphibolite terrains (Figure 6). A leaky aquifer is the least occurring aquifer system with just 13% found in both amphibolite and gneisses.

The dynamic water level developed in eight wells during the pumping phase. Four out of eight wells were on amphibolite terrains located at Ajegunle, Pako, Igboole I and II; three on gneissic terrains located at Apata, Abola and Agbede, and the last one on porphyritic granite bedrock terrains located at Ayete I. From the frequency of aquifer systems by bedrock (Figure 6), the dual and leaky aquifers are mostly associated with amphibolite and gneisses terrains. These aquifer systems supplied water at constant discharge and are characterised by low to minimal drawdowns during the entire pumping period. Aside from the nature of aquifer systems, another reason for the occurrence of more successful wells in amphibolite and gneisses was the hydro-geomorphic situations,

whereby the high-lying terrains mainly underlain by migmatite and granite are the recharge areas, whereas the low-lying terrains that are mostly underlain by amphibolite and gneisses are the discharge areas [4, 16].

Influence of Well Inventory on Transmissivity in Various Bedrocks

The plots of the transmissivities against well inventory along with the results of correlation coefficients (R) between transmissivities against well inventory are presented in Figure 7. The relationship between the aquifer transmissivities and well elevation is positive in amphibolite and granite but negative in migmatite and gneisses. The significance of this association is high only in gneisses, moderate in migmatite, low in granite and insignificant in amphibolite (Figure 7A). This shows that the relief of the well has little or no relevance to the aquifer transmissivities in amphibolite, whereas it does in other bedrocks, particularly in gneisses where $R = -0.62$. It is also deduced that the topography of a well does not have a significant effect on the drawdown and groundwater yield in amphibolite terrain (with $R = 0.08$). This is because the transmissivity of the aquifer is a function of the groundwater yield and drawdown during pumping. However, in migmatite, these hydraulic properties are moderately influenced by well relief with $R = -048$. This relationship is weak in porphyritic granite with $R = 0.27$ (Figure 7A). Moreover, the strong and moderate indirect relationships correspondingly obtained for gneisses and migmatite indicate that wells situated at low-lying areas will be characterised by fairly large transmissivity within these terrains. However, the wells on high-lying areas will be more likely to be prolific in the granitic terrain where the relationship is positive. This is corroborated by the wells at Idere on higher relief > 200 m (Table 1) underlain by granite. The two tested wells were characterised by large discharge and higher transmissivity of 2.95 and 1.19 m^2/day as compared to other wells on the granitic terrain.

The relationship between aquifer transmissivities and well depths is illustrated in Figure 7B. The relationship is direct and moderate in amphibolite terrain while it is indirect for other bedrock terrains. The indirect relationship is low for gneisses and porphyritic granite ($R = -0.33$ and -0.26, respectively). This implies that deep wells will not improve hydrau-

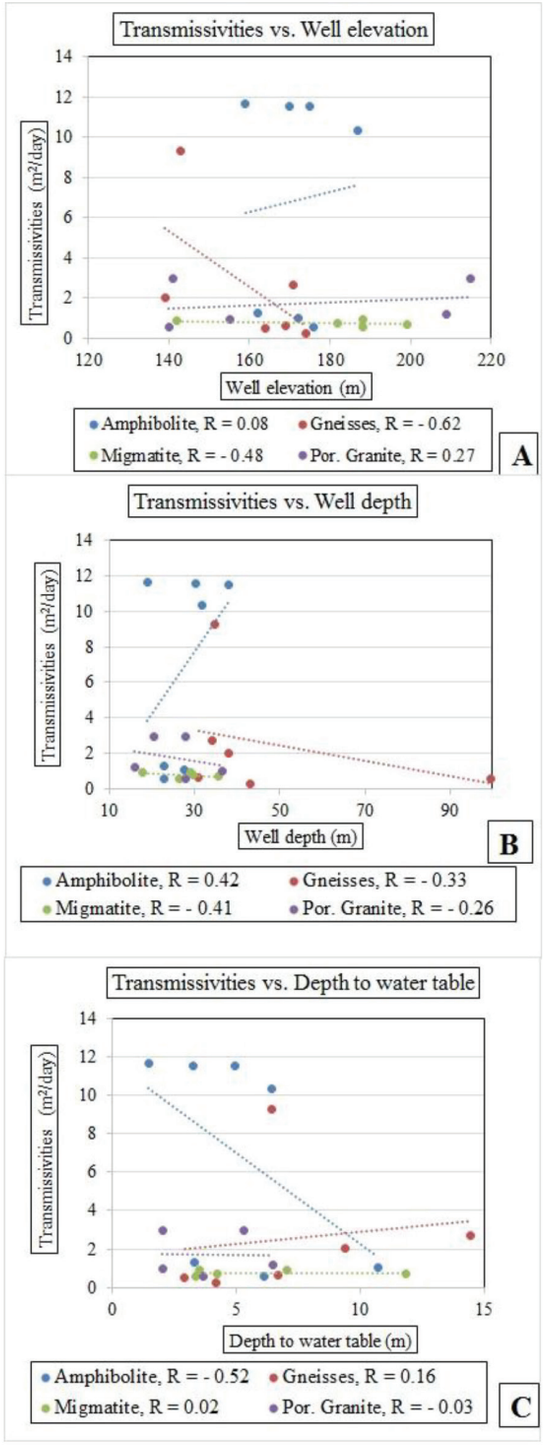

Figure 7: *Cross-plots and R coefficients of (A) transmissivity against wells' elevations, (B) transmissivity versus wells' depths and (C) transmissivity against water table by bedrocks.*

lic properties in gneisses and in granite, and to a larger extent in migmatite bedrocks where $R = -0.41$. However, the positive moderate relationship in amphibolite with $R = 0.42$ indicates that deep wells are expected to be more prolific in amphibolite. This is supported by the fact that amphibolite terrains have prominent occurrences of dual aquifer systems, which is an indication of the extensive subsurface weathering and fracturing [12]. However, shallow wells may also be prolific within amphibolite, like the well at Ajegunle (Tables 1). Normally, terrains underlain by gneisses were notably characterised by deeper wells with depth range of 30.9–99.5 m (Table 3). The linear relationship occurring between transmissivities and wells' depths is weak and indirect ($R = -0.33$; Figure 7B). This suggests that deep wells in gneissic bedrock terrains will not give large water transmission. This was buttressed by wells at Alaagba, where deeper wells did not have a positive effect on the transmission capacity of the aquifers with transmissivities of 0.25 and 0.55 m^2/day correspondingly for Alaagba I and II. However, other gneissic wells with depths between 34 and 36 m at Apata, Abola and Agbede were prolific. Hence, there is no guarantee of striking a fracture zone at depth beyond this range on gneissic terrains. This is also the case for wells in migmatite. The relationship is also indirect with $R = -0.41$ (Figure 7B), which means that deep wells will not necessarily be prolific as well. Similarly, the R relationship between transmissivities and well depths in granite is indirect, and the strength of relationship is low ($R = -0.26$) (Figure 7B). This explains the reason for a sharp drop in discharge for wells at Idere. Notably, the wells in granite are shallower (with the average depth of 25.7 m), compared to the averages of 27.47 m, 46.68 m and 27.72 m correspondingly for wells in amphibolite, gneisses and migmatite terrains (Table 3). The R value and the relatively shallower wells within granitic terrains indicated less weathering and infrequency of bedrock fractures within granitic terrains [12].

The only significant relationship existing between the aquifer transmissivities and the groundwater table in Figure 7C is within the amphibolite terrains with $R = -0.52$. This relationship is indirect and moderate. Shallow groundwater table is an indication of high aquifer pressure, which is most likely in amphibolite, whereby the regolith units are largely fine grained, and are acting as aquiclude over the largely fractured bedrock [3, 12]. This creates a confined aquifer system in amphibolite and the groundwater system is under pressure, leading to likely occurrences of artesian aquifers within this bedrock. The strength of the relationships between transmissivities and groundwater table is insignificant in other bedrocks (Figure 7C).

Groundwater Yield and Aquifer Sustainability

Eight wells located at Ajegunle, Igboole II, Igboole I, Pako, Agbede, Ayete I, Abola and Apata out of all tested boreholes are prolific and sustainable (Figure 8) due to comparatively larger transmissivity, smaller drawdown and constant discharge during the entire pumping period. The wells are either leaky or dual aquifer categories and are mainly restricted to terrains underlain by amphibolite and gneisses. The first four wells with the largest transmissivity within the range of 11.65–9.30 m^2/day are within amphibolite terrain. Wells at Agbede, Abola and Apata are on the gneissic bedrock, while Ayete I is the only prolific well tested on the porphyritic granite terrain.

Aside from the sustainable yield of leaky and dual aquifers, the water level attained a dynamic equilibrium level at the late pumping stage. These aquifers supplied water to the wells from the matrix/weathered layer and the fractured bedrocks. The depths of these prolific wells that penetrated the dual and leaky aquifers are mainly within 30–38 m, whereas the depths of the other wells that penetrate mere weathered-regolith aquifers are mostly below 30 m (Table 1). Estimably, sustainable groundwater-bearing zones can be said to be within the depth range of 30–38 m within the amphibolite and gneissic terrains.

Comparatively, from the mean in Table 2, the regolith aquifers were characterised by lower transmissivity of 0.92 m^2/day and higher total drawdown of 18.08 m, compared to 9.15 m^2/day and 5.42 m^2/day with a total drawdown of 10.27 m and 16.90 m for dual and leaky aquifers respectively. The regolith

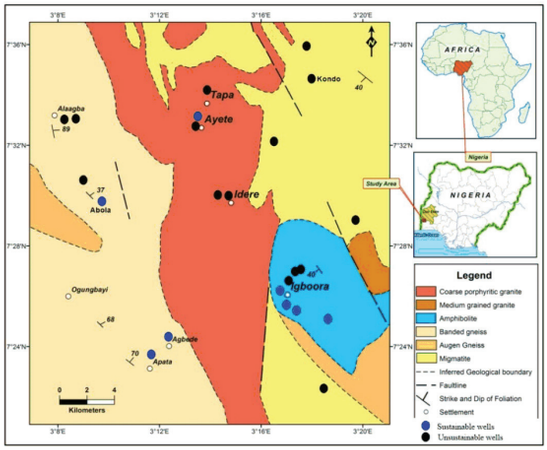

Figure 8: *Locations of sustainable and unsustainable wells on geological map.*

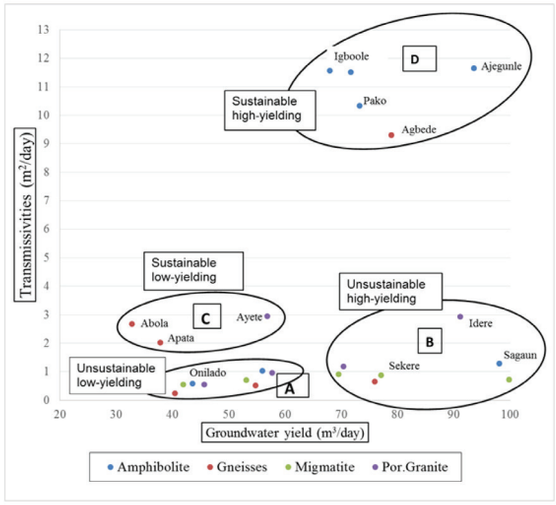

Figure 9: *Conceptual hydraulic models of basement aquifers across the study area.*

aquifers can be said to be terminated on either impermeable or sparsely fractured bedrock (or boundary). Hence, the drawdown drops drastically, and the yield is not sustainable for a long period of pumping. The discharge in the regolith aquifers was mostly influenced by well bore storage. The regolith aquifers are unsustainable and are the most widespread category, but they are usually associated with migmatite and granitic terrains (Figure 8).

Conceptual Models of Hydraulic Settings of the Aquifer Systems

The overall theoretical model of the hydraulic conditions of the basement aquifer of the Ibarapa region based on the plots of transmissivity against groundwater yield can be categorised into four major groups as illustrated in Figure 9. Groups A and B are regolith aquifers whose hydrogeological settings could not sustain a longer pumping period. However, the seven wells in Group B were characterised by large groundwater discharge greater than 70 m^3/day, but the yield is unsustainable over a long period. The discharge drops as pumping continues. The transmissivities of the aquifers in this group are typically greater than 1.0 m^2/day. Contrastingly, the transmissivities of the aquifers of under Group A are mostly below 1.0 m^2/day. Groundwater yield is lower and less than 60 m^3/day, but the aquifers can sustain a longer period of discharge.

The hydrogeological settings of eight aquifers in Groups C and D sustained continuous groundwater yield for hours of pumping. But in comparison, aquifers in Group C have lower transmissivities and smaller sustainable discharge than those in Group D (Figure 9). The transmissivities of aquifers in Group D exceeded 9.0 m^2/day and their discharge above 60 m^3/day. Lastly, migmatite and granitic aquifers are mainly regolith/weathered units whose yields are not sustainable either when large or when low. These aquifers can only sustain short pumping

period, which may be lengthened when the bedrock is fractured. Wells in Groups C and D are typically within amphibolite and gneisses terrains, where the bedrocks are largely fractured [12].

Conclusion

For sustainable groundwater development, the groundwater system should be used in a way that it can be conserved for an unlimited time without causing improper environmental, economic or social problems [17]. It is obvious from the responses of the basement aquifers to pumping that geological and structural heterogeneity have imprinted on the hydraulic settings across the study area. The subsurface groundwater-bearing zones in Igboora and the lower parts of the western block within the study area are sustainable and quite pro-

lific. These areas are underlain by amphibolite and gneisses, respectively. Wells drilled within these areas can be connected to provide town water supply for the entire Ibarapa region. This will ensure even distribution and judicious utilisation of groundwater system for the entire Ibarapa region, including areas such as Ayete and Tapa that are underlain by migmatite and granite where the water-bearing zones are not able to sustain a long period of pumping. Alternatively, groundwater may also be exploited from the overburden units within the latter areas through hand-dug wells. Although the yield will be low and will be adversely affected by seasonal variation during dry season, this will improve through meteoric recharge during the recurrent rainy season.

References

[1] Acworth, R.I. (1987): The development of crystalline basement aquifers in a tropical environment. *Quarterly Journal of Engineering Geology*, 20, pp. 265–272.

[2] Wright, E.P., Burgess, W.G. (1992): Hydrogeology of crystalline basement aquifers in Africa*. Geological Society Special Publication*, 66, pp. 1–27.

[3] Akanbi, O.A. (2016): Use of vertical electrical geophysical method for spatial characterisation of groundwater potential of crystalline crust of Igboora area, southwestern Nigeria. *International Journal of Scientific and Research Publications,* 6(3), pp. 399–406.

[4] Akanbi, O.A. (2017): *Hydrogeologic characterisation of crystalline basement aquifers of part of Ibarapa area, southwestern Nigeria*. Ph. D. Thesis. University of Ibadan, Faculty of Science, Department of Geology: Ibadan, 312 p.

[5] [5] Akanbi, O.A., Olukowade, J.O (2018): Lithologic Characterisation of the Basement Aquifers of Awe and Akinmorin Areas, Southwestern Nigeria. *Global journal of geological sciences*, 16, pp. 1–11, DOI: 10.4314/gjgs.v16i1.1.

[6] Dada, S.S. (1998): Crust-forming ages and Proterozoic evolution in Nigeria: a reappraisal of current interpretations. *Precambrian Research*, 87, pp. 65–74.

[7] NGSA, (2009): *Geological and mineral resources map of south-western zone, Nigeria*. Nigerian Geological Survey Abuja, Nigeria.

[8] 2006 population census [online]. National Bureau of Statistics [cited 7/26/2011]. Available on: *http://* www.nigerianstat.gov.ng.

[9] Singhal, B.B.S., Gupta R.P. (1999): *Applied hydrogeology of fractured rocks*. Kluwer Academic Publishers: Dordrecht, 400 p.

[10] Kruseman, G.P., de Ridder, N.A. (2000): *Analysis and evaluation of pumping test data*. 2nd edition. International institute for land reclamation and improvement: Wageningen, 377 p.

[11] Jones, H.A., Hockey, R.D. (1964): The geology of part of south-western Nigeria. *Bull. Geol. Surv. Nigeria*, 31.

[12] Akanbi, O.A. (2018): Hydrogeological characterisation and prospects of basement aquifers of Ibarapa region, SW Nigeria. *Applied Water Science,* 8(3), 89, DOI: 10.1007/s13201-018-0731-9.

[13] Phillippe, R., Damian, G., Miguel, M. (2008): Understanding diagnostic plots for well-test interpretation. *Hydrogeology Journal,* 17, pp. 589–600.

[14] Cooper, H.H., Jacob, C.E, (1946): A generalized graphical method for evaluating formation constants and summarising well field history. *American Geophysical Union Transactions*, 27, pp. 526–534.

[15] Fetter, C.W. (2007): *Applied hydrogeology*. 2nd edition. Merrill Publishing Company: USA, 592 p.

[16] Akanbi, O. A. (2018): Groundwater Occurrence from Hydrogeomorphological Study of Hard Rock Terrain of part of SW Nigeria. *Materials and Geoenvironment,* 65(3), pp. 131–143*,* DOI: 10.2478/ rmzmag-2018-0011.

[17] Alley, W.M., Reilly, T.E., Franke O.L. (1999): *Sustainability of groundwater resources.* U.S. Geological Survey Circular 1186.

Original scientific paper

Received: Aug 24, 2019
Accepted: Sep 09, 2019
DOI: 10.2478/rmzmag-2019-0012

Photovoltaic Solar Energy: Is It Applicable in Brazil? – A Review Applied to Brazilian Case

Fotovoltaična sončna energija: ali je uporabna v Brazliji? – Pregled, uporaben za primer Brazilije

Wilmer Emilio García Moreno[1,*], Andressa Ullmann Duarte[1], Litiéle dos Santos[1], Rogério Vescia Louregа[1,2]

[1] Graduation Program in Materials Engineering and Technology, Pontifical Catholic University of Rio Grande do Sul (PGETEMA/PUCRS), Brazil

[2] Pontifical Catholic University of Rio Grande do Sul (PUCRS), Brazil

* wilgm93@gmail.com

Abstract

The photovoltaic technologies have been developed year by year in different countries; however, there are some countries where this kind of energy is being born, such as the Brazilian case. In this paper, some important parameters are analysed and applied to different solar cell materials, identifying that if the fossil fuels were substituted by solar cells, it would reduce the CO_2 emissions by 93.2%. In addition, it is shown that the efficiency of solar cells is not as farther as it could be thought from coal thermoelectrical plants in Brazil and the cost of energy using solar cells could be as good as these thermoelectrical plants. Finally, the potentiality of Brazilian territory to implant this technology is presented, identifying that with the use of 0.2% of the territory, the energy demand could be supplied.

Key words: Solar cells, CO_2 Emissions, Fossil fuels, Brazil, Thermoelectrical plants

Povzetek

Fotovoltaične tehnologije se iz leta v leto razvijajo v različnih državah. Obstajajo nekatere države, kot na primer Brazilija, kjer ta vrsta energije igra pomembno vlogo. Zaradi tega smo v članku analizirali nekatere pomembne parametre, ki se nanašajo na različne material sončnih celic. Ugotovili smo, da bi se v primeru zamenjave fosilnih goriv s sončnimi celicami izpusti CO_2 lahko zmanjšali v najboljšem primeru za 93.2%. Prav tako smo pokazali, da učinkovitost sončnih celic in cena z njimi pridobljene energije ne zaostaja za termoelektrarnami v Braziliji. Na koncu je predstavljen potencial ozemlja Brazilije, kjer bi lahko z uporabo 0.2% ozemlja pokrili energetske potrebe.

Ključne besede: sončne celice, emisije CO_2, fosilna goriva, Brazilija, termoelektrarne

Introduction

Both economic and population growth have an effect on energy demand, having as principal consequence an accumulative increase in the use of fossil fuels, a way to supply this demand, increasing the average greenhouse gases concentration, being the CO_2 the principal gas among them [1]; therefore, the biggest challenge is to reduce the CO_2 emissions to the atmosphere by means of using diverse green energy sources, such as natural gas, ethanol, nuclear, wind and solar energy [2]. In this order of ideas, the concern in these alternative energies has been bigger in conformity of the growing global warming and air pollution [3].

Some countries have implemented the use of renewable energy in order to solve the environmental problems, solar photovoltaic systems being one of them [4] and is also placed as one of the most promising energies because of its potential to reduce greenhouse gases (GHG) emissions [5] and how not considering as it, when along its operational time it does not emit CO_2? [6] [7]. Also, an important parameter has been studied and it is its pricing by Wp (Watts Peak), being reported 1.60 US$/Wp in 2011, 0.34 US$/Wp in 2017 and reduced to 0.244 US$/Wp in January 2019 [8].

On the other hand, placing the focus on Brazil, its grid is composed by 67.9% of hydroelectrical sources; however, the photovoltaic energy occupies a low 0.7% [9]. Also even when the hydroelectrical source is considered clean, its application is restricted due to environmental impact, such as flooding in large areas, methane emissions from anaerobic degradation of organic material, dependence on local hydrological stability [10]. In addition, because of the climate change, more frequent, intense and prolonged droughts in Brazil are expected, which would affect dramatically the hydroelectrical source [11].

Hence, due to all the above mentioned environmental impact, this work tries to show a review focused on some specific parameters such as the GHG emission, energy payback time (EPBT), energy return on energy invested (ERoEI), efficiency, cost and irradiance potentiality and focused on different materials to know how green this energy (no matter about the solar cell material) can be and how it can be applied in Brazil, trying to illustrate how the country could be helped, due to its enormous capability [12] [13].

Cell Technologies

In brief, solar cells transform the solar power to electrical power. This photovoltaic cell is created by a semiconductor material which is exposed to the photons emerging from sunlight. This semiconductor has an absorption capacity, depending on its specific band gap energy that will absorb photons with the same energy (the band gap energy) and, if the energy is higher, these photons will release the surplus energy in heat form and, in that way, retaining the specific band gap energy of the material [14]. Having in consideration the different kinds of materials, the global share is illustrated in Figure 1.

Monocrystalline photovoltaic cells are made using a single and continuous crystal of silicon, having almost no impurities, obtaining a blue solid colour [15], sharing around 30% of

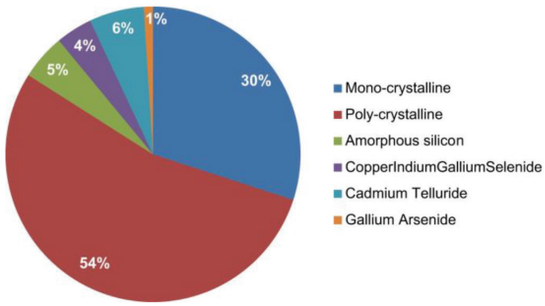

Figure 1: *Global market share of photovoltaic cells [14].*

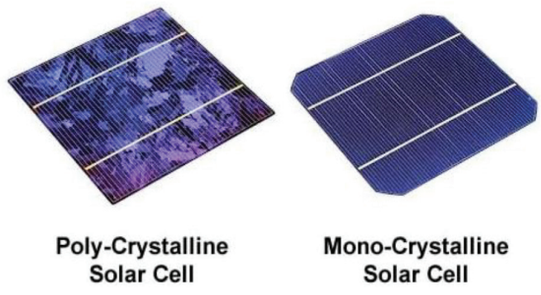

Figure *2: Silicon solar cells [19].*

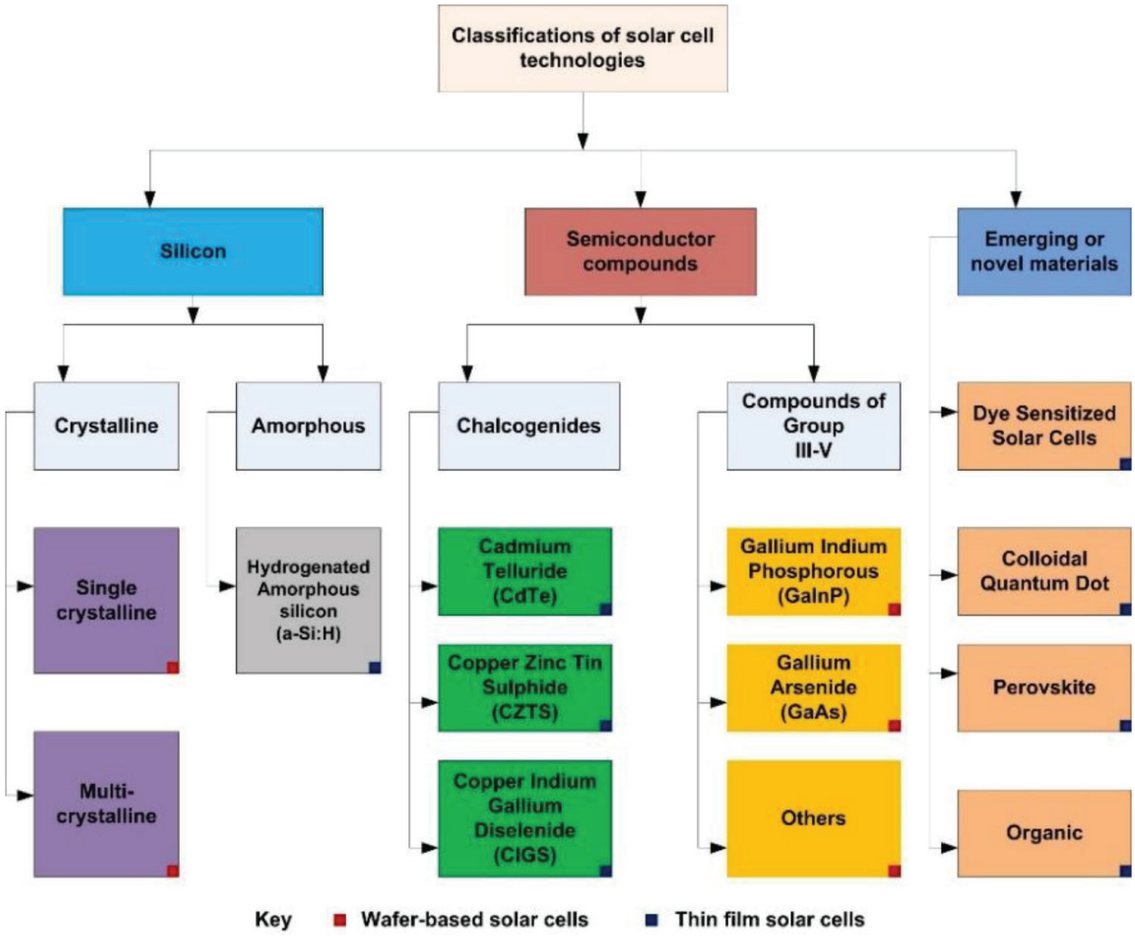

Figure 3: *Solar cell technologies classification [26].*

the market (Figure 1). The manufacturing of these cells is more expensive due to processing of high purity crystal and also guaranteeing a higher efficiency compared with polycrystalline cells [16] [17]. On the other hand, polycrystalline photovoltaic cells occupied most of the market share (more than 50%) (Figure 2). They are produced using several different monocrystalline silicon grains which are melted and consequently solidified slowly by cooling down [18].

Another kind of photovoltaic cells are thin films which are known as second generation of photovoltaic cells, having a range of thickness varying between 10 nm to 10 μm [20]. Also, it has been reported that in comparison with silicon solar cells (amorphous, polycrystalline and monocrystalline), the EPBT and the price of thin films have been lower, although the efficiency is not as high as silicon solar cells [21].

Nevertheless, in attempting to be a better contender in front of silicon photovoltaics, some materials have been performed. Copper indium gallium selenide (CIGS) is one of the best absorber materials in thin films, because it possesses a chalcopyrite crystal structure and can modify the band gap energy values changing indium by gallium and obtaining $CuInSe_2$ and $CuGaSe_2$ with 1.02 and 1.67 eV [22]. Another material is cadmium telluride (CdTe) with a band gap energy of 1.5 eV which gives it a theoretical efficiency of around 30% (see section 4.4) and the most attractive characteristic of this material is its chemical simplicity so that it could be applied to space applications [21]. Also, gallium arsenide (GaAs) is used in thin films and by the year 2014, this material had been shown the best efficiency by a single junction (27.6%) [23]. In addition, GaAs uses a band gap between 1.43 and 1.7 eV [14].

The next generation of solar cells is covered by organic solar cells (OSCs) or organic photovoltaics (OPV). These cells are based on photosynthesis process in order to absorbing light which is done by the dye that substitutes the silicon, compared with conventional cells; however, they have been demonstrated with low efficiency of around 3–5% [24] and they are still a promising alternative because of their low cost and relative ease of chemical synthesis [25]. Even though only some materials have been presented, there are a huge variety of solar cells materials. Figure 3 shows the three biggest blocks of these materials.

Applied Review Methodology

This methodology is based on a comprehensive method to evaluate and analyse, along the whole product lifetime, the environmental performance and energy consumption, covering the whole processes [27] having a life cycle assessment as principal analogy. Therefore, it has been proposed and standardised by ISO 14040 and ISO 14044 [28] [29] using some fundamental stages: first is goal and scope; second is life cycle inventory; third impacts assessment and fourth is the interpretation of the results [30]. Hence, taking the impact into consideration in this study, the following points were analysed: diverse aspects of GHG emissions, EPBT, ERoEI, the efficiency, how suitable it could be with respect to the potentiality of the territory and how much it could be, in order to demonstrate that this alternative can be a substitute of fossil fuels, being applied specifically to Brazil.

Results and Discussion

Efficiency

Efficiency of Solar Cells

The first essential point to be evaluated, which has been studied along the years, is the efficiency that most of the green parameters depend on the efficiency to be better, such as recovering the invested energy, trying to get shorter time and producing even more energy. Also, low equivalent CO_2 emissions are expected by energy produced along the lifetime, without affecting the efficiency. For this reason, the results from 39 different materials and studies are gathered and represented in Table 1. All these data are analysed by means of two graphs, first to com-

Table 1: *Efficiency by materials.*

Material	Efficiency (%)	Reference	Year
GaAs	23.5	[31]	2011
CZTS	7.3	[32]	2012
Poly-Si	20.3	[33]	2012
CZTS	8.9	[34]	2012
CIGS	15.5	[35]	2012
DSC	11.4	[36]	2012
OPV	8.4	[37]	2012
InGa/GaAs	26.6	[38]	2013
CZTS	12.6	[39]	2013
DSC	9.4	[40]	2013
CdTe	12.3	[41]	2013
CIGS	20.4	[42]	2013
CIGS	15.2	[43]	2013
CZTS	8.4	[44]	2013
OPV-triple junction	11.55	[45]	2014
CZTS	11.6	[46]	2014
Perovskite	11.13	[47]	2014
Poly-Si	18.45	[48]	2014
Mono-Si	25.6	[49]	2014
Perovskite	16.6	[50]	2014
Perovskite	15.07	[51]	2014
OPV	10.31	[52]	2014
Perovskite	17.6	[53]	2015
Mono-Si	20.6	[54]	2015
Mono-Si	22.5	[55]	2015
Perovskite	17.7	[56]	2015
Perovskite	18.3	[57]	2015
CIGS	21.7	[58]	2015
OPV	9.94	[59]	2015
GaAs	28	[60]	2015
CdTe	21	[60]	2015
OPV	11.25	[61]	2016
GaAs	15.3	[62]	2016
Poly-Si	21.25	[63]	2016
Mono-Si	19.42	[64]	2016
Poly-Si	16.7	[64]	2016
CdTe	17	[65]	2016
Poly-Si	18.62	[66]	2017
OPV	13.1	[67]	2017
Perovskite-silicon	26.4	[68]	2017

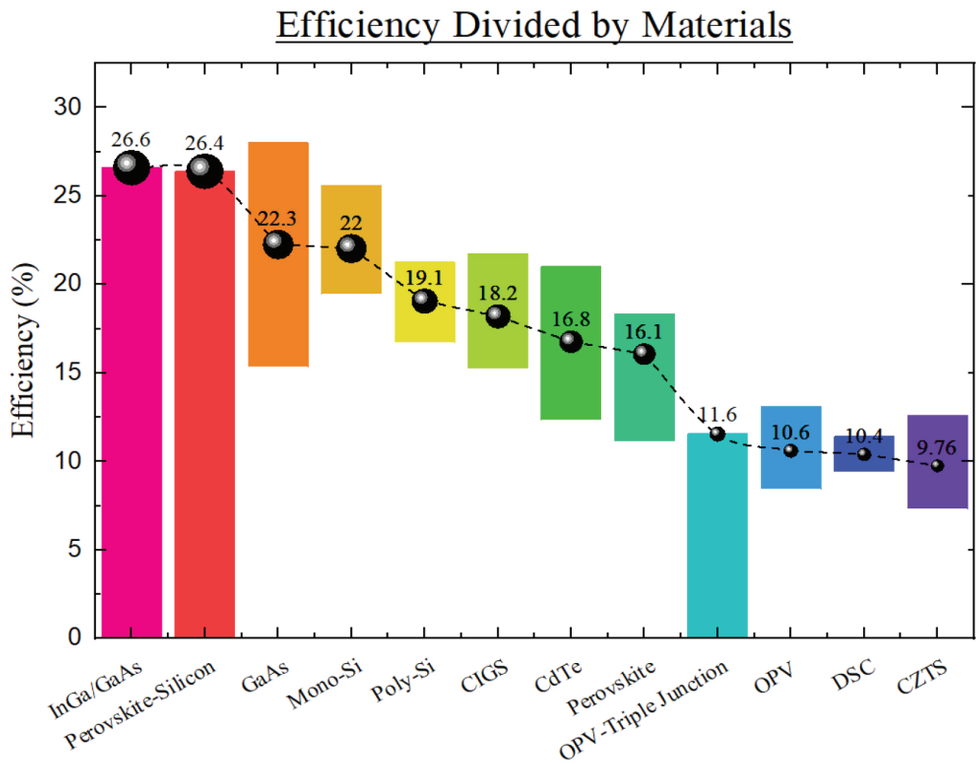

Figure *4: Efficiency divided by materials.*

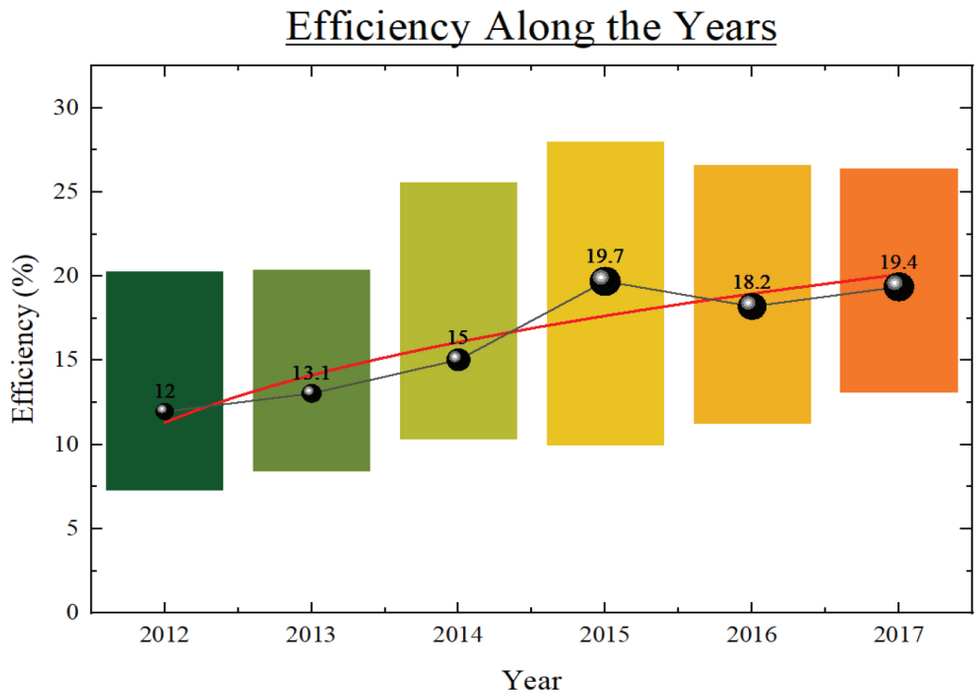

Figure 5: *Efficiency along the time.*

pare the efficiencies by materials (Figure 4), and the other, along the last years, to average the different studies (Figure 5).
When the materials are seen, it is possible noticing a top around 26% of efficiency; also, the first three materials correspond to newer technologies like tandem (InGa/GaAs and perovskite/silicon) and thin films (GaAs). However, monocrystalline and polycrystalline silicons (which are the most commonly used) are ubicated later with the efficiencies of approximately 19% and 18%. On the other hand, in recent years, the average efficiency of solar cells has been increasing.

Efficiency of solar cells in front of thermoelectrical plants
If the efficiency was compared with the thermoelectrical power plants, there would be still a gap between them, with a global average efficiency around 35% [69] [70], which represents almost the double if compared with silicon solar cells (1.85 times). Also, if it is considered on account of the Brazilian case, there are some carbon power plants which have a varied efficiency, being 20.5% in Charqueadas power plant, 25%, 29,4%, 36.1% and 35.8% corresponding to Jorge Lacerda A1, A2, B and C, the most 36.5% belonging to Candiota III [71], but this corresponds only to 1.88% of the total produced energy in Brazil and 8.51% of thermoelectrical plants [72]. Besides, the biggest part is taken by thermoelectrical gas plant (7.75% of total grid and 35.07% of thermoelectrical energy) which was reported a 42% of efficiency [71], obtaining a 5.14% of total energy grid by oil (23.25% of thermoelectrical energy) with 34% of efficiency [73]. The rest is corresponded to biomass (8.58% of total energy grid and 38.84% of thermoelectrical plants) having an efficiency around 23.05% in Brazil [72].
It could resemble that there is nothing to do against the efficiency of thermoelectrical power plants; however, observing the efficiency along the years, there has been a constant increase in efficiency which could then help developing better solar cells. Also, even when the carbon thermoelectrical efficiency is bigger than silicon solar cells, the CO_2 emission is 20 times higher and when it is used as natural gas, the emissions are 10 times higher and 16 times higher for oil thermoelectrical plants [74] (this point will be analysed later). Hence, it is possible asking, is it fear, right or correct using thermoelectrical plants just because of increasing efficiency? It does not look like.

Greenhouse Gases Emissions (Equivalent CO_2 Emissions)

CO_2 emissions by energy produced in solar cells
When evaluating the GHG emissions, the principal gas on which this parameter is based is CO_2, assessing it along the whole life of the studied material and expressing its value in CO_2 g/kWh. For that reason, in this section a total of 24 ref-

Table 2: *CO_2 emissions.*

Material	CO_2 emission (g/KWh)	Reference	Year	Average CO_2 emission (g/kWh)
Mono-Si	131	[75]	2009	131.00
CdTe	17	[76]	2010	36.00
CIGS	33	[76]	2010	
CIGS	44	[77]	2010	
CdTe	50	[77]	2010	
OPV	37.77	[78]	2011	47.21
OPV	56.65	[78]	2011	
Poly-Si	88.74	[79]	2012	63.01
DSSC	22.29	[80]	2012	
CdTe	48	[80]	2012	
CIGS	95	[80]	2012	
Mono-Si	61	[81]	2012	

Table 2: *CO_2 emissions (continue).*

Material	CO_2 emission (g/KWh)	Reference	Year	Average CO_2 emission (g/kWh)
CdTe	15.83	[82]	2013	
CdTe	20.11	[82]	2013	
CIGS	21.44	[82]	2013	
Poly-Si	27.2	[82]	2013	
CIGS	27.64	[82]	2013	
Mono-Si	38.06	[82]	2013	35.61
Poly-Si	49.7	[82]	2013	
Mono-Si	81.2	[82]	2013	
Mono-Si	47.9	[83]	2013	
GaInP/ GaInAs/Ge	27	[84]	2013	
CdTe	20	[85]	2014	
CIGS	22	[85]	2014	
OPV-Multi J.	48.18	[86]	2014	
CdTe	15.1	[87]	2014	
Poly-Si	31.5	[87]	2014	
Mono-Si	41.8	[87]	2014	
DSSC	28.1	[88]	2014	
CdTe	68	[88]	2014	
CIGS	70	[88]	2014	
Poly-Si	12.28	[89]	2014	36.73
Poly-Si	13.04	[89]	2014	
Poly-Si	18.11	[89]	2014	
Poly-Si	19.49	[89]	2014	
Poly-Si	51.68	[89]	2014	
Poly-Si	54.82	[89]	2014	
Poly-Si	55.89	[89]	2014	
Poly-Si	58.81	[89]	2014	
Poly-Si	31.8	[90]	2014	
Mono-Si	37.3	[90]	2014	
Poly-Si	50.9	[91]	2015	
Perovskite	60.1	[92]	2015	64.50
Perovskite	82.5	[92]	2015	
Mono-Si	5.6	[93]	2016	
Mono-Si	12.07	[93]	2016	
OPV	14.7	[94]	2016	
Poly-Si	60.1	[95]	2016	46.50
Mono-Si	65.2	[95]	2016	
Poly-Si	80.5	[95]	2016	
Mono-Si	87.3	[95]	2016	

Table 2: *CO_2 emissions (continue).*

Material	CO_2 emission (g/KWh)	Reference	Year	Average CO_2 emission (g/kWh)
CdTe	35	[14]	2017	40.50
CIGS	46	[14]	2017	
AZTS/Si	19.8	[96]	2018	24.72
CZTS/Si	20.4	[96]	2018	
CIGS/Si	27.8	[96]	2018	
Poly-Si	20.9	[97]	2018	
Poly-Si	29.2	[97]	2018	
Poly-Si	30.2	[97]	2018	

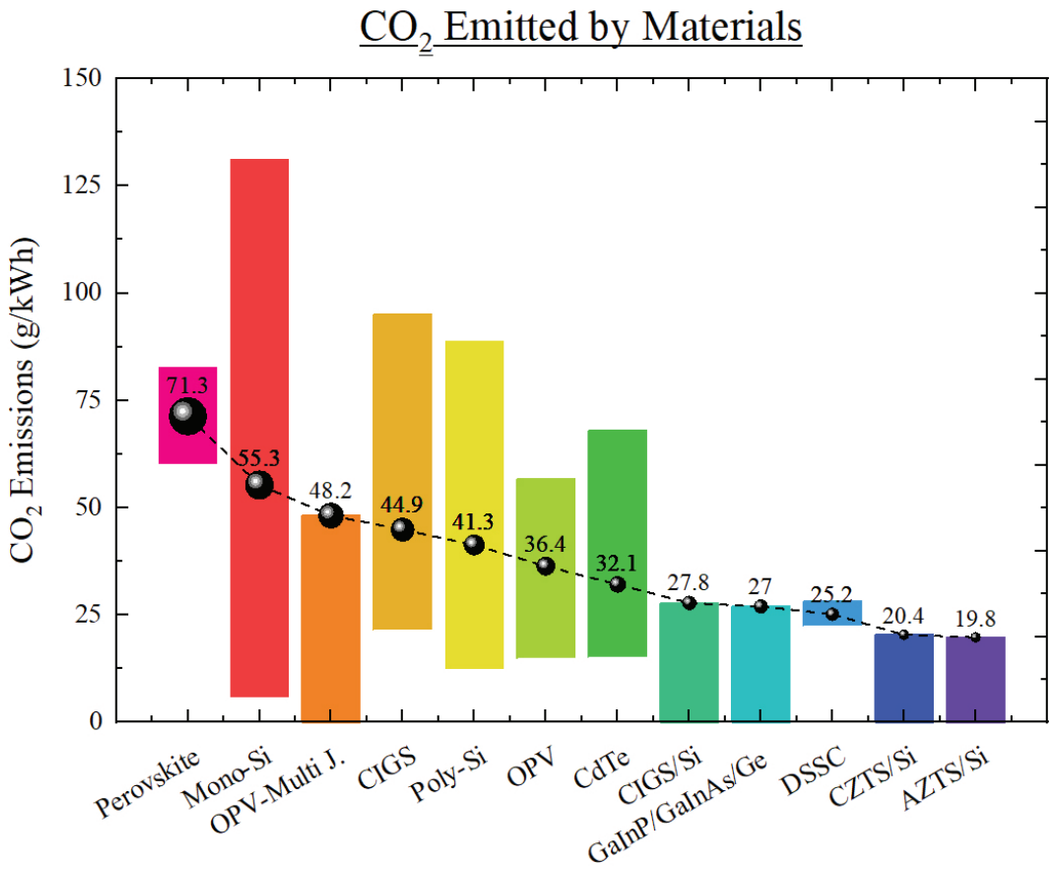

Figure 6: *CO_2 emission by different materials.*

erences, from 2009 to 2019 (Table 2), was gathered, obtaining a graph (Figure 6) where the highest value is 131 CO_2 g/kWh, and the values correspond to the oldest data (2009). However, the average values by materials vary in a range of ~20 to ~70 g/kWh which shows an improved, although, relatively low value when compared with fossil fuel emissions. This will be discussed in the next subsection.

CO_2 emission compared with fossil fuels

If all the data are averaged from Figure 6, it will be 42.15 CO_2 g/kWh. Also, using the data from International Energy Agency that pub-

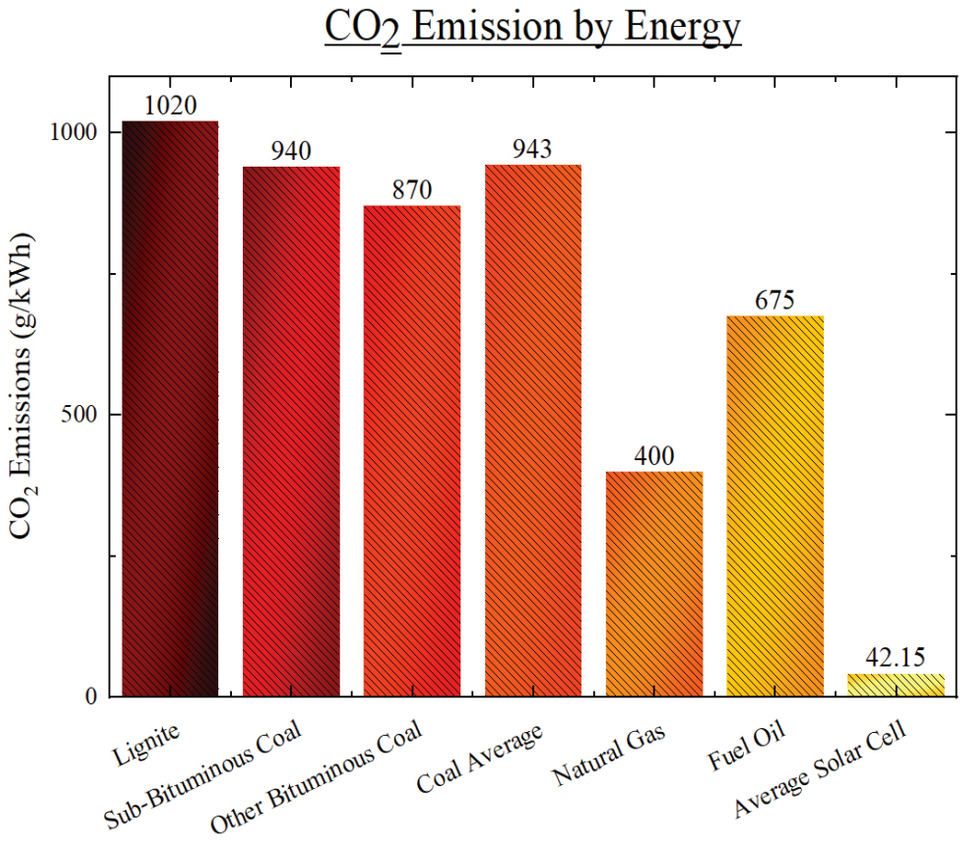

Figure 7: *CO_2 emission by energies.*

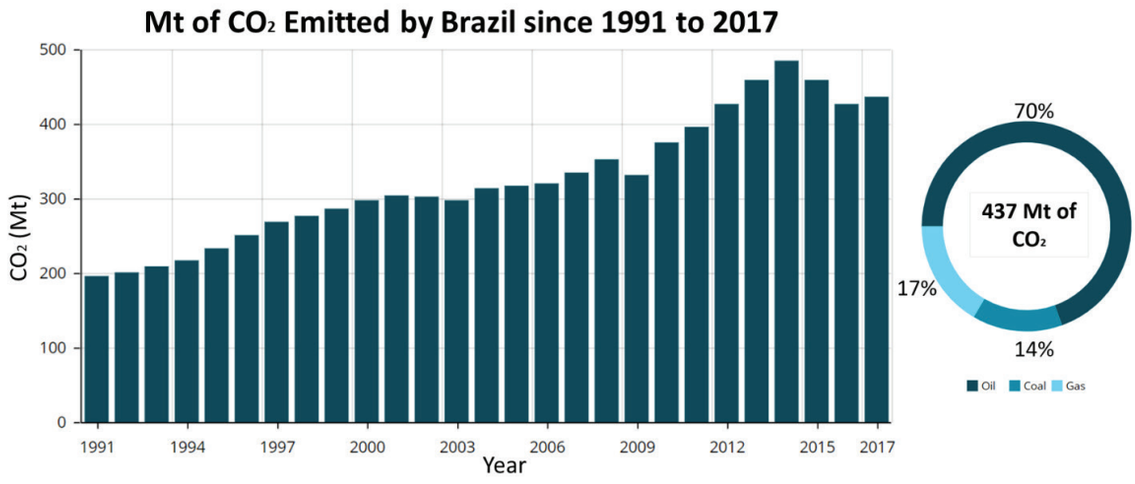

Figure 8: *CO_2 emitted by Brazil in 2017 [98].*

lished its report about CO_2 emissions from fuel combustion [74], a graph (Figure 7) is drawn to represent the big difference between them and a solar cell system; for this reason, the energy emitted by coal (average), natural gas and fuel oil contains approximately 22.37, 9.49 and 16.01 times more CO_2 than an average photovoltaic panel. This leads to analyse the case of Brazil, which is shown in Figure 8, with a focus on the year 2017 (the last obtained data), and

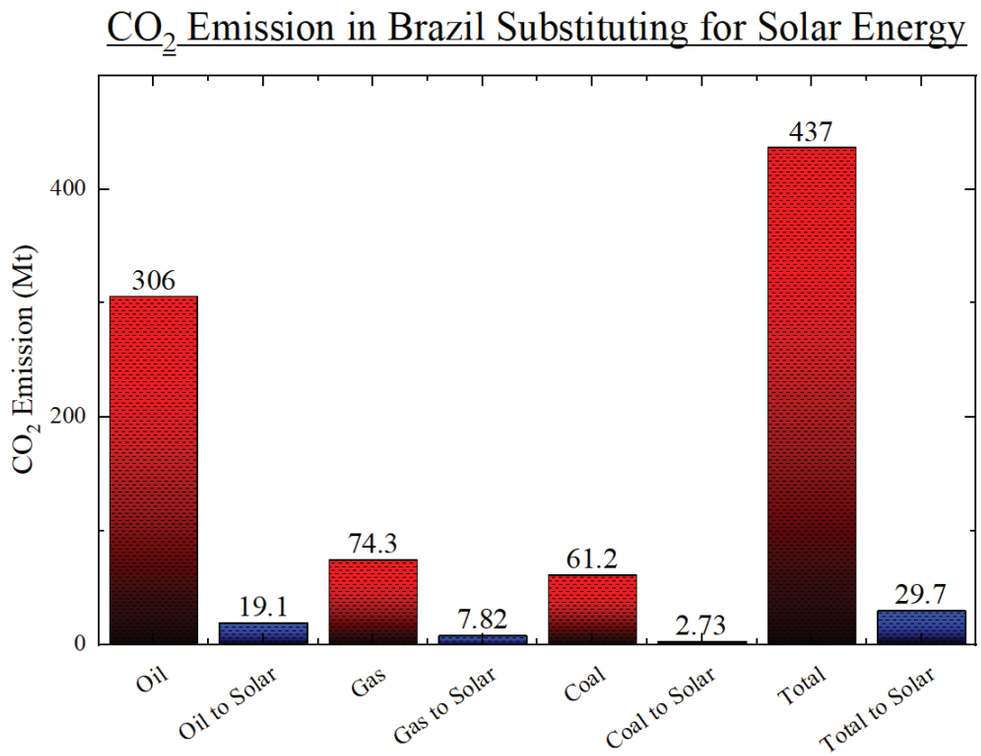

Figure 9: *Emissions of CO_2 if the fossil fuels are substituted by solar energy.*

the data is divided by the emission by the fossil fuels the emissions of CO_2 is calculated if they are substituted by solar panels (Figure 9), reducing from 437 to 29.7 Mt, being only 6.8% of the CO_2 emitted nowadays.

Energy Payback Time

This parameter refers to the required time that the system takes to recover all the used energy from its cradle to grave [84]; for this reason, even when a system has low CO_2 emission, it needs to recover its used energy as fast as possible, as a way to be sustainable. In this order of ideas, some studies have been gathered to analyse how these values have been developed (Table 3) by materials (Figure 10) and along the years (Figure 11).

Observing the graphs, it is notorious how the EPBT is decreasing with the years, varying with materials, getting even lower values than the average by year, nevertheless, there are no data in 2008, 2010 and also in 2009 but there was a data with a really high value. On the other hand, the evolution of EPBT could be defined in a range between 1 and 2.5 years, in average, to recover the used energy. However, it is valid asking if the obtained EPBT values are framing inside the lifetime of solar cells.

To answer the lifetime framework, an analytical review based on degradation rates of photovoltaics made by Jordan and Kurtz [106], the authors concluded that even when the companies warranty a lifetime of 25 years, moreover the reported report some panels with 40 years of duration. Also, they obtained degradation rates of 0.8% by year in average; in fact, 78% of their study reflected a degradation rate less than 1% by year, concluding that a range of 1 to 2.5 years to recover the energy is an excellent parameter. Additionally, in the Brazilian case, by the year of 2011, an EPBT was reported which varied between 3.1 and 4.1 years [107] (Figure 12), compared with the analysis in this review in the same year which was 3.9 years in average. Brazil fits good, besides, the tendency was from 3.9 years in 2011 to 1.26 years in 2018 for EPBT; for this reason, an interval could be proposed for Brazil (following the same tendency until 2018) from 1.085 to 1.435 years.

Table 3: *Energy payback time.*

Material	EPBT (year)	Reference	Year	EPBT average (year)
GaAs	5	[99]	2007	4.60
GaInP/GaAs	4.6	[99]	2007	
Poly-Si	4.2	[99]	2007	
Mono-Si	9.08	[75]	2009	9.08
OPV	2.02	[78]	2011	3.90
OPV	1.35	[78]	2011	
Mono-Si	8.04	[100]	2011	
Poly-Si	4.18	[100]	2011	
Poly-Si	4.17	[79]	2012	2.77
CIGS	2.8	[80]	2012	
DSSC	1.58	[80]	2012	
CdTe	1.5	[80]	2012	
Mono-Si	3.8	[81]	2012	
Mono-Si	2.34	[82]	2013	1.68
Mono-Si	1.96	[82]	2013	
Poly-Si	1.45	[82]	2013	
Poly-Si	1.24	[82]	2013	
CIGS	1.02	[82]	2013	
CIGS	1.01	[82]	2013	
CdTe	0.68	[82]	2013	
CdTe	0.68	[82]	2013	
Mono-Si	5.5	[83]	2013	
GaInP/GaInAs/Ge	0.9	[84]	2013	
OPV-Multi J.	0.24	[86]	2014	1.74
Mono-Si	3.11	[87]	2014	
Poly-Si	2.97	[87]	2014	
CdTe	0.94	[87]	2014	
CIGS	1.98	[88]	2014	
CdTe	1.95	[88]	2014	
DSSC	0.95	[88]	2014	
Mono-Si	1.9	[90]	2014	
Poly-Si	1.6	[90]	2014	
Mono-Si	4.1	[101]	2015	1.85
Poly-Si	3.5	[101]	2015	
CIGS	1.7	[101]	2015	
CdTe	1	[101]	2015	
Poly-Si	2.2	[91]	2015	
Perovskite	0.266	[92]	2015	
Perovskite	0.193	[92]	2015	
Mono-Si	0.91	[93]	2016	1.34
Mono-Si	0.42	[93]	2016	
OPV	0.34	[94]	2016	
Poly-Si	2.1	[95]	2016	
Mono-Si	2.06	[95]	2016	
Mono-Si	1.95	[95]	2016	

Table 3: *Energy payback time (continue).*

Material	EPBT (year)	Reference	Year	EPBT average (year)
Poly-Si	1.6	[95]	2016	1.34
Perovskite-Si	1.1	[102]	2017	0.92
Perovskite-CIGS	0.625	[102]	2017	
Perovskite-CZTS	0.21	[102]	2017	
Perovskite-perovskite	0.11	[102]	2017	
GaAs	1.67	[14]	2017	
CIGS	1	[14]	2017	
CdTe	0.75	[14]	2017	
Perovskite	0.5	[14]	2017	
Poly-Si	2.3	[103]	2017	
Perovskite-Si	0.88	[104]	2018	1.26
Perovskite-CIGS	0.5	[104]	2018	
Perovskite-CZTS	0.45	[104]	2018	
CIGS/Si	1.4	[96]	2018	
CZTS/Si	1.3	[96]	2018	
AZTS/Si	1.3	[96]	2018	
Poly-Si	1.11	[97]	2018	
Poly-Si	1.08	[97]	2018	
Poly-Si	1.01	[97]	2018	
CdTe	3.6	[105]	2018	

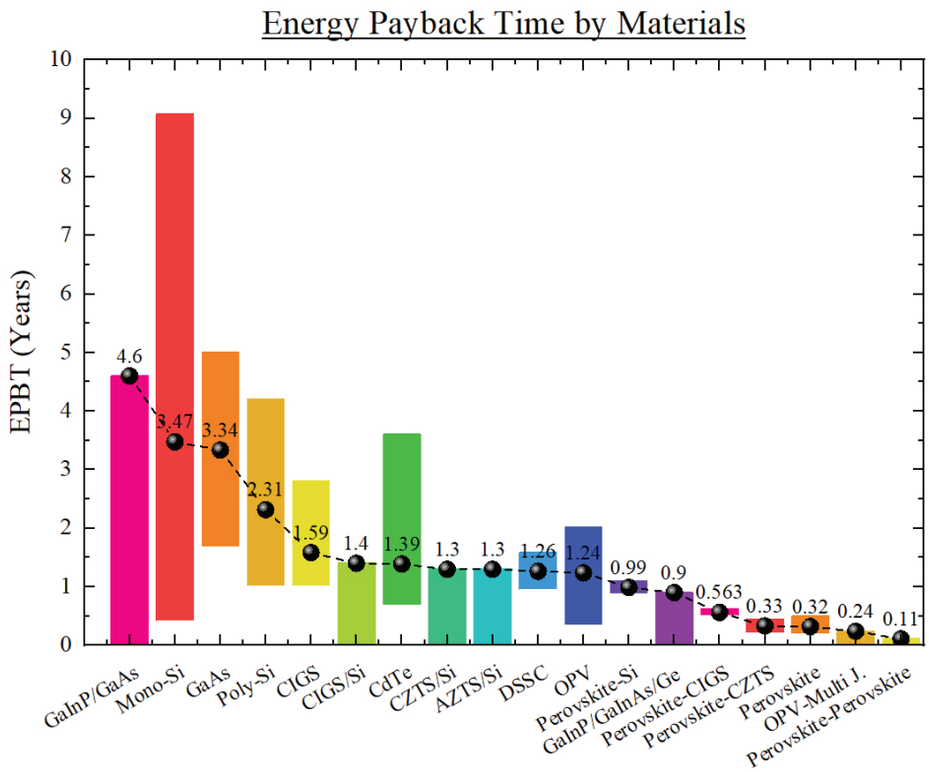

Figure 10: *EPBT corresponding to each material.*

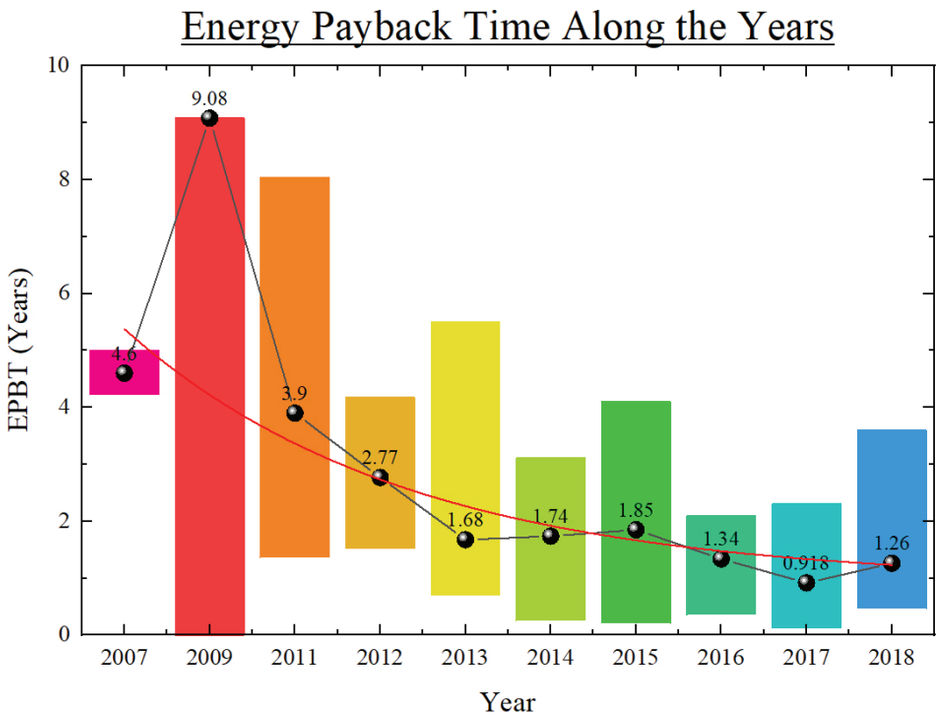

Figure 11: *EPBT along the years with its corresponding average values and tendency.*

Figure 12: *EPBT in Brazil using a low-cost solar system [107].*

Energy Return on Energy Invested

ERoEI in solar cells

Another important parameter to be assessed is the ERoEI, which refers to the ratio between the energy generated and given to commercial usage and the input system energy along its lifetime, since cradle to its final dead use which can be recycled [108]. Having this data into consideration, the results from 19 different materials from 2012 to 2018 are considered (Table 4) and this parameter is graphed with respect to different materials (Figure 13), obtaining that the ERoEI varies from 5.2 to 16.9; however, as it is known that silicon panels are the most common, it can be taken in a range between 8.5 and 10.4 which are the average values for monocrystalline and polycrystalline silicon panels.

Table 4: *ERoEI studies.*

Material	ERoEI	Reference	Year
Poly-Si	4.83	[79]	2012
CdTe	13.33	[80]	2012
CIGS	7.14	[80]	2012
DSSC	12.67	[80]	2012
Mono-Si	6	[109]	2012
Poly-Si	6	[109]	2013
CdTe	12	[109]	2014
Mono-Si	16.1	[90]	2014
Poly-Si	19.1	[90]	2014
CdTe	34.2	[101]	2015
CIGS	19.9	[101]	2015
Mono-Si	8.7	[101]	2015
Poly-Si	11.6	[101]	2015
CdTe	8	[110]	2016
Mono-Si	3.3	[110]	2017
Mono-Si	8.45	[111]	2017
Perovskite-CIGS	9.2	[104]	2018
Perovskite-CZTS	8.1	[104]	2018
Perovskite-Si	5.2	[104]	2018

ERoEI of solar cells in front of Brazilian grid

The range of solar cells obtained earlier has to be compared with those values corresponding to other energies, especially non-renewable energies, and some studies are shown in Table 5 and graphed (Figure 14) together with solar cells data, which were divided into two, only silicon solar cells (Solar-Si) and the average between solar cell materials (Solar-System).

If the Brazilian energy grid was analysed, it could be possible to notice that only 22.10% of the total energy is produced by thermoelectrical source, which is the most common pollutant (Figure 15). Also, as shown in Figure 14, the ERoEI could be reduced from a range between 18.3 and 13.1 (thermoelectrical plants from fossil fuels) to 9.45, which has to be re-

Table 5: *Different energies and their ERoEI.*

Energy	ERoEI	Reference	Year
Oil and gas	5.02	[113]	2007
Oil and gas	10.65	[113]	2007
Oil and gas	16	[114]	2008
Oil and gas	13	[114]	2008
Oil and gas	20	[114]	2009
Gas	20	[114]	2009
Coal	12	[108]	2010
Coal	16	[108]	2010
Oil	5.9	[108]	2010
Oil	5	[108]	2010
Gas	4.8	[108]	2010
Gas	8.2	[108]	2010
Oil and gas	10	[115]	2010
Coal	27	[115]	2010
Coal	28	[116]	2012
Oil and gas	17	[116]	2012
Hydroelectric	84	[116]	2012
Coal	30	[117]	2013
Gas	28	[117]	2013
Hydroelectric	35	[117]	2013
Coal	12	[108]	2015
Gas	11	[110]	2016
Coal	3	[110]	2016
Oil	1.7	[110]	2016
Hydroelectric	58	[110]	2016

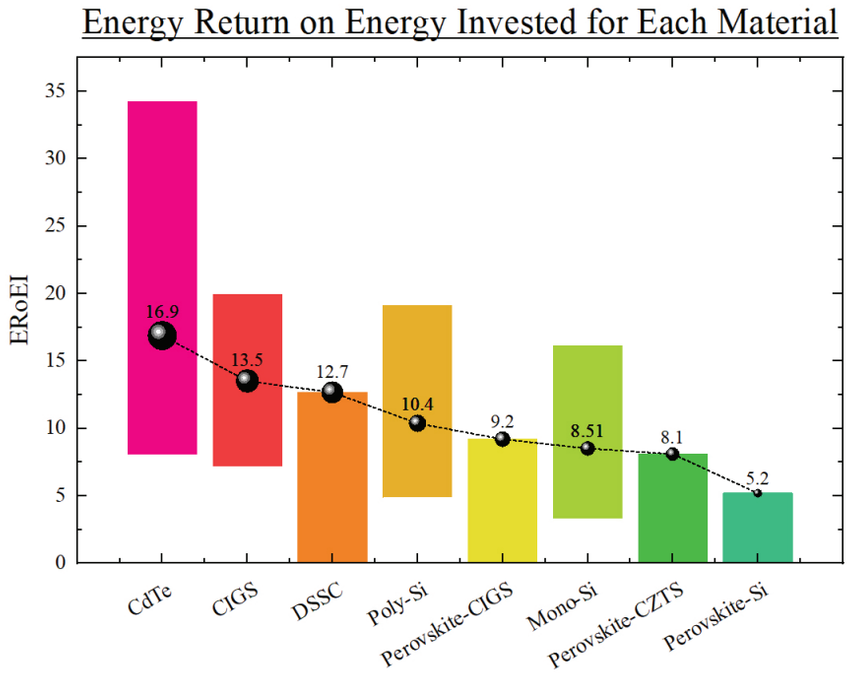

Figure 13: *ERoEI corresponding to different materials and their average.*

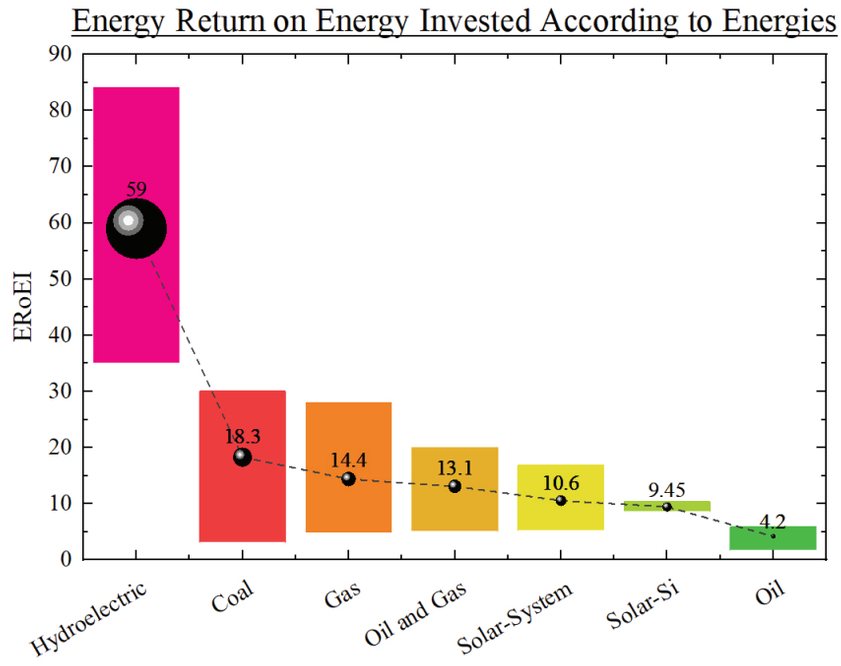

Figure *14: Different energies and their ERoEI.*

duced further. However, analysing the total energy capacity in Brazil which is 156.4 GW [9], getting its maximum peak in the same month (70.66 GW) [112] and having thermoelectrical potential energy as 34.56 GW, then without this energy, the total capacity in Brazil would be 121.84 GW. Therefore, even when the ERoEI of solar cells is lower than the thermoelectrical

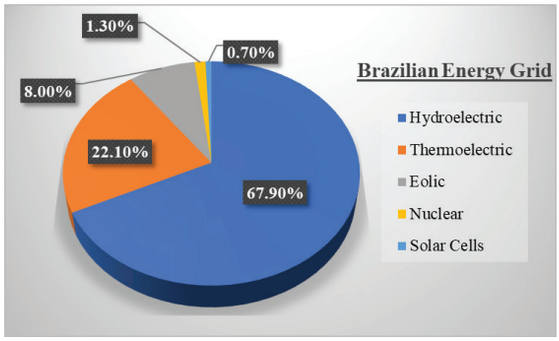

Figure *15: Brazilian energy grid (March 2018).*

plants, the country would be stable if thermoelectrical plants were substituted by solar cells.

The Brazilian Scenario

Potentiality of the territory

The four important parameters to be evaluated in the performance of a green energy have been analysed; however, the economical aspect and application potentiality of the region have to be investigated. First, the irradiance is analysed (Figure 16) where Brazil is compared with Europe, obtaining similar, and even better, values, compared with other countries, such as Portugal, Spain and Germany, where the solar energy has been applied [118]. Also, the potential system that could exist in Brazil is 5153 Wh/m^2 [119], and knowing they are of the country (8.52 × 1012 m^2) the potential energy is 43.96 PWh (4.396 × 1016 Wh). Compared with the maximum energy demand (≈85,000 GW) [120], it is 0.085 PW and 0.193% of the potentiality of solar cells energy; therefore, this result might be translated as 0.193% of the Brazilian territory could supply the energy demand.

Economic aspect

Another point is the economic aspect. It was analysed how could cost the energy by MWh, obtaining the levelised cost of energy (LCOE), in 2019, with the corresponding value of solar energy 45.7 US$/MWh, compared with 39.1 US$/MWh in hydroelectrical industry, 104.3 US$/MWh for thermoelectrical plant using coal and 46.3 US$/MWh when the thermoelectrical plant is used for natural gas [121].

On the other hand, in 2015, the cost in Brazil for solar energy was studied, getting around 175 US$/MWh [10], but using the tendency from 2015 to 2019 it could be reduced from around 0.6 to 0.244 US$/Wp [8], the value being 40.67% compared with the value 4 years ago. Therefore, it could be thought that in Brazil, nowadays, the projected value for solar

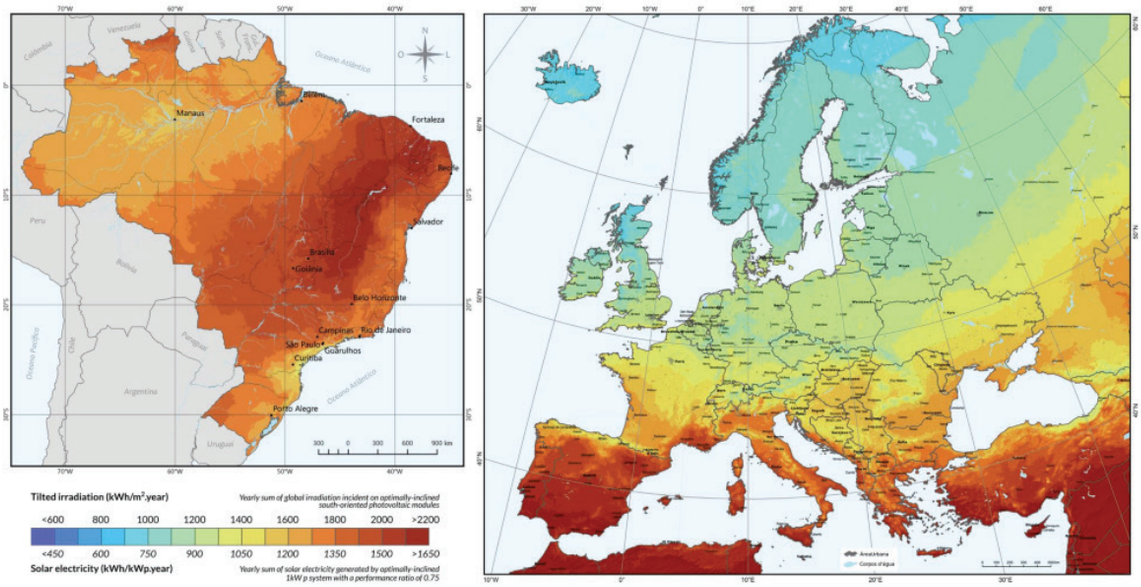

Figure 16: *Solar irradiance in Brazil (left) and in Europe (right) [118].*

energy could cost 71.17 US$/MWh which is more competitive. Also, another studied value for Brazil is the price of carbon thermal plant-with a value between 70.9 and 100.6 US$/MWh [71], being better using the solar energy.

Conclusions

In addition to all those mentioned and explained earlier, five critical points were analysed, observing the behaviour of solar cells and how they could act in the Brazilian scenario, and they are summarised below.

CO_2 emissions: In this point, the emission generated by different solar panels along their lifetime was obtained, from the factory to the grave getting values from 19.8 to 71.3 CO_2 g/kWh and being much lower than the energy from coal (943 CO_2 g/kWh). For this reason, if Brazil substitutes its fossil fuels to solar energy, the emissions could be reduced from 437 to 29.7 Mt of CO_2 by year, which is 6.8% of the actual emissions.

EPBT: Here, the time to recover all the used energy by solar panels varies from 0.11 to 4.6 years and in Brazil the value is around 3 to 4 years. There are improvements every year, having in consequence a reduction of this value. Also, they are good values that some companies offer a warranty of 25 years.

ERoEI: One of the most remarkable points was that photovoltaic panels can be compared with fossil fuels, showing better values than oil.

Efficiency: The efficiency has been a point with a constant increase every year, reaching 20% of efficiency easily, being rival to Brazilian thermoelectrical plants.

Cost and irradiance: Analysing the Brazilian case directly, the photovoltaic panels are more expensive than in Europe; nonetheless, they show a cheaper price than energy from coal. Also, the irradiance in Brazil is thus big that it is needed 0.2% of their territory to supply the national energy demand.

Finally, the solar energy presents low CO_2 emissions, a fast payback time, good efficiency and lower prices every year showing how green it could be, and in the Brazilian case it is perfectly suitable because of all those points mentioned earlier, and the Brazilian territory presents a wonderful irradiance potential.

Acknowledgements

First, we acknowledge PUCRS because without the university this paper could have not happened. Also, we acknowledge CAPES, due to the scholarships received from them, which let us being at PUCRS.

References

[1] IPCC, "Climate Change 2014 Synthesis Report Summary for Policymakers," 2014.

[2] M. Zhang and S. Bachu, "Review of integrity of existing wells in relation to CO_2 geological storage: What do we know?," *International Journal of Greenhouse Gas Control,* vol. 5, pp. 826–840, 2011.

[3] J.Y. Lee, M.S. Yu, K.H. Cha, S.Y. Lee, T.W. Lim and T. Hur, "A study on the environmental aspects of hydrogen pathways in Korea," *International Journal of Hydrogen Energy,* vol. 34, no. 20, pp. 8455–8467, 2009.

[4] H. Kim, K. Cha, V.M. Fthenakis, P. Sinha and T. Hur, "Life cycle assessment of cadmium telluride photovoltaic (CdTe PV) system," *Solar Energy,* vol. 103, pp. 74–88, 2014.

[5] Y. Wang, S. Zhou and H. Huo, "Cost and CO_2 reductions of solar photovoltaic power generation in China: Perspectives for 2020," *Renewable and Sustainable Energy Reviews,* vol. 39, pp. 370–380, 2014.

[6] R. Kannan, K.C. Leong, H.K. Ho and C. Tso, "Life cycle assessment study of solar PV systems: An example of a 2.7 kWp distributed solar PV system in Singapore," *Solar Energy,* vol. 8, no. 5, 2006.

[7] J. Peng, L. Lu and H. Yang, "Review on life cycle assessment of energy payback and greenhouse gas emission of solar photovoltaic systems," *Renewable and Sustainable Energy Reviews,* vol. 19, pp. 255–274, 2013.

[8] ITRPV, "International Technology Roadmap for Photovoltaic Results 2018," ITRPV, 2019.

[9] Operador Nacional do Sistema Elétrico, "ONS," March 2018. [Online]. Available: http://ons.org.br/Paginas/resultados-da-operacao/historico-da-operacao/capacidade_instalada.aspx. [Accessed 7 April 2019].

[10] A. Ferreira, S.S. Kunh, K.C. Fagnani, T.A. De Souza, C. Tonezer, G. Dos Santos and C.H. Coimbra-Araújo,

"Economic overview of the use and production of photovoltaic solar energy in brazil," *Renewable and Sustainable Energy Reviews,* vol. 81, 2018.

[11] P. d. Jong, T.B. Barreto, C.A. Tanajura, D. Kouloukoui, K.P. Oliveira-Esquerre, A. Kiperstok and E.A. Torres, "Estimating the impact of climate change on wind and solar energy in Brazil using a South American regional climate model," *Renewable Energy,* 2019.

[12] F. Martins, E. Pereira, S. Silva, S. Abreu and S. Colle, "Solar energy scenarios in Brazil, Part one: Resource assessment," *Energy Policy,* vol. 36, pp. 2853–2864, 2088.

[13] F. Martins, R. Rüther, E. Pereira and S. Abreu, "Solar energy scenarios in Brazil. Part two: Photovoltaics applications," *Energy Policy,* vol. 36, pp. 2865–2877, 2008.

[14] O.O. Ogbomo, E.H. Amalu, N. Ekere and P. Olagbegi, "A review of photovoltaic module technologies for increased performance in tropical climate," *Renewable and Sustainable Energy Reviews,* vol. 75, 2017.

[15] S.A. Kalogirou, "Photovoltaic Systems- Processes and Systems," in *Solar Energy Engineering,* Academic Press, 2009, pp. 469–519.

[16] R.H. Plante, "Solar Photovoltaic Systems," in *Solar Energy, Photovoltaics, and Domestic Hot Water A Technical and Economic Guide for Project Planners, Builders, and Property Owners*, 2014, pp. 75–92.

[17] A.E. Brooks, "Solar Energy: Photovoltaics," in *Future Energy (Second Edition) - Improved, Sustainable and Clean Options for our Planet*, T.M. Letcher, Ed., 2014, pp. 383–404.

[18] L. Dobrzański, A. Drygała, M. Giedroć and M. Macek, "Monocrystalline silicon solar cells applied in photovoltaic system," *The Journal of Achievements in Materials and Manufacturing Engineering,* vol. 53, no. 1, July 2012.

[19] "Tindo Solar," [Online]. Available: http://www.tindosolar.com.au/learn-more/poly-vs-mono-crystalline/. [Accessed 4 April 2019].

[20] W. Hoffma and T. Pellkofer, "Thin films in photovoltaics: Technologies and perspectives," *Thin Solid Films,* vol. 520, pp. 4094–4100, 2012.

[21] S. Sundaram, K. Shanks and H. Upadhyaya, "Thin Film Photovoltaics," in *A Comprehensive Guide to Solar Energy Systems With Special Focus on Photovoltaic Systems*, 2018, pp. 361–370.

[22] Y. Tang, "Copper Indium Gallium Selenide Thin Film Solar Cells," in *Nanostructured Solar Cells*, 2017.

[23] N. Ekins-Daukes, "III-V Solar Cells," in *Solar Cell Materials: Developing Technologies*, G. Conibeer and A. Willoughby, Eds., 2014.

[24] S. Bhatia, "Solar photovoltaic systems," in *Advanced Renewable Energy Systems*, 2014, pp. 144–157.

[25] C. Amador-Bedolla, R. Olivares-Amaya, J. Hachmann and A. Aspuru-Guzik, "Organic Photovoltaics," in *Informatics for Materials Science and Engineering Data-driven Discovery for Accelerated Experimentation and Application*, 2013, pp. 423–442.

[26] T. Ibn-Mohammed, S.C.L. Koh, I.M. Reaney, A. Acquaye, G. Schileo, K.B. Mustapha and R.M. Greenough, "Perovskite solar cells: An integrated hybrid lifecycle assessment and review in comparison with other photovoltaic technologies," *Renewable and Sustainable Energy Reviews,* vol. 80, 2017.

[27] N.A. Ludin, N.I. Mustafa, M.M. Hanafiah, M.A. Ibrahim, M.A.M. Teridi, S. Sepeai, A. Zaharim and K. Sopian, "Prospects of life cycle assessment of renewable energy from solar photovoltaic technologies: A review," *Renewable and Sustainable Energy Reviews,* vol. 96, pp. 11–28, 2018.

[28] ISO, "ISO 14044 - Environmental management – Life cycle assessment – Requirements and guidelines," 2006.

[29] ISO, "ISO 14040 - Environmental management – Life cycle assessment – Principles and framework," 2006.

[30] S. Gerbinet, S. Belboom and A. Léonard, "Life Cycle Analysis (LCA) of photovoltaic panels: A review," *Renewable and Sustainable Energy Reviews,* vol. 38, pp. 747–753, 2014.

[31] L.S. Mattos, S.R. Scully, M. Syfu, E. Olson, L. Yang, C. Ling, B.M. Kayes and G. He, "New module efficiency record: 23.5% under 1-sun illumination using thin-film single-junction GaAs solar cells," in *2012 38th IEEE Photovoltaic Specialists Conference*, 2012.

[32] S. Ahmed, K.B. Reuter, O. Gunawan, L. Guo, L.T. Romankiw and H. Deligianni, "A High Efficiency Electrodeposited Cu2ZnSnS4 Solar Cell," *Advanced Energy Materials,* vol. 2, no. 2, pp. 253–259, 2012.

[33] Z. Wang, P. Han, H. Lu, H. Qian, L. Chen, Q. Meng, N. Tang, F. Gao, Y. Jiang, J. Wu, W. Wu, H. Zhu, J. Ji, Z. Shi, A. Sugianto, L. Mai, B. Hallam and S. Wenham, "Advanced PERC and PERL production cells with 20.3% record efficiency for standard commercial p-type silicon wafers," *Progress in Photovoltaics,* vol. 20, no. 3, pp. 260–268, 2012.

[34] B. Shin, Y. Zhu, N.A. Bojarczuk, S.J. Chey and S. Guha, "Control of an interfacial MoSe2 layer in Cu2ZnSnSe4 thin film solar cells: 8.9% power conversion efficiency with a TiN diffusion barrier," *Applied Physics Letters,* vol. 101, no. 5, 2012.

[35] F. Karg, "High Efficiency CIGS Solar Modules," *Energy Procedia,* vol. 15, pp. 275–282, 2012.

[36] L. Han, A. Islam, H. Chen, C. Malapaka, B. Chiranjeevi, S. Zhang, X. Yang and M. Yanagida, "High-efficiency dye-sensitized solar cell with a novel co-adsorbent," *Energy & Environmental Science,* vol. 5, no. 3, 2012.

[37] T. Yang, M. Wang, C. Duan, X. Hu, L. Huang, J. Peng, F. Huang and X. Gong, "Inverted polymer solar cells with 8.4% efficiency by conjugated polyelectrolyte," *Energy & Environmental Science,* vol. 5, no. 8, 2012.

[38] D. Shahrjerdi, S.W. Bedell, C. Bayram, C.C. Lubguban, K. Fogel, P. Lauro, J.A. Ott, M. Hopstaken, M. Gayness and D. Sadana, "Ultralight High-Efficiency Flexible InGaP/(In)GaAs Tandem Solar Cells on Plastic," *Advanced Energy Materials,* vol. 3, no. 5, pp. 566–571, 2013.

[39] W. Wang, M.T. Winkler, O. Gunawan, T. Gokmen, T.K. Todorov, Y. Zhu and D.B. Mitzi, "Device Characteristics of CZTSSe Thin-Film Solar Cells with 12.6% Efficiency," *Advanced Energy Materials,* vol. 4, no. 7, 2014.

[40] H.-S. Kim, J.-W. Lee, N. Yantara, P.P. Boix, S.A. Kulkarni, S. Mhaisalkar, M. Grätzel and N.-G. Park, "High Efficiency Solid-State Sensitized Solar Cell-Based on Submicrometer Rutile TiO2 Nanorod and CH3NH3PbI3 Perovskite Sensitizer," *Nano Letters,* vol. 13, no. 6, p. 2412–2417, 2013.

[41] M.G. Panthani, J.M. Kurley, R.W. Crisp, T.C. Dietz, T. Ezzyat, J.M. Luther and D.V. Talapin, "High Efficiency Solution Processed Sintered CdTe Nanocrystal Solar Cells: The Role of Interfaces," *Nano Letter,* vol. 14, no. 2, p. 670–675, 2014.

[42] A. Chirilă, P. Reinhard, F. Pianezzi, P. Bloesch, A.R. Uhl, C. Fella, L. Kranz, D. Keller, C. Gretener, H. Hagendorfer, D. Jaeger, S.N. Rolf Erni, S. Buecheler and A.N. Tiwari, "Potassium-induced surface modification of Cu(In,Ga)Se2 thin films for high-efficiency solar cells," *Nature Materials,* vol. 12, pp. 1107–111, 2013.

[43] T.K. Todorov, O. Gunawan, T. Gokmen and D.B. Mitzi, "Solution-processed Cu(In,Ga)(S,Se)2 absorber yielding a 15.2% efficient solar cell," *Progress in Photovoltaics,* vol. 21, no. 1, pp. 83–87, 2013.

[44] B. Shin, O. Gunawan, Y. Zhu, N.A. Bojarczuk, S.J. Chey and S. Guha, "Thin film solar cell with 8.4% power conversion efficiency using an earth-abundant Cu2ZnSnS4 absorber," *Progress in Photovoltaics,* vol. 21, no. 1, pp. 72–76, 2012.

[45] C. Chen, W. Chang, K. Yoshimura, K. Ohya, J. You, J. Gao, Z. Hong and Y. Yang, "An Efficient Triple-Junction Polymer Solar Cell Having a Power Conversion Efficiency Exceeding 11%," *Advanced Materials,* vol. 26, no. 32, pp. 5670–5677, 2012.

[46] Y.S. Lee, T. Gershon, O. Gunawan, T.K. Todorov, T. Gokmen, Y. Virgus and S. Guha, "Cu2ZnSnSe4 Thin-Film Solar Cells by Thermal Co-evaporation with 11.6% Efficiency and Improved Minority Carrier Diffusion Length," *Advanced Energy Materials,* vol. 5, no. 7, 2015.

[47] D.-Y. Son, J.-H. Im, H.-S. Kim and N.-G. Park, "11% Efficient Perovskite Solar Cell Based on ZnO Nanorods: An Effective Charge Collection System," *The Journal of Physical Chemistry,* vol. 118, no. 30, p. 16567–16573, 2014.

[48] X. Ye, S. Zou, K. Chen, J. Li, J. Huang, F. Cao, X. Wang, L. Zhang, X. Wang, M. Shen and X. Su, "18.45%-Efficient Multi-Crystalline Silicon Solar Cells with Novel Nanoscale Pseudo-Pyramid Texture," *Advanced Functional Materials,* vol. 24, no. 42, 2014.

[49] K. Masuko, M. Shigematsu, T. Hashiguchi, D. Fujishima, M. Kai, N. Yoshimura, T. Yamaguchi, Y. Ichihashi, T. Mishima, N. Matsubara, T. Yamanishi, T. Takahama, M. Taguchi, E. Maruyama and Shing, "Achievement of More Than 25% Conversion Efficiency With Crystalline Silicon Heterojunction Solar Cell," *Shingo Okamoto,* vol. 4, no. 6, p. IEEE Journal of Photovoltaics, 2014.

[50] H. Zhou, Q. Chen, G. Li, S. Luo, T.-b. Song, H.-S. Duan, Z. Hong, J. You, Y. Liu and Y. Yang, "Interface engineering of highly efficient perovskite solar cells," *Science,* vol. 345, no. 6196, 2014.

[51] W. Ke, G. Fang, J. Wang, P. Qin, H. Tao, H. Lei, Q. Liu, X. Dai and a. X. Zhao, "Perovskite Solar Cell with an Efficient TiO2 Compact Film," *Applied Materials Interfaces,* vol. 6, no. 18, 2014.

[52] S.-H. Liao, H.-J. Jhuo, P.-N. Yeh, Y.-S. Cheng, Y.-L. Li, Y.-H. Lee, S. Sharma and S.-A. Chen, "Single Junction Inverted Polymer Solar Cell Reaching Power Conversion Efficiency 10.31% by Employing Dual-Doped Zinc Oxide Nano-Film as Cathode Interlayer," *Nature,* 2014.

[53] C. Tao, S. Neutzner, L. Colella, S. Marras, A.R.S. Kandada, M. Gandini, M.D. Bastiani, G. Pace, L. Manna, M. Caironi, C. Bertarelliac and A. Petrozza, "17.6% stabilized efficiency in low-temperature processed planar perovskite solar cells," *Energy & Environmental Science,* vol. 8, pp. 2365–2370, 2015.

[54] S. Zhang, X. Pan, H. Jiao, W. Deng, J. Xu, Y. Chen, P.P. Altermatt, A. i. o. Z. Feng and P.J. Verlinden, in *2015 IEEE 42nd Photovoltaic Specialist Conference (PVSC)*, New Orleans, 2015.

[55] E. Kobayashi, Y. Watabe, R. Hao and T.S. Ravi, "High efficiency heterojunction solar cells on n-type kerfless mono crystalline silicon wafers by epitaxial growth," *Applied Physics Letter,* vol. 106, 2015.

[56] W. Nie, H. Tsai, R. Asadpour, J.-C. Blancon, A.J. Neukirch, G. Gupta, J.J. Crochet, M. Chhowalla, S. Tretiak, M.A. Alam, H.-L. Wang and A.D. Mohit, "High-efficiency solution-processed perovskite solar cells with millimeter-scale grains," *Science,* vol. 347, no. 6221, pp. 522–525, 2015.

[57] N. Ahn, D.-Y. Son, I.-H. Jang, S.M. Kang, M. Choi and N.-G. Park, "Highly Reproducible Perovskite Solar Cells with Average Efficiency of 18.3% and Best Efficiency of 19.7% Fabricated via Lewis Base Adduct of Lead(II) Iodide," *Journal of The American Chemical Society,* vol. 137, no. 27, p. 8696–8699, 2015.

[58] T.M. Friedlmeier, P. Jackson, A. Bauer, D. Hariskos, O. Kiowski, R. Wuerz and M. Powalla, "Improved photocurrent in Cu(In,Ga)Se2 solar cells: From 20.8% to 21.7% efficiency," in *2015 IEEE 42nd Photovoltaic Specialist Conference (PVSC)*, New Orleans, 2015.

[59] Z. He, B. Xiao, F. Liu, H. Wu, Y. Yang, S. Xiao, C. Wang, T.P. Russell and Y. Cao, "Single-junction polymer solar cells with high efficiency and photovoltage," *Nature Photonics,* vol. 9, p. 174–179, 2015.

[60] R.M. Geisthardt, M. Topič and J.R. Sites, "Status and Potential of CdTe Solar-Cell Efficiency," *IEEE Journal of Photovoltaics,* vol. 5, no. 4, pp. 1217 - 1221, 2015.

[61] W. Zhao, D. Qian, S. Zhang, S. Li, O. Inganäs, F. Gao and J. Hou, "Fullerene-Free Polymer Solar Cells with over 11% Efficiency and Excellent Thermal Stability," *Advanced Materials,* vol. 28, p. 4734–4739, 2016.

[62] I. Åberg, G. Vescovi, D. Asoli, U. Naseem and J.P. Gilboy, "A GaAs Nanowire Array Solar Cell With 15.3% Efficiency at 1 Sun," *IEEE Journal of Photovoltaics,* vol. 6, no. 1, pp. 185–190, 2016.

[63] W. Deng, F. Ye, Z. Xiong, D. Chen, W. Guo, Y. Chen, Y. Chen, P.P. Altermatt, Z. Feng and P.J. Verlinden, "Development of High-efficiency Industrial p-type Multi-crystalline PERC Solar Cells with Efficiency Greater Than 21%," *Energy Procedia,* vol. 92, pp. 721–729, 2016.

[64] A. Tihane, M. Boulaid, L. Boughamrane, M. Nya, K. Bouabid and A. Ihlal, "Modeling and seasonal performance analysis of two monocrystalline and polycrystalline silicon photovoltaic modules," *Materials Today: Proceedings,* vol. 3, no. 7, pp. 2562–2569, 2016.

[65] Y. Zhao, M. Boccard, S. Liu, J. Becker, X.-H. Zhao, C.M. Campbell, E. Suarez, M.B. Lassise, Z. Holman and Y.H. Zhang, "Monocrystalline CdTe solar cells with open-circuit voltage over 1 V and efficiency of 17%," *Nature Energy,* vol. 1, 2016.

[66] Y. Jiang, H. Shen, T. Pu, C. Zheng, Q. Tang, K. Gao, J. Wu, C. Rui, Y. Li and Y. Liu, "High efficiency multi-crystalline silicon solar cell with inverted pyramid nanostructure," *Solar Energy,* vol. 142, no. 15, pp. 91–96, 2017.

[67] W. Zhao, S. Li, H. Yao, S. Zhang, Y. Zhang, B. Yang and J. Hou, "Molecular Optimization Enables over 13% Efficiency in Organic Solar Cells," *Journal of the American Chemical Society,* vol. 139, no. 21, pp. 7148–7151, 2017.

[68] T. Duong, Y. Wu, H. Shen, J. Peng, X. Fu, D. Jacobs, E. Wang, T.C. Kho, K.C. Fong, M. Stocks, E. Franklin, A. Blakers, N. Zin, K. McIntosh, W.Li,Y. Cheng, T.P. White, K. Weber and K. Catchpole, "Rubidium Multication Perovskite with Optimized Bandgap for Perovskite-Silicon Tandem with over 26% Efficiency," *Advanced Energy Materials,* vol. 7, no. 14, 2017.

[69] J. Wachsmuth, B. Dransfeld, H. Fekete, V. Duscha, M. Hagemann, N. Höhne, M. Reuter and F. Röben, "How Energy Efficiency Cuts Costs for a 2-Degree-Future," Fraunhofer Institute for Systems and Innovation Research ISI, 2015.

[70] G.C. Institute, "Efficiency in Thermal Power Generation," [Online]. Available: https://hub.globalccsinstitute.com/publications/energy-efficiency-technologies-overview-report/5-efficiency-thermal-power-generation. [Accessed 11 April 2019].

[71] E. d. P. E. (EPE), "Energia Termelétrica: Gás Natural, Biomassa, Carvão, Nuclear," Empresa de Pesquisa Energética (EPE), Rio de Janeiro, 2015.

[72] ANEEL, "Brazilian Energy Grid," 2018. [Online]. Available: http://www2.aneel.gov.br/aplicacoes/capacidadebrasil/OperacaoCapacidadeBrasil.cfm. [Accessed 26 April 2019].

[73] IEMA, "Uso de água em termoelétricas," 2016.

[74] I. E. Agency, "CO_2 emissions from fuel combustion," 2017.

[75] R. García-Valverde, C. Miguel, R. Martínez-Béjar and A. Urbina, "Life cycle assessment study of a 4.2 kWp stand-alone photovoltaic system," *Solar Energy,* vol. 83, no. 9, pp. 1434–1445, 2009.

[76] A. Dominguez-Ramos, M. Held, R. Aldaco, M. Fischer and A. Irabien, "Prospective CO_2 emissions from energy supplying systems: photovoltaic systems and conventional grid within Spanish frame conditions," *The International Journal of Life Cycle Assessment,* vol. 15, no. 6, pp. 554–566, 2010.

[77] M. Ito, K. Komoto and K. Kurokawa, "Life-cycle analyses of very-large scale PV systems using six types of PV modules," *Current Applied Physics,* vol. 10, no. 2, 2010.

[78] N. Espinosa, R. García-Valverde, A. Urbina and F.C. Krebs, "A life cycle analysis of polymer solar cell modules prepared using roll-to-roll methods under ambient conditions," *Solar Energy Materials and Solar Cells,* vol. 95, no. 5, pp. 1293–1302, 2011.

[79] U. Desideri, S. Proietti, F. Zepparelli, P. Sdringola and S. Bini, "Life Cycle Assessment of a ground-mounted 1778 kWp photovoltaic plant and comparison with traditional energy production systems," *Applied Energy,* vol. 97, pp. 930–943, 2012.

[80] M.L. Parisi, A. Sinicropi and R. Basosi, "Life cycle assessment of thin film non conventional photovoltaics: the case of dye sensitized solar cells," in *The 25th International Conference on Efficiency, Cost, Optimization, Simulation and Environmental Impact of Energy Systems*, 2012.

[81] M.J.R. Perez, V. Fthenakis, H. Kim and A.O. Pereira, "Façade–integrated photovoltaics: a life cycle and performance assessment case study," *Progress in Photovoltaics,* vol. 20, no. 8, pp. 975–990, 2012.

[82] M.J.D. Wild-Scholten, "Energy payback time and carbon footprint of commercial photovoltaic systems," *Solar Energy Materials and Solar Cells,* vol. 119, pp. 296–305, 2013.

[83] U. Desideri, F. Zepparelli, V. Morettini and E. Garroni, "Comparative analysis of concentrating solar power and photovoltaic technologies: Technical and environmental evaluations," *Applied Energy,* vol. 102, pp. 765–784, 2013.

[84] V.M. Fthenakis and H.C. Kim, "Life cycle assessment of high-concentration photovoltaic systems," *Progress in Photovoltaics,* vol. 21, no. 3, pp. 379–388, 2013.

[85] J.D. Bergesen, G.A. Heath, T. Gibon and S. Suh, "Thin-Film Photovoltaic Power Generation Offers Decreasing Greenhouse Gas Emissions and Increasing Environmental Co-benefits in the Long Term," *Environmental Science & Technology,* vol. 48, no. 16, pp. 9834–9843, 2014.

[86] N. Espinosa and F.C. Krebs, "Life cycle analysis of organic tandem solar cells: When are they warranted?," *Solar Energy Materials and Solar Cells,* vol. 120, pp. 692–700, 2014.

[87] H. Kim, K. Cha, V.M. Fthenakis, P. Sinha and T. Hur, "Life cycle assessment of cadmium telluride photovoltaic (CdTe PV) systems," *Solar Energy,* vol. 103, pp. 78–88, 2014.

[88] M.L. Parisi, S. Maranghi and R. Basosi, "The evolution of the dye sensitized solar cells from Grätzel prototype to up-scaled solar applications: A life cycle assessment approach," *Renewable and Sustainable Energy Reviews,* vol. 39, pp. 124–138, 2014.

[89] N. Stylos and C. Koroneos, "Carbon footprint of polycrystalline photovoltaic systems," *Journal of Cleaner Production,* vol. 64, pp. 639–645, 2014.

[90] D. Yue, F. You and S.B. Darling, "Domestic and overseas manufacturing scenarios of silicon-based photovoltaics: Life cycle energy and environmental comparative analysis," *Solar Energy,* vol. 105, pp. 669–678, 2014.

[91] Y. Fu, X. Liu and Z. Yuan, "Life-cycle assessment of multi-crystalline photovoltaic (PV) systems in China," *Journal of Cleaner Production,* vol. 85, pp. 180–190, 2015.

[92] J. Gong, S.B. Darling and a. F. You, "Perovskite photovoltaics: life-cycle assessment of energy and environmental impacts," *Energy & Environmental Science,* vol. 8, no. 7, pp. 1953–1968, 2015.

[93] W. Chen, J. Hong, X. Yuan and J. Liu, "Environmental impact assessment of monocrystalline silicon solar photovoltaic cell production: a case study in China," *Journal of Cleaner Production,* vol. 112, pp. 1025–1032, 2016.

[94] D. Hengevoss, C. Baumgartner, G. Nisato and C. Hugi, "Life Cycle Assessment and eco-efficiency of prospective, flexible, tandem organic photovoltaic module," *Solar Energy,* vol. 131, pp. 317–327, 2016.

[95] G. Hou, H. Sun, Z. Jiang, Z. Pan, Y. Wang, X. Zhang, Y. Zhao and Q. Yao, "Life cycle assessment of grid-connected photovoltaic power generation from crystalline silicon solar modules in China," *Applied Energy,* vol. 164, pp. 882–890, 2016.

[96] M.M. Lunardi, S. Moore, J.P. Alvarez-Gaitan, C. Yan, X. Hao and R. Corkish, "A comparative life cycle assessment of chalcogenide/Si tandem solar modules," *Energy,* vol. 145, pp. 700–709, 2018.

[97] W. Luo, Y.S. Khoo, A. Kumar, J.S.C. Low, Y.Li,Y.S. Tan, Y. Wang, A.G. Aberle and S. Ramakrishna, "A comparative life-cycle assessment of photovoltaic electricity generation in Singapore by multicrystalline silicon technologies," *Solar Energy Materials and Solar Cells,* vol. 174, pp. 157–162, 2018.

[98] Enerdata, "Global Energy Statistical Yearbook 2018," 2018. [Online]. Available: https://yearbook.enerdata.net/co2-fuel-combustion/CO2-emissions-data-from-fuel-combustion.html. [Accessed 7 April 2019].

[99] N.J. Mohr, J.J. Schermer, M.A.J. Huijbregts, A. Meijer and L. Reijnders, "Life cycle assessment of thin-film GaAs and GaInP/GaAs solar modules," *Progress in Photovoltaics,* vol. 15, no. 2, pp. 163–179, 2007.

[100] A. Sumper, M. Robledo-García, R. Villafáfila-Robles, J. Bergas-Jané and J. Andrés-Peiró, "Life-cycle assessment of a photovoltaic system in Catalonia (Spain)," *Renewable and Sustainable Energy Reviews,* vol. 15, no. 8, pp. 3888–3896, 2011.

[101] K.P. Bhandari, J.M. Collier, R.J. Ellingson and D.S. Apul, "Energy payback time (EPBT) and energy return on energy invested (EROI) of solar photovoltaic systems: A systematic review and meta-analysis," *Renewable and Sustainable Energy Reviews,* vol. 47, pp. 133–141, 2015.

[102] I. Celik, A.B. Phillips, Z. Song, Y. Yan, R.J. Ellingson, M.J. Heben and D. Apul, "Environmental analysis of perovskites and other relevant solar cell technologies in a tandem configuration," *Energy & Environmental Science,* vol. 10, pp. 1874–1884, 2017.

[103] P. Wu, X. Ma, J. Ji and Y. Ma, "Review on Life Cycle Assessment of Energy Payback of Solar Photovoltaic Systems and a Case Study," *Energy Procedia,* vol. 105, pp. 68–74, 2017.

[104] I. Celik, A.B. Philips, Z. Song, Y. Yan, R.J. Ellingson, M.J. Heben and D. Apul, "Energy Payback Time (EPBT) and Energy Return on Energy Invested (EROI) of Perovskite Tandem Photovoltaic Solar Cells," *IEEE Journal of Photovoltaics,* vol. 8, no. 1, pp. 305 - 309, 2018.

[105] P. Rajput, Y.K. Singh, G. Tiwari, O. Sastry, S. Dubey and K. Pandey, "Life cycle assessment of the 3.2 kW cadmium telluride (CdTe) photovoltaic system in composite climate of India," *Solar Energy,* vol. 159, pp. 415–422, 2018.

[106] D.C. Jordan and S.R. Kurtz, "Photovoltaic Degradation Rates – An Analytical Review," National Renewable Energy Laboratory, 2012.

[107] F.R. Martins and E.B. Pereira, "Enhancing information for solar and wind energy technology deployment in Brazil," *Energy Policy,* vol. 39, no. 7, pp. 4378–4390, 2011.

[108] A. Arvesen and E.G. Hertwich, "More caution is needed when using life cycle assessment to determine energy return on investment (EROI)," *Energy Policy,* vol. 76, pp. 1–6, 2015.

[109] M. Raugei, P. Fullana-i-Palmer and V. Fthenakis, "The energy return on energy investment (EROI) of photovoltaics: Methodology and comparisons with fossil fuel life cycles," *Energy Policy,* vol. 45, pp. 576–582, 2012.

[110] M. Raugei and E. Leccisi, "A comprehensive assessment of the energy performance of the full range of electricity generation technologies deployed in the United Kingdom," *Energy Policy,* vol. 90, pp. 45–59, 2016.

[111] M. Raugei, S. Sgouridis, D. Murphy, V. Fthenakis, R. Frischknecht, C. Breyer, U. Bardi, C. Barnhart, A. Buckley, M. Carbajales-Dale, D. Csala, M. de Wild-Scholten, G. Heath, A. Jæger-Waldau, C. Jones, A. Keller, E. Leccisi, P. Mancarella, N. Pearsall, A. Siegel, W. Sinke and P. Stolz, "Energy Return on Energy Invested (ERoEI) for photovoltaic solar systems in regions of moderate insolation: A comprehensive response," *Energy Policy,* vol. 102, pp. 377–384, 2017.

[112] Operador Nacional do Sistema Elétrico, "ONS," March 2018. [Online]. Available: http://ons.org.br/Paginas/resultados-da-operacao/historico-da-operacao/carga_energia.aspx. [Accessed 7 April 2019].

[113] M.C. Guilford, C.A. Hall, P. O'Connor and C.J. Cleveland, "A New Long Term Assessment of Energy Return on Investment (EROI) for U.S. Oil and Gas Discovery and Production," *Sustainability,* vol. 3, no. 10, pp. 1866–1887, 2011.

[114] J. Freise, "The EROI of Conventional Canadian Natural Gas Production," *Sustainability,* vol. 3, no. 11, pp. 2080–2104, 2011.

[115] Y. Hu, C.A. Hall, J. Wang, L. Feng and A. Poisson, "Energy Return on Investment (EROI) of China's conventional fossil fuels: Historical and future trends," *Energy,* vol. 54, pp. 352–364, 2013.

[116] J. Lambert, C. Hall, S. Balogh, A. Poisson and A. Gupta, "EROI of Global Energy Resources Preliminary Status and Trends," 2012.

[117] D. Weißbach, G. Ruprecht, A. Huke, K. Czerski, S. Gottlieb and A.H. Hussein, "Energy intensities, EROIs (energy returned on invested), and energy payback times of electricity generating power plants," *Energy,* vol. 52, pp. 210–221, 2013.

[118] E. Bueno, "Overview of Solar Energy in Brazil," Fundación de Apoyo a la Investigación del Estado de São Paulo, São Paulo, 2017.

[119] INPE, "Brazilian Atlas of Solar Energy," 2017.

[120] H.H. Zurn, D. Tenfen, J.G. Rolim, A. Richter and I. Hauer, "Electrical energy demand efficiency efforts in Brazil, past, lessons learned, present and future: A critical review," *Renewable and Sustainable Energy Reviews,* vol. 67, pp. 1081–1086, 2017.

[121] U.S. Energy Information Administration, "Levelized Cost and Levelized Avoided Cost of New Generation Resources in the Annual Energy Outlook 2019," 2019.

Original scientific paper

Received: Jul 17, 2018
Accepted: Mar 08, 2019
DOI: 10.2478/rmzmag-2019-0004

Electrical Resistivity Tomography for Sustainable Groundwater Development in a Complex Geological Area

Električna Upornostna Tomografija v Razvoju Sonaravne Oskrbe z Vodo v Kompleksnem Geološkem Območju

Adedibu Sunny Akingboye, Isaac Babatunde Osazuwa, Muraina Zaid Mohammed
Department of Earth Sciences, Adekunle Ajasin University, P.M.B. 001, Akungba-Akoko, Ondo State, Nigeria
adedibu.akingboye@aaua.edu.ng, iosazuwa@yahoo.com, muraina.mohammed@aaua.edu.ng

Abstract

Electrical resistivity tomography (ERT) was used for delineating significant subsurface hydrogeological features for sustainable groundwater development in Etioro-Akoko area, Southwestern Nigeria. This study was necessitated by challenges posed on groundwater supplies from wells and boreholes in Etioro-Akoko and the neighbouring fast growing towns and villages. Field data were acquired over the area with ABEM Lund Resistivity Imaging System and were subsequently processed and inverted through RES2DINVx64 software. Results showed four distinct subsurface layers: topsoil, weathered layer, fractured bedrock and fresh bedrock (basal unit). Localised bedrock depressions occasioned by fracturing and deep weathering of less stable bedrock minerals were delineated with resistivity and thickness values ranging from 50 to 650 Ωm and 12 to > 25 m, respectively. The localised depressions mirrored uneven bedrock topography and served as the preferential groundwater storage and hydrogeological zones in the area. The two hydrogeological zones significant for groundwater development included overburden-dependent aquifers and fractured dependent bedrock aquifers. It was, therefore, concluded that groundwater storage potential was depended on hydrogeological zones particularly at major localised bedrock depressions where fractures and groundwater recharges/discharges were evident. Wells and boreholes were proposed at bedrock depressions with thickness value not less than 12 and > 25 m, respectively, for enhanced groundwater sustainability and quality assurance in the area.

Key words: electrical resistivity tomography (ERT), subsurface conduits, hydrogeological zones, groundwater, Etioro-Akoko.

Povzetek

Električno upornostno tomografijo (Electrical Resistivity Tomography, ERT) so uporabili za omejitev hidrogeoloških značilnosti, pomembnih za oceno potenciala talne vode na območju Etioro-Akoko v jugozahodni Nigeriji. Potrebo po študiji so sprožile težave oskrbe s podtalnico iz vodnjakov in vrtin v Etioro-Akoku in sosednjih naglo razvijajočih se mestih in vaseh. Terenske podatke s področja so pridobili z ABEM Lundovim upornostnim prikazovalnim sistemom in jih zatem obdelali z računalniško opremo RES2DINVx64. Rezultati so nakazali štiri različne podpovršinske nivoje: vrhnja tla, preperinska plast, kamnine razpokane podlage in nepreperele kamnine podlage. Lokalizirane depresije v podlagi, nastale z drobljenjem in globokim preperevanjem manj obstojnih mineralov v kamninah podlage so omejili z dobljenimi vrednostmi upornosti in debeline na 50–650 Ωm oziroma 12 – > 25 m. Ugotovljene depresije, ki nakazujejo neravno površino podlage, predstavljajo ugodne hidrogeološke cone za zbiranje vode na raziskovanem območju. Dve hidrogeološki coni, obetavni za razvoj vodnih virov, obsegata vodonosnike, vezane na prekritje in vodonosnike v razpokani kamnini podlage. Raziskavo so zato sklenili z ugotovitvijo, da je potencial vodnih zalog odvisen od hidrogeoloških con zlasti v glavnih ugotovljenih depresijah podlage, kjer so očitni razpokanost in sledovi gibanja podtalnice. Lokacije vodnjakov in vrtin so predlagali nad depresijami podlage z vrednostmi debeline vsaj 12 m, oziroma nad 25 m za zagotovitev boljše trajnosti in kakovosti oskrbe z vodo na tem območju.

Ključne besede: električna upornostna tomografija (ERT), podzemni kanali, hidrogeološke cone, podtalnica; Etioro-Akoko.

Introduction

Globally, people express a desire for abundant and potable groundwater for consumption and other purposes. Thus, exploration for the abundance of this hidden resource in the subsurface necessitates advancement in electrical resistivity imaging via the development of fast automated multi-electrode array systems and new inversion algorithms [1–5]. These systems clearly reveal the characteristics and conditions of the subsurface geology for sustainable groundwater development, particularly in the areas of complex geology.

Exploitation of groundwater in basement terrain depends on weathering thickness and bedrock structures such as grabens and fractures. Generally, overburden thicknesses are somewhat very thin across some sections of the Southwestern Basement Complex of Nigeria [6]. This development leaves aquifer systems in substantial parts of the terrain with few localised subsurface structures and bedrock depressions serving as conduits for groundwater recharge and storage, respectively. However, the unconfined and near-surface nature of most aquifer systems within the basement terrain may be challenged by contamination arising from surficial impurities and run-offs. Therefore, groundwater deficit due to thin overburden and vulnerability is evident in the study area.

Geophysical investigations using both conventional electrical resistivity and other integrated geophysical probes have been carried out in parts of Etioro-Akoko with its adjoining towns in the recent past. The efforts have been to determine aquifer regimes and potentials, as well as subsurface geology [6–8]. Moreover, borehole projects such as *Kamomi* water project and mechanised handpump borehole have been conducted in the study area. However, these investigations have not fully solved the challenges posed on groundwater supplies in the area. Lack of good knowledge of the subsurface strata, bedrock topography, bedrock structures and degree of the susceptibility of the aquifers in the area are possible challenges. Therefore, groundwater resources in Etioro-Akoko must be developed and exploited in a sustainable manner.

Studies have shown that there exists a direct relationship between electrical resistivity and geological factors such as soil water content, lithology, size and pores, as well as fluid saturating the pores [6, 9, 10]. Earth materials are generally resistive, and the presence of groundwater decreases the resistivity of total saturated volume of rock/deposit. Consequently, ERT remains a versatile technique for evaluating these geological factors for groundwater development and sustainability. ERT is a non-invasive surveying technique that images the subsurface from electrical resistivity measurements made at the earth's surface along a series of constant traverse separation with increasing electrode spacing at successive station positions [1, 5, 11]. This study, therefore, aimed at determining viable subsurface hydrogeological zones for groundwater development in Etioro-Akoko, a complex geological area where a layer of aquitard developed on the thin overburden, through the delineation of subsurface layers, structures/weak zones, and aquifer geometry and productivity.

Location and Geological Setting

Etioro-Akoko is located along Owo – Ikare-Akoko road in Akoko Southwest Local Government Area of Ondo State, Nigeria. It is located between latitudes 07°26′ and 07°27′ N and longitudes 005°43′and 005°44′ E (Figure 1). The adjoining towns include the following: Ayegunle and Oba-Akoko to the South, Supare-Akoko to the West, Akungba-Akoko to the North and Iwaro and Oka-Akoko to the Northeast of the study area.

Etioro-Akoko is located in the tropical rainforest belt of Nigeria. The climate is dictated by the southwestern monsoon winds characterised by the tropical wet and dry climate. Rain starts in March with peaks during July to September while the dry season starts between October and November with annual mean variation between 1000 and 1500 mm [12]. The general pattern of drainage in the area is dendritic except in few cases where trellis patterns are observed. The area is characterised by three distinct landforms, which include hills, plains and valleys; these together constitute the topographic relief of the area, generally with aver-

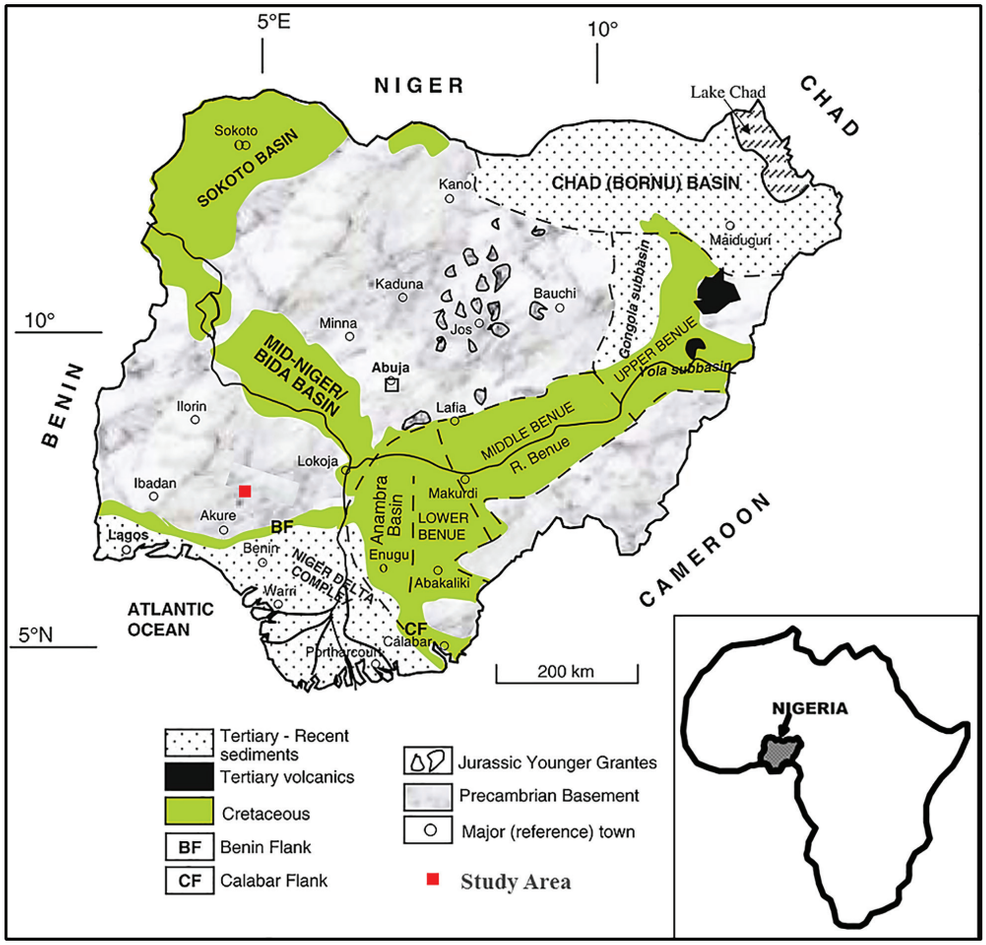

Figure 1: *Geological map of Nigeria showing the study area (modified after [14]) [Inset: Map of Africa showing Nigeria].*

age elevation between 320 and 350 m above the mean sea level.

The area is underlain by rocks of the Migmatite-Gneiss Complex of the Precambrian Southwestern basement rocks of Nigeria [13] (Figure 1). The rocks in the area include granite gneiss which is the widely spread rock and other minor intrusives such as aplite, pegmatite and vein quartz. The rocks show great variations in grain size and in mineral composition. The overburden in the area is generally thin. The basement outcrops in few places across the area. The basement rocks of the area have undergone at least two episodes of tectonic deformation, which have helped in the development of a series of simple and complex structures in the rocks.

Materials and Methods

The study involved a reconnaissance geological survey for field observation of the various rock types in the area. This was followed by geo-reference/establishment of geophysical traverses across the areas of interest to produce a geophysical acquisition map and selection of the array/protocol type for the resistivity field measurements.

Field Measurements

The ABEM Lund Resistivity Imaging System was used for the data collection. The field data acquisition employed the use of ABEM Tetrameter SAS 4000 Resistivity Meter, two sets of 100 m cable reels with pinouts of 5 m spacing, a 64-electrode unrestricted electrode selector (switching unit) – ES 10–64C, a set of 41 stainless steel electrodes and a car battery. Cables

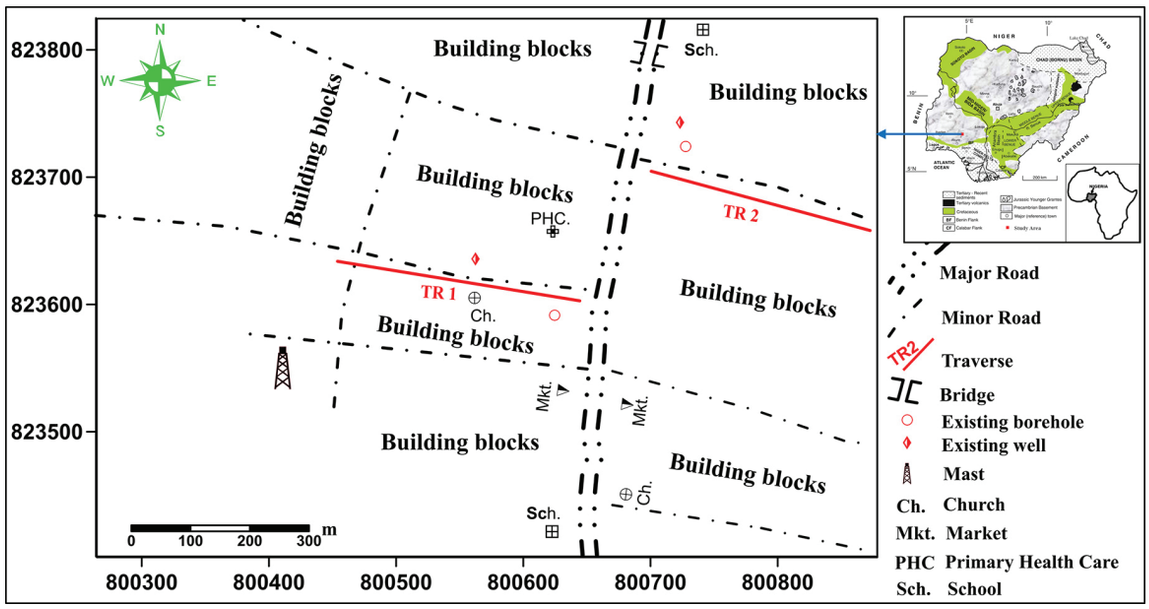

Figure 2: *Data acquisition map of the study area.*

were laid out and pinouts were connected to the grounded electrodes via cable jumpers. This was followed by the connection of the two terminal ends of the multicore cables to the electrode selector, and the electrode selector was then connected to the resistivity metre by a special cable. The resistivity metre was switched on after being connected to the car battery to select the array protocol (array configuration), and other measurement settings were adjusted for the measurements to be taken automatically.

In this study, the Wenner protocol was employed for the tomographic surveying due to its high signal-to-noise ratio and resolution. Measurements were acquired along two traverses (TRs 1 and 2) in the study area (Figure 2). TR 1 was laid approximately in E–W direction along *Iyanu Jesu Street*, where the *Kamomi* borehole was situated while TR 2 was laid about 50 m away along a street vertically opposite to TR 1. The topography of TR 2 is rugged, showing a low-lying basement outcrop of about 15 m extent from station 100 m and plunges downward towards the eastern end of the traverse. Each of the traverses (TRs 1 and 2) has a spread length of 200 m, with a spacing of 5 m between the respective electrodes.

Field Data Processing and Inversion

The field converted apparent resistivity data from .s4k to .dat format through SAS 4000 Utility software were reduced, inverted and modelled sequentially by using RES2DINVx64 software. The data reduction phase involved the extermination of bad data points with too large or too small resistivity values corresponding to high or low spikes, respectively. Bad data points were due to the failure of the relays at one of the electrodes, poor electrode contact arising from dry soil, and/or shorting across the cables.

Least square inversion modelling was employed to determine the subsurface apparent resistivity distribution through adjusted change and inversion setting parameters. The adjusted parameters included model refinement using cell widths of half electrode spacing for optimum results and finite element method of 4 nodes to achieve accurate calculated apparent resistivity values, particularly for large resistivity contrasts. L_1 norm (robust inversion) was employed for more stable results [15, 16]. The vertical/horizontal flatness ratio filter of 0.5 was used for better resolution of anomaly appearances. Damping factor of 0.1 with minimum of 0.02 (one-fifth of the initial value) was used to stabilise the inversion process and to increase the certainty that the identified anomalies actually exist [17, 18]. Inverse model convergence

RMS limit below 10% was chosen for a maximum of 10 iterations. Finally, standard Gauss–Newton method was used for the calculation of sensitivity matrix.

Results and Discussion

The detailed interpretation of inverse model resistivity section from electrical imaging demands considerable practical experience of the method on the one hand, and on the other hand, a sound knowledge of the geology of the area under consideration. The interpretation of the inverse model resistivity sections is done using the geological information (rocks and structural features) of the study area and environs provided in the works of Refs. [6-8] and other information from failed hand-dug wells; such information includes but not limited to the nature of subsurface constituents and depth to bedrock. The above mentioned information with the range of resistivity values encountered in the inverse model resistivity sections, a detailed subsurface interpretation of the inverse model resistivity sections, is obtained.

The 2D resistivity inversion considerably provides robust image of the subsurface geology. It places the structures at approximately their correct depths and provides acceptable estimates of their true resistivities. The 2D inverse model resistivity sections of high resolution and quality target definition for the area investigated are shown in Figures 3 and 4.

A 2D inverse model resistivity section of TR 1 along *Iyanu Jesu* Street in Etioro-Akoko is shown in Figure 3. The subsurface is characterised by four distinct subsurface layers of varying resistivity responses. The first layer (topsoil) is characterised by surficial soil typical of clay medium with resistivity generally below 100 Ωm and thickness of about 0.4–2.0 m. The second layer is characterised by weathered materials typical of clayey sand/sandy clay/sand with resistivity ranging from 50 to 450 Ωm and depth of about 12 m. The partially weathered bedrock intersperse the topsoil at stations 17–20 m, 120–125 m and 170 m and beyond. Stations 10–60 m, 100–120 m and 150–160 m along the traverse are delineated as possible weak zones marked by resistivity patterns ranging from 480 to 800 Ωm. These sections are indicative of the partially weathered/fractured bedrock (third layer). The fresh bedrock which is the basal unit has resistivity that is generally greater than 1000 Ωm. The fresh bedrock is marked by gently undulating to broad crested surface. It extends to the surface between stations 160 and 170 m. The topsoil and weathered bedrock form the overburden with thickness ranging from < 4 to 15 m. Sections with high overburden thicknesses are characterised by localised bedrock depressions occasioned by fracturing (F–F') and deep weathering of less stable rock minerals such as feldspar and amphiboles. The zones are suggestive of the accumulation and conduits for groundwater. Stations 40 m and 110 m of TR 1 display these characteristics. The aquifer characteristics and geometries of these two groundwater zones have potential for high groundwater yield due to aquifer characteristics such as low clayey content, trough-like structures and appreciable overburden thicknesses as conduits and groundwater storage/collecting centres. However, other stations on the traverse are zones with shallow overburden thicknesses. The groundwater productivity level of the *Kamomi* community borehole, which is the most productive borehole in the area, corroborates the success rate of the result for station 40 m.

Figure 4 shows the inverse model resistivity section of TR 2 along a rugged street from surface observation. TR 2 shows four distinct subsurface layers of varying resistivity responses. The first layer (topsoil) is characterised by surficial soil typical of clayey medium, with resistivity generally below 150 Ωm and thickness of about 0.3–1.5 m. The topsoil is interspersed by high resistivity responses particularly at stations 20–60 m, 120–135 m and 145 m. The second layer is characterised by weathered materials typical of clayey sand/sandy clay/sand with resistivity ranging from 160 to 650 Ωm. The weathered materials show evidence of low resistivity response that extends to the depth of about 25 m and 11 m at stations 85–128 m and 157 m westward respectively. This low resistivity response is suggestive of saturated weathered bodies. Partially weathered/fractured bedrock (third layer) is delineated at stations 130–160 m with resistivity values

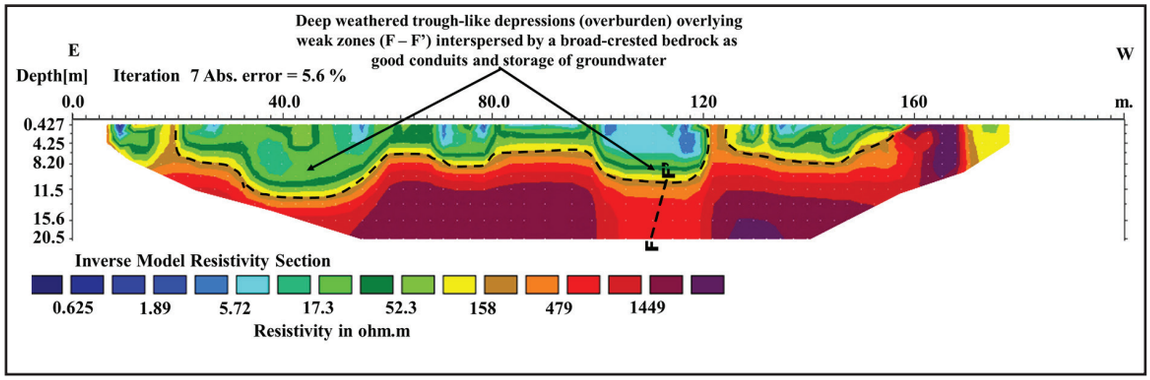

Figure 3: *The inverse model resistivity section of traverse (TR) 1.*

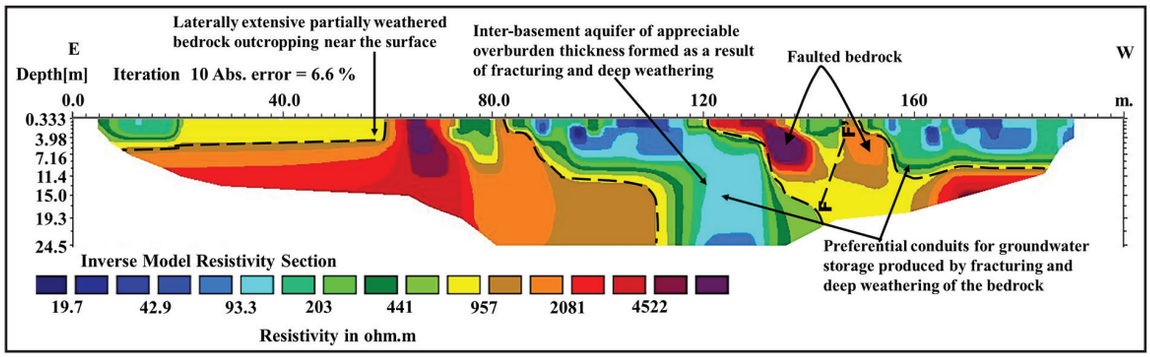

Figure 4: *The inverse model resistivity section of traverse (TR) 2.*

of 660–900 Ωm. The basal unit which is the fresh bedrock is characterised by resistivity generally above 1000 Ωm. The fresh bedrock is discontinued at some sections by fractures and deep weathered troughs to produce localised depressions which may have resulted from active fluids/seepages and other geological activities. The localised depressions extend beyond the depth of 24.5 m and 12 m at stations 110–128 m and 160 m westward respectively. These delineated features enhance the groundwater potential of the area in spite of its ruggedness.

Station 120 m of TR 2 is considered as probable zone for the siting of borehole because the zone is suggestive of high groundwater yield owing to good degree of water saturation and overburden thickness greater than 25 m. From station 160 m westward, points are considered to have moderate groundwater yield. The mechanised hand-pump borehole is situated about 20 m northward from these stations.

As shown in Figures 3 and 4, two hydrogeological/aquifer zones were identified. The hydrogeological zones include the following: overburden-dependent aquifers on the fairly and highly deep weathered bedrock, and fractured dependent aquifers on the fractured bedrock column. The hydrogeological zones are significant for high yielding groundwater boreholes and wells in the area. Possible hydrogeological zones aside the locations of the existing wells/boreholes include zones between stations 90 m and 120 m of TR 1 and stations 110 m, 120 m and 160 m of TR 2. These zones are characterised by zones of weaknesses (fractured/faulted bedrocks) with localised deep and elongated weathered bedrock troughs (bedrock depressions) of appreciable overburden thicknesses not less than 12 m. The deep and elongated weathered/fractured bedrock depressions are envisaged for high groundwater storage and discharge tendencies in few places in the study area.

Conclusion

In this study, multi-electrode electrical resistivity tomography was employed for delineating the subsurface hydrogeological features for sustainable groundwater development to ameliorate the challenges posed on groundwater supplies in Etioro-Akoko, southwestern Nigeria. The results of the inverse model resistivity sections along two traverses generally show four subsurface layers. These include the topsoil, fairly to highly weathered layer, partially weathered/fractured bedrock and fresh bedrock. The overburden section is composed of constituents of the topsoil and weathered/partially weathered bedrock. The overburden-dependent and fractured dependent aquifers were delineated as the hydrogeological zones/aquifer regimes in the area. The depth to bedrock varied from less than 4 m to greater than 12 m. Deep and elongated weathered columns are indicative of localised bedrock depressions in few places. The depressions are occasioned by weathering of less stable minerals such as amphibole, feldspar and mica within the bedrock. These features enhance the channelling and accumulation of groundwater. It is envisaged that the proposed hydrogeological zones are significant for the siting of wells and boreholes in addition to the existing servicing wells and boreholes for sustainable groundwater supply in Etioro-Akoko community.

However, indiscriminate siting of dumpsite practices be disabused in the study area as the thin overburden covers (< 4 m) in most places may not act as effective barriers/filters against surface contaminants or leachates that degrade groundwater quality. Biochemical and microbial analyses of groundwater may be carried out to ascertain the quality of groundwater for consumption by inhabitants in the study area.

Acknowledgements

The authors are grateful to Messers Abimbola C. Ogunyele, Olaniyi R. Ijaleye and Moses Salami for their field assistance. Anonymous reviewers are acknowledged for comments that have made the manuscript more readable.

References

[1] Griffiths, D.H., Barker, R.D. (1993): Two-dimensional resistivity imaging and modeling in areas of complex geology. *Journal of Applied Geophysics*, 29, pp. 211–226.

[2] Barker, R., Moore, J. (1998): The application of time-lapse electrical tomography in groundwater studies. *Leading Edge*, 17, pp. 1454–1458.

[3] Osazuwa, I.B., Chii, E.C. (2010): Two-dimensional electrical resistivity survey around the periphery of an artificial lake in Precambrian Basement Complex of Northern Nigeria*. International Journal of Physical Sciences*, 5(3), pp. 238–245.

[4] Costall, A., Harris, B., Pigois, J.P. (2018): Electrical Resistivity Imaging and the Saline Water Interface in High-Quality Coastal Aquifers. *Survey Geophysics*, pp. 1–64. https://doi.org/10.1007/s10712-018-9468-0.

[5] Akingboye, A.S., Ogunyele, A.C. (2019): Insight into seismic refraction and electrical resistivity tomography techniques in subsurface investigations. *The Mining-Geology-Petroleum Engineering Bulletin*, 34(1), pp. 93–111. doi: 10.17794/rgn.2019.1.9.

[6] Aminu, M.B. (2015): Electrical Resistivity Imaging of a Thin Clayey Aquitard Developed on Basement Rocks in Parts of Adekunle Ajasin University Campus, Akungba-Akoko, South-western Nigeria. *Environmental Research, Engineering and Management,* 71(1), pp. 47–55. http://dx.doi.org/10.5755/j01.erem.71.1.9016.

[7] Mohammed, M.Z., Ogunribido, T.H.T., Adedamola, T.F. (2012): Electrical Resistivity Sounding for Subsurface Delineation and Evaluation of Groundwater Potential of Araromi Akungba-Akoko. Ondo State, Southwestern Nigeria. *Journal of Environment and Earth Science*, 2(7), pp. 29–40.

[8] Okpoli, C., Saba, E.A. Oduneye, O.C. (2014): Geophysical Investigation of Groundwater Regime: Case Study of Etioro-Akoko, Southwestern Nigeria. *Environmental Research, Engineering and Management*, 69(3), pp. 29–39. http://dx.doi.org/10.5755/j01.erem.69.3.5334.

[9] Abu-Hassanein, Z., Benson, C., Blotz, L. (1996). Electrical resistivity of compacted clays. *Journal of Geotechnical Engineering*, 122, pp. 397–406. https://doi.org/10.1061/(ASCE)0733-9410.

[10] Hassan, A.A. (2014): Electrical Resistivity Method for Water Content Characterisation of Unsaturated Clay Soil. Durham Theses, Durham University. Available from: Durham e-theses online. http://etheses.dur.ac.uk/10806/.

[11] Merritt, A.J. (2014): 4D Geophysical Monitoring of Hydrogeology Precursors to Landslide Activation. PhD Thesis, School of Earth and Environmental, University of Leeds, UK. 1–276.

[12] Ojo, S.O. (2000): Factor productivity in maize production in Ondo state Nigeria. *Applied Tropical Agriculture*, 23, pp. 25–26.

[13] Rahaman, M.A. (1989): Review of the Basement Geology of South-Western Nigeria. In: Kogbe, C.A. (eds.). *Geology of Nigeria* (2nd eds.). Rockview Nige Limited, Jos., pp. 39–56.

[14] Obaje N.G. (2009): *Geology and Mineral Resources of Nigeria*. Heidelberg, Berlin: Springer-Verlag. 221 p. doi: 10.1007/978-3-540-92685-6.

[15] Zhou, B., Dahlin, T. (2003): Properties and effects of measurement errors on 2D resistivity imagine survey. Near surface geophysics, 1(3), 105–117.

[16] Dahlin, T., Zhou, B. (2004): A numerical comparison of 2D resistivity imaging using 10 electrode arrays. *Geophysical Prospecting*, 52, 379–398.

[17] deGroot-Hedlin, C., Constable, S.C. (1990): Occam's inversion to generate smooth two-dimensional models from magnetotelluric data. *Geophysics*, 55, 1613–1624.

[18] Loke, M.H. (2004): Rapid 2D resistivity and IP inversion using the least-square method. Manual for RES2DINV, version 3.54. 53 p.

Original scientific paper

Received: Jul 10, 2019
Accepted: Sep 02, 2019
DOI: 10.2478/rmzmag-2019-0010

Lean Concept in Small and Medium Enterprises

Lean koncept v malih in srednjih podjetjih

Zorana Tanasić[1,*], Goran Janjić[1], Borut Kosec[2]

[1] University of Banja Luka, Faculty of Mechanical Engineering, Bulevar Vojvode Stepe Stepanovića 71, 78 000 Banja Luka, Bosnia and Herzegovina

[2] University of Ljubljana, Faculty of Natural Sciences and Engineering, Aškerčeva cesta 12, 1000 Ljubljana, Slovenia

* zorana.tanasic@mf.unibl.org

Abstract

The Lean concept is recognisable by how fast innovations are implemented and production processes are improved. Likewise, analysis of the implementation of Lean concepts so far has shown that Lean methods and tools cannot be applied to small and medium enterprises (SMEs) in the same measure as they can be applied to large enterprises.

This paper aims to present a critical review of the implementation of Lean concepts in SMEs with the claim that Lean concept can be successfully applied in all branches of industry, provided that the Lean concept is fully understood, and it's meaning, principles and practice. Given that SMEs have limited resources, they often face difficulties during the implementation of all Lean tools and methods.

Depending on the type of improvement in Kaizen activities, the Poka Yoke and Jidoka tools should be applied. Every improvement in the production process needs to be standardised as soon as possible so that the processes can become more continuous and efficient.

Key words: Lean concept, SMEs, Model, Methods, Tools

Povzetek

Lean koncept je poznan po hitrosti implementacije inovacij in napredovanja procesa proizvodnje. Prav tako kaže analiza dosedanje implementacije Lean koncepta, da Lean metode in orodja niso v enaki meri uporabni v malih in srednjih podjetjih (MSP) v primerjavi z velikimi.

Cilj tega dela je prikazati kritičen pogled na uporabo Lean koncepta v malih in srednjih podjetjih ob predpostavki, da se lahko Lean koncept uspešno uporabi v vseh vejah industrije, vendar pod Pogojem da je koncept v popolnosti apliciran oziroma njegov pojem, principi in prakse. Glede na to, da imajo mala in srednja podjetja omejene vire, se pogosto soočajo s težavami pri implementaciji vseh Lean orodij in metod.

V odvisnosti od vrste napredovanja v Kaizen aktivnostih je potrebno uporabiti orodja Poka Yoke in Jidoka. Vsak napredek v proizvodnem procesu je potrebno čimprej standardizirati, da postanejo procesi kontinuirni in učinkovitejši.

Ključne besede: Lean koncept, MSP, Model, Metode, Orodja

Introduction

Business processes and the environment in which the business world is located are changing at a high rate due to globalisation, the Internet, e-commerce, and so on. Companies that do not follow these changes in the business remain far behind their competitors. To establish the realistic basis for the development of the company, continuous communication of management as well as the involvement of all stakeholders is needed. The only way to achieve sustained success is to establish an innovative organisation, which is flexible, quickly adapts to changes in the environment and learns quickly. The key to success lies in establishing an organisational culture in which all employees feel not for the obligation but a need for constant innovation and improvement of their own work. By this approach, employees provide for themselves a secure job and survival on the market.

The management of production systems is very demanding and is often very unpredictable. The company behaves like a living organism, that is, all processes take place simultaneously with one goal, which is survival along with profit. To successfully manage the production enterprice, it is necessary to integrate human, material and financial resources into efficient systems. This is a major challenge because a full understanding of the system is needed with the ability to anticipate the behaviour of the company's macro environment.

Many agree that Japanese companies are one of the best and most effective companies, but no one explains in detail why and how they have become so successful. The most common explanation is their culture and traditions, but their investments in scientific and technical technological research are emphasised as one of the key aspects of their success in the world market. In this paper, it is intended to present and demonstrate that Lean methods and tools can be applied in small and medium enterprises (SMEs). Also, it should be emphasised that the active participation of the management and well-trained staff may contribute to business environment in which problems are solved; occurrence of errors and dissipation in the work process are prevented by the implementation of systematic approach and teamwork.

Literature Review

Many examples of the implementation of Lean production in large enterprises can be found in professional and academically literature, while there is very little literature available on the implementation of Lean concept in SMEs. Only a few authors, such as Achanga et al., White and Conner, recommended the implementation of Lean production in SMEs [1–3]. Most often, management in SMEs is not sure of the results of the implementation of Lean concepts or is not able to invest money in the Lean concept. Studies have shown that SMEs, which adopted the Lean concept, have benefitted through increased competitiveness, faster development of innovations, shorter production cycle, increased flexibility and reduced expenses [4].

However, a large number of authors believe that the introduction of Lean concepts or the implementation of tools and methods to improve productivity conceals only certain problems [5–8] in enterprises' business. For this reason, Hayes [9] argues that the successful realisation of the Lean concept in SMEs requires correct planning before implementation to avoid certain difficulties and problems.

In a study from 2007, Baker and McInturff [10] presented their observations during their visits to a certain number of industrial plants in Southern California where they had conversations with business owners. The authors have emphasised that the small companies are more competitive than the large enterprises, but they continue to face competition, tax burdens, ecological regulations and so on. In such circumstances, the Lean concept can affect small businesses to reduce operating costs and increase productivity. Several research were carried out aiming to get answers to the questions: why don't most SMEs today apply Lean methods? and where do managers of SMEs see difficulties in the implementation of Lean methods?

The results of the research of available literature [11] are as follows:

— Lean methods are not well-known in many companies.
— Companies often try to increase the efficiency of production through the large series that minimises the capacity of machines.

— Lean thinking, if it exists, is applied only in the process of production.
— There is a lack of knowledge in employees and management education.
— Small companies rarely employ qualified workers and there is a necessity of transferring knowledge in small businesses.

Implementation of Lean Concept in SMEs

In a Lean enterprise, noncompliance is seen as an opportunity for improvement and not just something that needs to be identified and eliminated in the work processes. It is an endless journey for perfection through the continuous improvement of the work process. It is carried out through the constant pursuit and implementation of better ways of performing the process in relation to the way it was previously used by Ohno in 1988 and Grasso in 2005. In industrial systems, the Lean concept is based on designing a workflow that is applicable, flexible, consistent and sustainable in space and time [12].
The word Lean is of English origin and it means thin, slim and slender. The term Lean is used to mark a modern and successful business philosophy, or a world-class organisation characteristic of contemporary business. The goal of this philosophy is to enable the company to achieve a satisfactory market position, in the conditions of turbulent competition, the decline in customer loyalty, constant technological innovations, short product lifespan, and so on. For the implementation of Lean concepts in production systems, the necessary abilities have to be developed to give priority to Lean behaviour and Lean thinking. The basic preconditions for creating an environment for the application of the Lean concept are as follows:
— Lean behaviour of management structure and
— Lean thinking of management structure and other employees.

Lean thinking can be described as the ability of people to make effective and efficient solutions that provide profit to organisation and satisfaction to employees and customers. It provides the ability to determine and define activities that create value, to manage them continuously and to perform those activities daily on a more cost-effective and efficient basis. The implementation of Lean production aims to respond the demands of the customers with less human effort, inventory and time and to develop the desired product, that is, to produce a product of superior quality in the most efficient and cost-effective way [13].
Permanent changes in the environment in which companies operate and the trends of the 21st century imposed the need for design/redesign of business systems. These changes have led to further changes of influential factors and requirements based on which the organisations are designed.
Lean thinking can be described as the ability of people to achieve effective solutions that provide a profit to the organisation as well as the satisfaction to employees and consumers. It provides the ability to define all activities that add value to the product from the user's perspective [14]. The Lean concept is a developed model of production management in the context of improving the quality and engineering processes, which performs a process of reorganisation by identifying the following five principles [15]:
1. Defining the value of the product to the customer,
2. Determining the value of the currents,
3. Creating the value of the currents,
4. Implementation of the "pulling" principle and
5. Striving for perfection.

Lean production is a set of methods and techniques that aim to largely reduce any losses occurring during the process of production and during all other processes in the company. These five principles lead to the understanding of Lean philosophy in companies, and their joint application in all processes of the production system can significantly improve the efficiency of the same. To implement the Lean concept, to adopt a new behaviour – *Lean behaviour* and a new way of thinking – *Lean thinking*, ability and will are required. This way the manpower is being developed and training for the use of Lean tools and methods is necessary

for achieving the defined goals of the business system [15].

At the beginning of the 21st century, the application of Lean principles has had a significant impact on many manufacturing companies. Based on the statistics and analysis of the economic importance of SMEs, it can be observed that they are more numerous and generate a significant portion of the total value in the business economy. In economic theory, there is a series of advantages for SMEs compared with large enterprises. SMEs are flexible in terms of products and adapting to the changes in the market. It is up to the managers of SMEs to correctly understand the change process and the application of appropriate skills and techniques to constantly increase the efficiency and effectiveness of the organisation. To survive and to improve their businesses, use of modern tools and quality techniques, as well as concepts and methodology in the management of business systems, is required.

For this reason, at the beginning of the 21st century, SMEs are the subject of research of many authors in their scientific work. The solution to the current crisis is not only of economic importance but also of social and human importance, which requires a radical change of consciousness and this can be achieved by implementing Lean concepts in SMEs.

Based on the data from the Agency for Statistics, B&H has ended the first half of 2017 with 35,710 registered companies, of which 74.7% are micro-enterprises, 18.3% are small enterprises, 6.0% are medium-sized and only 1% are large enterprises, which employ more than 250 workers.

Implementation of Lean concepts in SMEs is one of the ways to increase productivity and competitiveness. After the decision to realise Lean principles in SMEs, managers come up with better results in a very short period of time comparing with what could be achieved in large enterprises. SMEs are more flexible and faster in the implementation of changes due to less bureaucracy and shorter communication links. On the other hand, SMEs are faced with several internal weaknesses and limitations, such as low level of knowledge about new technologies, access to finance, low bargaining power, low productivity, lack of entrepreneurial skills and lack of knowledge regarding the proper management of human resources.

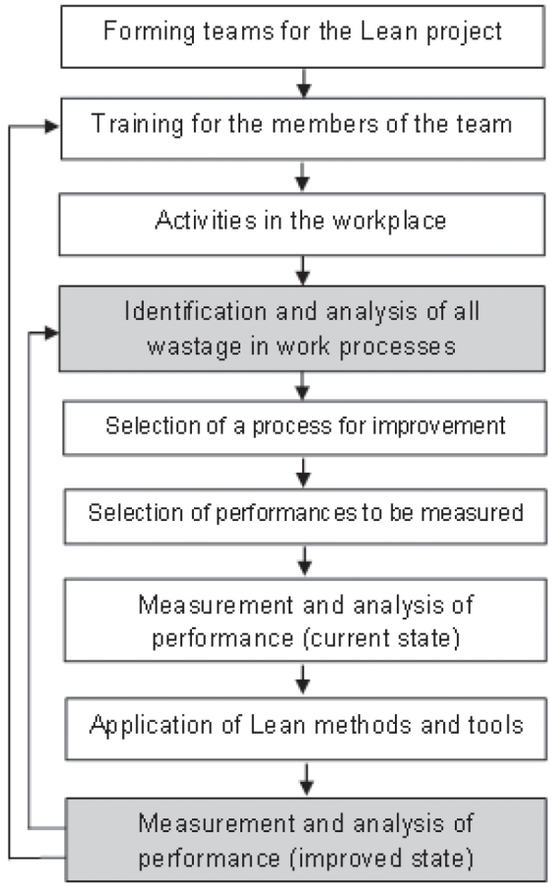

Figure 1: *Model for the implementation of the Lean concept in SMEs [17].*

Aside from the Lean concept, in practice, there are different approaches to creating value in the process of the realisation of the product, such as "pull" manufacturing, total productive maintenance, standardised operation, quality management and so on [16].

Keeping in mind that the availability of material, human and financial resources of SMEs is much lower than that of large enterprises, any additional expense or hiring people for the implementation of the Lean concept has to be planned in detail. Based on these facts, Figure 1 presents the model for the implementation of Lean concepts in SMEs. Beginning of the implementation of Lean concept in SMEs starts with the decision of top management teams to form and implement training for all employees,

which is usually organised by outside consultants [17].
The team should consist of employees from all organisational units (sectors) who will be the first to adopt a new way of thinking, which is Lean business culture. The training should be organised in such a way that as little additional burden is placed on the employees and to make it easier for them to operate in the workplace []. The main objective of the training is to introduce employees with certain methods and tools that will enable them to recognise and see the wastage in their work processes, and to understand the distinction between activities that add value and those that do not add value to the product. The tools that are commonly used by all employees in their daily work are priority matrix, mapping the value stream, the cause and effect diagrams, analysis of five-why and so on.
After successfully completing the training, an identification of a process for improvement is conducted. The emphasis is on finding ways to improve the process so as to enable a quick return on investment for the implementation of the improvement process. This step can be considered as one of the main drivers for the adoption and implementation of Lean principles by the owners and/or managers of companies [16].
Based on the selection of the improvement process, problems are defined and the causes of the problems are identified, after which actions to eliminate the cause or wastage are taken and specific strategies to minimize the wastage are proposed. Also, it is necessary to generate measurable parameters for monitoring the performance of certain processes of the current state, implementation of the improvement methods and monitoring of an improved state.

Lean Methods and Tools in Medium Enterprises

The Lean concept includes a set of principles, methods, techniques and tools that emphasise the identification and elimination of all activities that do not add value, that is, eliminating dissipation from the workflow process in business systems. This develops and empowers human resources to use the Lean tools and methods necessary to achieve the functions of the production system's goal and its pursuit of perfection (Figure 2).

Kaizen

Kaizen is a term composed of two Japanese words: kai (change) and zen (to good), which would mean in free translation – continuous improvement. It represents the way of managing a company focussed on continuous improvement and philosophy according to which every aspect of life should be constantly improved. As the words themselves state, it is necessary to isolate the problem first, then analyse, solve it and ultimately implement the solution. Kaizen is based on the teachings of Edward Deming and his PDCA cycle. Kaizen is a continuous improvement method to be applied by all employees in the company. The result of Kaizen activities is the tools, Poka Yoke, Jidoka, Smed, balancing the production process and so on. Poka Yoke is created by the implementation of Kaizen activities, solving a particular cause of problems in the work processes. Kaizen activities should be carefully prepared, effectively managed and implemented if successful results are sought. The time of the Kaizen event can be divided into three major units: 40% of the time should be spent on preparation (problem isolation and statistical analysis), 40% on finding solutions and 20% on the implementation of the solution [19].
In the company, the application of Kaizen is shown in the assembly process, where the product cable laying is made. The cable laying was made using a template drawing, indicating which hardware was embedded in the product and the device coupling scheme.
The cables were made in accordance with the template, where the template was placed on the desk and ergonomically was not suitable, that is, it was not sufficiently mobile and flexible. The biggest problem was a large number of different wires that were used, but they did not have their stand and place on the desk. Hence, the wires should have been pre-prepared with certain lengths to be tied to the table, which took a long time.
Figure 3 shows a work desk that has been improved in relation to the existing one and the

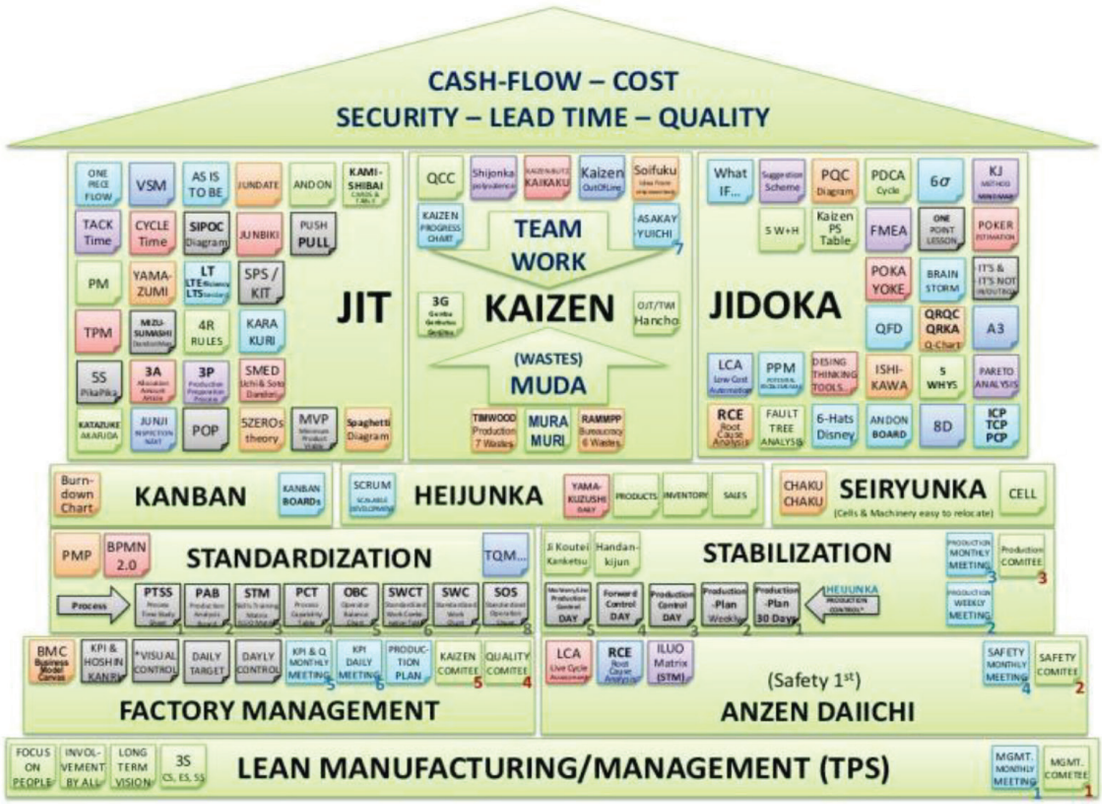

Figure 2: *Lean concept – methods and tools [18].*

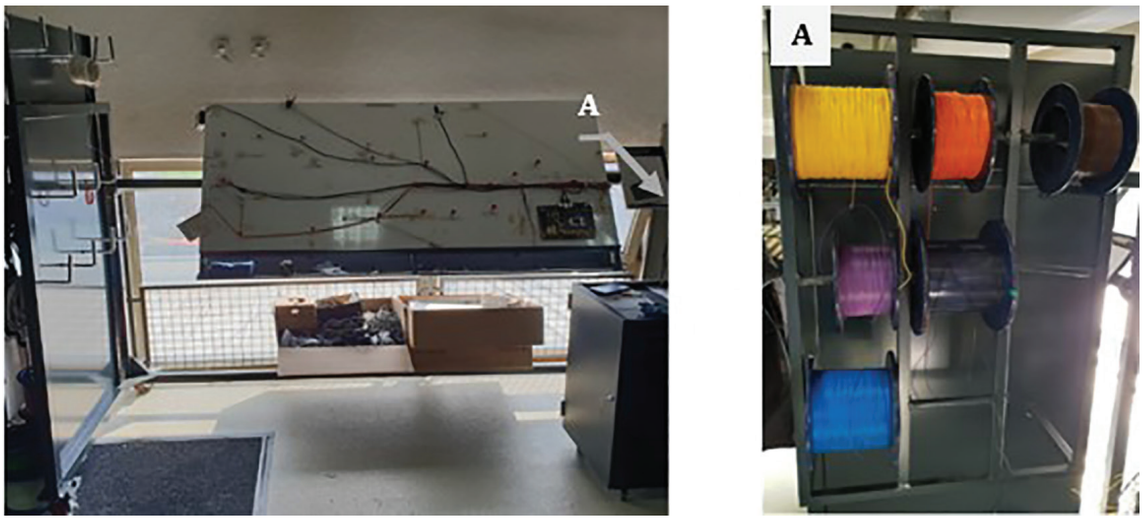

Figure 3: *Improvement of working table for assembling cable [19].*

team facilitates and accelerates the work on the processes of making cable laying for the products.

On the left side of the table are hooks for connectors, and in the middle there is a template for cables that can be changed because each

product requires another cable. Below the table, there is a toolbox and there are wheels for making it easier to transport. On the right side, there are carriers of different wires that pass through the right panel and are directly placed on the template.

Poka Yoke

Poka Yoke has a great application for parts that are welded in the metal industry. Regardless of what is indicated on the workshop drawing, it often happens that the left and right sides are incorrectly welded. These errors are usually detected too late or when the product enters the final stage. This requires the product to return to the initial stage. To prevent these errors, the parts which are welded into the circuit have a "hole slot". By adding hole slot, we enable assembly of two parts in only one way. Figure 4 shows an example of three parts that are welded into one circuit, and it is possible to fit them in only one way [20].

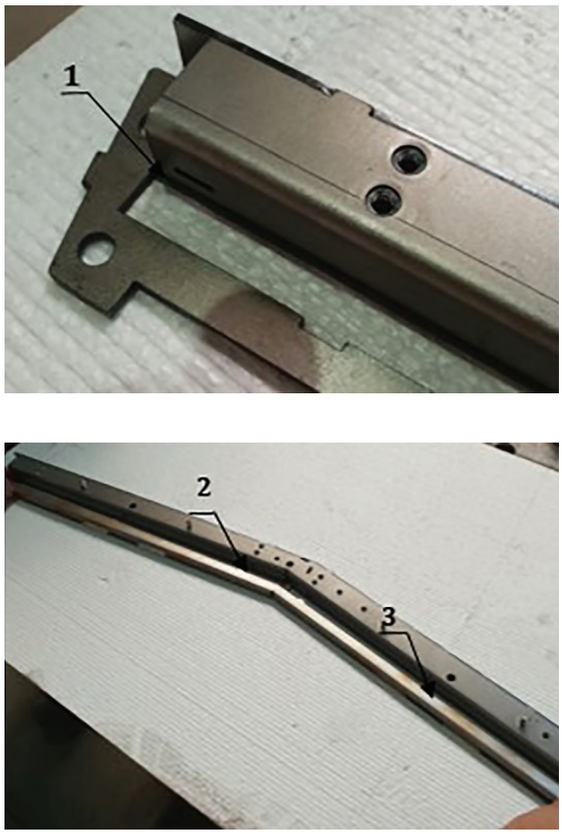

Figure 4: *Poke Yoke – application.*

Kanban

The company uses a Kanban board for better communication between the sales and the development, and technical bureaus on projects take place through an electronic cannon table. The company works simultaneously on 10–15 projects, and it was very complicated to conduct and keep track of projects before the introduction of the electronic Kanban board. Kanban board enables engineers to receive project assignments, instructions, deadlines and all other necessary information for their work on their orders (Figure 5).

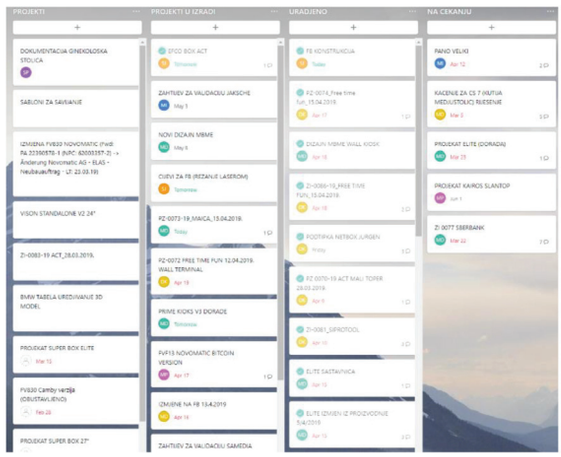

Figure 5: *Electronic Kanban board [19].*

Discussion and Conclusion

Available literature and data on the number of registered enterprises indicate that SMEs support the national economy, but the application of Lean practices and its success in these companies are very little explored. In this regard, the above studies indicate resource limitations in SMEs that put them at a disadvantage when it comes to the adoption and implementation of Lean principles and methods. Given the limitations, a strategy is proposed for implementing Lean concepts in SMEs. The concept includes the formation of different teams of employees, training by outside consultants, researching ways to improve processes and elimination of waste. The project of implementation of Lean concept in SMEs begins with activities that do not require large investments and large ex-

penses, but perseverance and commitment of all employees from top management to operational workers.

The basic preconditions for the proposed model for the application of Lean concept in SMEs can be shown through

— necessity to adopt the Lean way of thinking by investors and top managements in SMEs, even in micro-enterprises, to spread the culture of continuous improvement;
— willingness of management to involve all employees in training at the cost of halted production due to the limited number of employees in SMEs;
— monitoring and analysis of all wastes in all work processes and
— investment in the Lean project with an estimated amount of savings based on the minimisation of waste in the company and return on investment.

For the purpose of research, it is necessary to conduct additional studies on the implementation of Lean concepts and challenges of implementing Lean principles and culture in SMEs.

The implementation of Poke Yoke in the welding department has prevented the incorrect welding of the parts and the possibility of errors has been reduced. The Kanban electronic board, which is used in the technical bureau, made it possible to make a clear overview of the active projects and planned tasks, which resulted in increased flexibility and efficiency of operations.

Based on the above examples, it can be concluded that the use of certain Lean tools in SMEs has affected the reduction of total time in certain activities and thus increased the efficiency of the realisation of the planned operations. Finally, it should be noted that all departments in the enterprise (production and administration) can influence the reduction of losses and dissipation in their processes by applying Lean methods and techniques.

References

[1] Achanga, P., Shehab, E., Roy, R., Nelder, G. (2005): Critical success factors for lean implementation within SMEs. *Journal of Manufacturing Technology Management*, 17(4), pp. 460–471.

[2] White, R.E. (1999): An empirical assessment of JIT in US manufacturers. *Production & Inventory Management Journal*, 34(2), pp. 38–42.

[3] Conner, G. (2001). *Lean Manufacturing for the Small Shop*. Society of Manufacturing Engineers, 1. edition, Dearborn, MI, 275 p.

[4] Meredith, J. (1987): The strategic advantages of new manufacturing technologies for small firms. *Strategic Manufacturing Journal*, 8, pp. 249–258.

[5] Denton, P.D., Hodgson, A. (1997): Implementing strategy-led BPR in a small manufacturing company. In: Proceedings of the Fifth International Conference on FACTORY 2000 – The Technology Exploitation Process Conference Publication. Venue Churchill College, Cambridge, UK, pp. 1–8.

[6] Safayeni, F., Purdy, L., Van Engelen, R., Pal, S. (1991): Difficulties of just-in-time implementation. *International Journal of Operations & Production Management*, 2(7), pp. 27–36.

[7] Hanga, P., Taratoukhine, V., Roy, R., Nelder, G. (2004): The application of lean manufacturing within small and medium sized enterprises. In: Proceedings of International Conference on Manufacturing Research, Sheffield Hallam University, Sheffield.

[8] Achanga, P., Shehab, E., Roy, R., Nelder, G. (2005): Lean manufacturing to improve cost effectiveness of SMEs. In: Proceedings of the 7th International Conference on Stimulating Manufacturing Excellence in SMEs, University of Strathclyde, Glasgow.

[9] Assessing for lean six sigma implementation and success [online]. Six Sigma Advantage, 2000 [cited 10/10/2005]. Available on: http://software.isixsigma.com.

[10] Baker, J., McInturff, P. (2007): Small shop dynamics: time and technology. *Communications of the IIMA*, California, 7(3), pp. 109–118.

[11] Matt, D.T., Rauch E. (2013): Implementation of Lean Production in small sized Enterprises, 8th CIRP Conference on Intelligent Computation in Manufacturing Engineering.

[12] James, J., Frederick, M. (2001): *The Lean Company Making The Right Choices*, Society of Manufacturing Engineers, Dearborn, Michigan.

[13] Smith, R., Hawkins, B. (2004). *Lean Maintenance*, Elsevier Inc., Oxford, 278 p.

[14] Tanasić, T., Kosec, B., Janjić G., Soković M. (2014): LEAN and LCA – system approach, ETIKUM 2014, Novi Sad.

[15] Womack, J.P., Jones, D.T. (1996). *Lean Thinking*, Simon & Schuster, New York, 350 p.

[16] Doolen, T., Hacker, M. (2005): A Review of Lean Assessment in Organizations: An exploratory study of lean practices by electronics manufacturers. *Journal of Manufacturing Systems*, 24(1), pp. 55–67.

[17] Martić, R., Tanasić, Z., Janjić, G. (2017): Implementation of LEAN Concept in SMEs. In: 13th International Conference on Accomplishments in Mechanical and Industrial Engineering – DEMI 2017, Banja Luka, 26–27 May 2017, pp. 773–778.

[18] The Structure of Lean Manufacturing & Lean Management: All tools and concepts [online]. The house of lean, [cited 4/10/2019]. Available on: https://www.slideshare.net.

[19] Tanasić, Z., Petković S., Janjić, G., Kosec, B. (2019): Application of Lean concept in the ELAS Metalexpert company. In: 14th International Conference on Accomplishments in Mechanical and Industrial Engineering – DEMI 2019, Banja Luka, 24–25 May 2019, pp. 597–603.

[20] Tanasić, Z., Janjić, G., Bobrek, M., (2016). *Organizacija i menadžment*, University of Banja Luka, Faculty of Mechanical Engineering.

Instructions for Authors

RMZ – MATERIALS & GEOENVIRONMENT (RMZ – Materiali in geookolje) is a periodical publication with four issues per year (established in 1952 and renamed to RMZ – M&G in 1998). The main topics are Mining and Geotechnology, Metallurgy and Materials, Geology and Geoenvironment.
RMZ – M&G publishes original scientific articles, review papers, preliminary notes, and professional papers in English. Only professional papers will exceptionally be published in Slovene. In addition, evaluations of other publications (books, monographs, etc.), in memoriam, presentation of a scientific or a professional event, short communications, professional remarks and reviews published in RMZ – M&G can be written in English or Slovene. These contributions should be short and clear.
Authors are responsible for the originality of the presented data, ideas and conclusions, as well as for the correct citation of the data adopted from other sources. The publication in RMZ – M&G obligates the authors not to publish the article anywhere else in the same form.

Specification of the Contributions

Optimal number of pages is 7 to 15; longer articles should be discussed with the Editor-in-Chief prior to submission. All contributions should be written using the ISO 80000.

- Original scientific papers represent unpublished results of original research.
- Review papers summarize previously published scientific, research and/or expertise articles on a new scientific level and can contain other cited sources which are not mainly the result of the author(s).
- Preliminary notes represent preliminary research findings, which should be published rapidly (up to 7 pages).
- Professional papers are the result of technological research achievements, application research results and information on achievements in practice and industry.
- Publication notes contain the author's opinion on newly published books, monographs, textbooks, etc. (up to 2 pages). A figure of the cover page is expected, as well as a short citation of basic data.
- In memoriam (up to 2 pages), a photo is expected.
- Discussion of papers (Comments) where only professional disagreements of the articles published in previous issues of RMZ – M&G can be discussed. Normally the source author(s) reply to the remarks in the same issue.
- Event notes in which descriptions of a scientific or a professional event are given (up to 2 pages).

Review Process

All manuscripts will be supervised shall undergo a review process. The reviewers evaluate the manuscripts and can ask the authors to change particular segments, and propose to the Editor-in-Chief the acceptability of the submitted articles. Authors are requested to identify three reviewers and may also exclude specific individuals from reviewing their manuscript. The Editor-in-Chief has the right to choose other reviewers. The name of the reviewer remains anonymous. The technical corrections will also be done and the authors can be asked to correct the missing items. The final decision on the publication of the manuscript is made by the Editor-in-Chief.

Form of the Manuscript

All papers must be submitted via the online system.
The original file of the Template is available on RMZ – Materials and Geoenvironment Home page address: **www.rmz-mg.com**.

The contribution should be submitted in Microsoft Word. Manuscript should be written in Arial font and 12 pt font with 1.5 line spacing and should contain all figures, tables and formulas. Headings should be written in Arial bold font and shuold not be numbered. Subheadings should be written in Arial italic font. The electronic version should be simple, without complex formatting, hyphenation, and underlining. For highlighting, only bold and italic types should be used.

Annexes

Annexes are images, spreadsheets, tables, and mathematical and chemical formulas. Math formulas should be included in article as editable text and not as images.
Annexes should be included in the text at the appropriate place, and they should also be submitted as a separate document, i.e. separated from the text in the article.
Annexes should be originals, made in an electronic form (Microsoft Excel, Adobe Illustrator, Inkscape, AutoCad, etc.) and in .eps, .tif or .jpg format with a resolution of at least 300 dpi.
The width of the annex should be at least 152 mm. They should be named the same as in the article (Figure 1, Table 1). The text in the annexes should be written in typeface Arial Regular (6 pt).
The title of the image (also schemes, charts and graphs) should be indicated in the description of the image.
When formatting spreadsheets and tables in text editors, tabs, and not spaces, should be used to separate columns.
Each formula should have its number written in round brackets on its right side.
References of the annexes in the text should be as follows: “Figure 1…” and not “as shown below:”. This is due to the fact that for technical reasons the annex cannot always be placed at the exact specific place in the article.

Composition of the Manuscript

Title
The title of the article should be precise, informative and not longer that 100 characters. The author should also indicate the short version of the title. The title should be written in English as well as in Slovene..

Information on the Authors
Information on the authors should include the first and last name of the authors, the address of the institution and the e-mail address of the corresponding author.

Abstract
The abstract presenting the purpose of the article and the main results and conclusions should contain no more than 180 words. It should be written in Slovene and English.

Key words
A list of up to 5 key words (3 to 5) that will be useful for indexing or searching. They should be written in Slovene and English.

Introduction

Materials and methods

Results and discussion

Conclusions

Acknowledgements

References

The references should be cited in the same order as they appear in the article. **Where possible the DOI for the reference should be included at the end of the reference.** They should be numbered in square brackets. References should be cited according SIST ISO 690:1996 standards.

Book:
[1] Reynolds, J.M. (2011). *An introduction to Applied and Environmental Geophysics*. New York: Wiley, 710 p.

Unpublished Master thesis or PhD dissertation:
[2] Trček, B. (2001): *Solute transport monitoring in the unsaturated zone of the karst aquifer by natural tracers*. Ph. D. Thesis. Ljubljana: University of Ljubljana 2001; 125 p.

Chapter in an edited book:
[3] Blindow, N., Eisenburger, D., Illich, B., Petzold, H., Richer, T. (2007): *Ground Penetrating Radar*. In: Environmental Geology: Handbook of Field Methods and Case Studies, Knödel, K., Lange, G., Voigt, H.J. (eds.). Springer: Berlin; pp. 283–335.

Journal article : Journal title should be complete and not abbreviated.
[4] Higashitani, K., Iseri, H., Okuhara, K., Hatade, S. (1995): Magnetic Effects on Zeta Potential and Diffusivity of Nonmagnetic Particles. *Journal of Colloid and Interface Science*, 172, pp. 383–388.
[5] Mcmechan, G.A, Loucks, R.G, Mescher, P.A, Xiaoxian, Z. (2002): Characterization of a coalesced, collapsed paleocave reservoir analog using GPR and well-core data. *Geophysics*, 67, pp. 1148–1158. doi: 10.1190/1.1500376

Proceedings Paper:
[6] Benac, Č., Gržančić, Ž., Šišić, S., Ružić, I. (2008): Submerged Karst Phenomena in the Kvarner Area. In: Proceedings of the 5th International ProGEO Symposium on Conservation of the Geological Heritage, Rab, Croatia, Marjanac, T (ed.). Pro GEO Croatia: Zagreb; pp. 12–13.

Electronic source:
[7] CASREACT – Chemical reactions database [online]. Chemical Abstracts Service, 2000, renewed 2/15/2000 [cited 2/25/2000]. Available on: <http://www.cas.org/casreact.html>.

Scientific articles, review papers, preliminary notes and professional papers are published in English. Only professional papers will exceptionally be published in Slovene.

Units

SI System should be used for units. Physical quantities should be written in Italics (e.g. m, l, v, T). Symbols for units should be in plain text with spaces (e.g. 10 m, 5.2 kg/s, 2 s-1, 50 kPa). All abreviations should be spelt out in full on first appearance.

Manuscript Submission

Please submit your article via RMZ-M&G Editorial Manager System. You can find it on the address:
http://edmgr.editool.com/rmzmag/default.htm

Log in as an author and submit your article.
You can follow the status of your submission in the system manager and your e-mail.

Information on RMZ – M&G

— Assistant editor
  Jože Žarn
  E-mail address: joze.zarn@ntf.uni-lj.si

— Secretary
  Vukič Nivesč
  Telephone: +386 01 47 04 610
  E-mail address: nives.vukic@ntf.uni-lj.si

These instructions are valid from April 2017.